Moment matching based model order reduction in computational electromagnetism

Von der
Carl-Friedrich-Gauß-Fakultät
der Technischen Universität Carolo-Wilhelmina zu Braunschweig

zur Erlangung des Grades eines
Doktoringenieurs (Dr.-Ing.)

genehmigte Dissertation

von
André Bodendiek (M. Sc.)
geboren am 19.12.1985
in Braunschweig

Eingereicht am:	19.09.2013
Disputation am:	10.12.2013
1. Referent:	Prof. Dr. Matthias Bollhöfer
2. Referent:	Prof. Dr. Karl Meerbergen

(2014)

Bodendiek, André
Moment matching based model order reduction in computational electromagnetism
Dissertation,
Technische Universität Carolo Wilhelmina Braunschweig, 2014.

For
Cornelia and Edmund,
&
Margot and Rigo,
&
Anna-Lena.

Summary

In the thesis at hand, we will provide a comprehensive discussion on the application of structure-preserving moment matching methods in model order reduction of the first- and second-order Maxwell's equations. The model problems of the three-dimensional Maxwell's equations arise in the context of semiconductor structures, e.g. in order to analyse the influence of parallel conducting strip lines in the design of electric circuits. More precisely, the numerical simulation shall provide an appropriate analysis of the appearing parasitic effects, e.g. crosstalk or signal delay.

Since the resulting linear dynamical systems of Maxwell's equations are of high dimension, the application of model order reduction leads to a reduced order model of significantly smaller dimension. The key feature of model order reduction is the preservation of the input-output behaviour of the linear dynamical system such that the reduced order model allows for an efficient numerical simulation within a given accuracy. Due to the fact that the application of moment matching methods is still restricted by the lack of an a-priori error estimation, the achievement of a given accuracy in the reduced order model requires a reliable adaptive expansion point selection in order to properly benefit from the multiple expansion of the transfer function at each expansion point. Therefore, we will introduce an adaptive greedy-type expansion point selection based on a suitable approximation of the output moment error. In this context, the Galerkin projection for the computation of the reduced order model is obtained via the adaptive-order rational Arnoldi (AORA) method, which allows for an efficient computation of the required sequence of Krylov subspaces corresponding to different expansion points.

Although the application of model order reduction leads to an efficient numerical simulation of a high-dimensional linear dynamical system, we will additionally discuss the computational effort for the computation of the (Petrov-) Galerkin projection in moment matching model order reduction. For efficiently computing the solution to a sequence of high-dimensional shifted linear systems appearing in the computation of the reduced order model, we provide a new framework for the offline-stage in model order reduction. Thereby, we will show that the modified AORA (mAORA) method allows for the reuse of the orthonormal vec-

tors from different Krylov subspaces during the computation of a sequence of reduced order models.

Moreover, we will introduce an algebraic two-level method (ATLM) for solving a high-dimensional shifted linear system corresponding to first-order Maxwell's equations based on direct solvers. The main computational effort of the ATLM arises out of solving a linear system corresponding to the Schur complement of the discretized first-order Maxwell's equations, which refers to a discretized Maxwell's equation in the second-order formulation. For efficiently solving a sequence of high-dimensional shifted linear systems with multiple right hand sides required in moment matching methods, we will also review (recycling) Krylov subspace methods. Typically, recycling Krylov subspace methods offer a significant improvement of the convergence behaviour due to the employment of a recycling subspace. In this context, a structure-preserving solution technique for a complex symmetric, but highly indefinite second-order Maxwell's equations is achieved by the recycling simplified quasi-minimal residual (rSQMR) method.

Finally, we demonstrate by numerical experiments that the application of the modified AORA method in combination with the recycling SQMR method leads to an efficient offline-stage for moment matching methods in model order reduction with respect to the computational effort and the memory requirement.

Zusammenfassung

Die vorliegende Arbeit beschäftigt sich mit der Anwendung von strukturerhaltenden Momenten-Abgleich-Verfahren in der Modellreduktion der Maxwell-Gleichungen erster und zweiter Ordnung. Die zugehörigen Modellprobleme der dreidimensionalen Maxwell-Gleichungen resultieren aus dem Anwendungsgebiet der Halbleiterstrukturen, um den Einfluss von parallelen Leiterbahnen innerhalb der Entwicklung von elektrischen Schaltkreisen zu analysieren. In diesem Zusammenhang benötigt man eine zuverlässige Aussage über die auftretenden Störeffekte, zum Beispiel durch Übersprechen oder Signalverzögerung.

Aufgrund der Tatsache, dass die linearen dynamischen Systeme der Maxwell-Gleichungen hoch-dimensional sind, liefert die Modellreduktion eine Möglichkeit zur effizienten numerischen Simulation der Modellprobleme innerhalb einer vorgegebenen Genauigkeit. Hierbei liegt die wesentliche Eigenschaft der Modellreduktion in der Beobachtung, dass das Übertragungsverhalten des hoch-dimensionalen linear dynamischen Systems im reduzierten Modell wiederzufinden ist. Die derzeit fehlende a-priori Fehlerschranke für Momenten-Abgleich-Verfahren erfordert hinsichtlich der vorgegebenen Genauigkeit der reduzierten Modelle eine zuverlässige Auswahl an Entwicklungspunkten, um einen Vorteil aus der mehrfachen Entwicklung der Übertragungsfunktionen in jedem Entwicklungspunkt gewinnen zu können. Daher werden wir im weiteren Verlauf auf der Basis einer geeigneten Approximation des Momentenfehlers eine Greedy-artige Entwicklungspunktauswahl einführen. Hierbei erhalten wir die zugehörige Galerkin-Projektion zur Berechnung des reduzierten Modells mit Hilfe des adaptiven, rationalen Arnoldi (AORA) Verfahrens, welches eine effiziente Berechnung der einzelnen Krylov-Unterräume für eine gegebene Menge an Entwicklungspunkten ermöglicht.

Obwohl die Anwendung der Modellreduktion eine effiziente numerische Simulation des zugehörigen Modellproblemes erlaubt, soll im weiteren Verlauf zusätzlich der Rechenaufwand für die Berechnung der Galerkin-Projektion im Vordergrund stehen. Typischerweise benötigen wir in diesem Zusammenhang die Lösung einer Folge hoch-dimensionaler, geshifteter linearer Gleichungssysteme für ausgewählte Entwicklungspunkte. Aus diesem Grund haben wir für die sogenannte Offline-Phase der Modellreduktion eine entsprechende Erweiterung der bisherigen Verfahren eingeführt. Hierbei erlaubt die Anwendung des modifizierten adaptiven,

rationalen Arnoldi-Verfahrens die Wiederverwendung einer bekannten Sequenz orthonormaler Vektoren innerhalb der Berechnung einer Folge von reduzierten Modellen.

Weiterhin führt das sogenannte algebraische Zwei-Level-Verfahren zur Lösung geshifteter linearer Gleichungssysteme der Maxwell-Gleichungen erster Ordnung auf ein effizientes Verfahren mittels der Anwendung direkter Löser. Der wesentliche Rechenaufwand des algebraischen Zwei-Level-Verfahrens ergibt sich aus der Lösung eines Gleichungssystems mit dem Schur-Komplement der diskretisierten Maxwell-Gleichungen erster Ordnung. Dabei beschreibt das Schur-Komplement eine diskretisierte Maxwell-Gleichung zweiter Ordnung. Für die effiziente Lösung der Sequenz geshifteter linearer Gleichungssysteme mit mehrfachen rechten Seiten innerhalb der Momenten-Abgleich-Verfahren werden wir die recycling Krylov-Unterraum-Verfahren in Betracht ziehen. Aufgrund der Anwendung eines recycling Unterraumes führen recycling Krylov-Unterraum-Verfahren typischerweise auf ein wesentlich verbessertes Konvergenzverhalten. In diesem Zusammenhang beschreibt das recycling simplified quasi-minimal residual (rSQMR) Verfahren ein strukturerhaltendes Verfahren zur Lösung der (komplex-) symmetrischen, aber hochgradig indefiniten Maxwell-Gleichungen zweiter Ordnung.

Zum Abschluss werden numerische Experimente verdeutlichen, dass die Anwendung des modifizierten adaptiven, rationalen Arnoldi-Verfahrens in Kombination mit dem rSQMR-Verfahren auf eine effiziente Offline-Phase der Modellreduktion mittels Momenten-Abgleich-Verfahren im Hinblick auf den zugehörigen Rechen- und Speicheraufwand führt.

Acknowledgement

The thesis at hand would have never been written without the support and help of many different people. First of all, I would like to grateful thank my supervisor Prof. Dr. M. Bollhöfer for the numberless fruitful discussions and his motivation words during the difficult times of the research work. Furthermore, I acknowledge the German Federal Ministry of Education and Research for their funding of the MoreSim4Nano research project, where the essential components of the research work of the thesis have been worked out. I would also like to thank Prof. Dr. H. Faßbender for the given comments on the research work and along with Prof. Dr. M. Bollhöfer providing me the possibility to visit a large number of workshops and conferences. Especially, the SIAM Conference on Computational Science & Engineering in Boston had a significant impact on the progress of my research work. I am also pleased that Prof. Dr. K. Meerbergen and Prof. Dr. A. Kemnitz have spend their time being the second referee of the thesis and the chair of the corresponding oral examination, respectively.

During my work on the MoreSim4Nano research project, I have been working in the workgroup numerical mathematics of the Institute Computational Mathematics at the Technical University Braunschweig. Here, I would like to thank my colleagues André Eppler, Tanja Schenk, Peter Stange, Andreas Soppa, Alexander Vendl and Ralf Zimmermann for the fruitful discussions and the comfortable working atmosphere. In particular, I apologise Tanja Schenk and Peter Stange for the large number of coffee cups and the (un-) mathematical discussions. Moreover, the business trips with Alexander Vendl have always been a pleasure particularly with regard to the meal from the room service in Novi Sad (Serbia). Moreover, I thank Wolfgang Ackermann, Amir Geranmayeh, Martin Heß and Judith Schneider for the fruitful cooperation in the MoreSim4Nano research project. Finally, I would like to acknowledge my former fellow students Christian Kruschel and Mark Kuschkowitz for having several discussions on the time before starting to write the thesis.

Finally, I thank my parents Cornelia and Edmund and my grand parents Margot and Rigo Schall for their extensive support and love during the research work for the thesis. Thank you that you have never stopped to believe in the possibility to finish the PhD thesis. I would also like to mention my girl friend Anna-Lena Behrens who spend all her love in helping me to

come a little bit closer to the end at each day. Finally, I thank all other friends and colleagues, who have not been mentioned here, but who helped to find the right way to the end.

Contents

List of Figures

List of Tables

List of Algorithms

Nomenclature

Abbreviations

ADI	alternating direct implicit
AORA	adaptive-order rational Arnoldi
AORGA	adaptive-order rational global Arnoldi
ATLM	algebraic two-level method
AWE	asymptotic wave evaluation
BiCG	biconjugate gradient
BT	balanced truncation
FEM	finite element method
FIT	finite integration technique
GMRES	generalized minimal residual
IRKA	iterative rational Krylov algorithm
LR	low-rank
mAORA	modified adaptive-order rational Arnoldi
MIMO	multiple-input, multiple-output
PCA	principal component analysis
PCB	Printed Circuit Board
POD	proper orthogonal decomposition
PVL	Padé-via-Lanczos
QMR	quasi-minimal residual
rBiCG	recycling biconjugate gradient
rQMR	recycling quasi-minimal residual
rSQMR	recycling simplified quasi-minimal residual
s.p.d.	symmetric positive definite
SAORA	second- and adaptive-order rational Arnoldi

SI	International System of Units
SISO	single-input, single-output
SOAR	second-order Arnoldi
SPRIM	structure-preserving reduced order interconnect macromodeling
SQMR	simplified quasi-minimal residual
WCAWE	well-conditioned asymptotic waveform evaluation

Discretization of Maxwell's equations

$\mathcal{E}_{\#}$	number of local basis functions of ansatz space
$\widehat{\widehat{b}}$	magnetic grid flux
$\widehat{\widehat{d}}$	electrical grid flux
$\mathcal{T}$	tetrahedron of triangulation
$\mathcal{T}^o$	interior of tetrahedron $\mathcal{T}$
λ	wavelength according to frequency range
$\lambda_{\max}$	maximum wavelength
λ_i	i-th Barycentric coordinate
$\mathcal{G}$	grid of computational domain (FIT)
$n_{\#}$	number of grid points (FIT)
Ω	computational domain
Ω_h	triangulation of computational domain (FEM)
$\tilde{\mathcal{G}}$	dual grid of computational domain (FIT)
$\widehat{e}$	electrical grid voltage
$\widehat{h}$	magnetic grid voltage
C_E, C_H	discrete curl-operator w.r.t. electric and magnetic field strength
D_E, D_H	discrete divergence operator w.r.t. electric and magnetic field strength
h	step size of discretization of computational domain
V	Hilbert space
V_h	finite-dimensional subspace of Hilbert space

Symbols in (recycling) Krylov subspace methods

$\mathcal{K}_j(A, r_0)$	Krylov subspace for iterative Krylov subspace methods
$\mathcal{L}_j(A^*, \tilde{r}_0)$	dual Krylov subspace for iterative Krylov subspace methods
θ	harmonic Ritz value
$\underline{H}_j$	upper Hessenberg matrix from Arnoldi method

$\underline{T}_j$	tridiagonal matrix from Lanczos method
A	coefficient matrix of sparse linear system $Ax = f$
A'	preconditioned coefficient matrix of linear system
f	right-hand side of sparse linear system $Ax = f$
f'	preconditioned right-hand side of linear system
k	number of eigenvectors kept for recycling subspace
$m - k$	number of iteration steps before update of recycling subspace
M_1	left preconditioning matrix
M_2	right preconditioning matrix
r_j	j-th residual corresponding to iterative solution
S	Schur complement of algebraic two-level method
U	recycling subspace
V	(bi-) orthonormal basis of Krylov subspace $\mathcal{K}_j(A, r_0)$
W	(bi-) orthonormal basis of Krylov subspace $\mathcal{L}_j(A^*, r_0^*)$
x	solution to sparse linear system $Ax = f$
x'	preconditioned solution to linear system
x_j	j-th iterate of approximate solution to linear system

Mathematical symbols

$(\mathbf{u}, \mathbf{v})_0$	scalar product: $\int_\Omega \boldsymbol{u} \cdot \boldsymbol{v}\ d\boldsymbol{x}$ with $\boldsymbol{u}, \boldsymbol{v} \in [\mathbb{L}_2(\Omega)]^n$ and $n \in \mathbb{N}$
0	zero matrix
$[\mathbb{L}_2(\Omega)]^n$	extension of $L_2(\Omega)$ for vector fields $F : \mathbb{C}^m \to \mathbb{C}^n$
$\mid z \mid$	absolute value: $\sqrt{\alpha^2 + \beta^2}$ with $z = \alpha + \imath\beta \in \mathbb{C}$
$\bar{z}$	complex conjugate: $\alpha - \imath\beta$ with $z = \alpha + \imath\beta \in \mathbb{C}$
$\mathbb{C}$	field of complex numbers
$\mathbb{C}^{n\times m}$	field of complex $n \times m$ matrices
$\mathbb{C}^n$	vector space of dimension $n > 0$ with complex entries
$\mathbb{C}_+$	complex numbers with positive real part
$\mathbb{C}_-$	complex numbers with negative real part
$\mathrm{colspan}(V)$	span of the columns of the matrix V
δ_{ij}	Kronecker delta: $\delta_{ij} = 1$ for $i = j$, otherwise $\delta_{ij} = 0$
$\emptyset$	empty set
$\mathrm{Im}(z)$	imaginary part of complex number $z \in \mathbb{C}$

$\imath = \sqrt{-1}$	imaginary unit
$\mathbb{L}_2([0,t],\mathbb{R}^m)$	space of square integrable and Lebesgue measurable functions $u : [0,t] \to \mathbb{R}^m$ with $\| u \|_2 < \infty$
$\mathbb{L}_2(\Omega)$	space of square integrable and Lebesgue measurable functions
$\lambda E - A$	matrix pencil of generalized eigenvalue problem $Ax = \lambda Ex$, $x \neq 0$, $\lambda \in \mathbb{C}$
$\mathbb{H}_p$	Hardy space: $\left\{F : \mathbb{C} \to \mathbb{C}^{r\times m} : \| F \|_{\mathbb{H}_p} < \infty\right\}$ $(p = 1, \ldots, \infty)$
$\mathbb{N}$	set of natural number: $1, 2, \ldots$
$\mathbb{Z}$	set of integer numbers
$\mathcal{I} = [a,b]$	real-valued interval: $\{x \in \mathbb{R} : a \leq x \leq b\}$
$\mathcal{K}_j(A,b)$	Krylov subspace: $\mathrm{span}\left\{b, Ab, \ldots, A^{j-1}b\right\}$ with $A \in \mathbb{C}^{n\times n}$ and $b \in \mathbb{C}^n$
$\nabla \cdot F$	divergence operator: $\frac{\partial F_1}{\partial x_1} + \ldots + \frac{\partial F_n}{\partial x_n}$ with $F \equiv (F_1, \ldots, F_n)$
$\nabla \times F$	curl-operator: $\left(\frac{\partial F_z}{\partial y} - \frac{\partial F_y}{\partial z}, \frac{\partial F_x}{\partial z} - \frac{\partial F_z}{\partial x}, \frac{\partial F_y}{\partial x} - \frac{\partial F_x}{\partial y}\right)^{\mathrm{T}}$ with $F \equiv (F_x, F_y, F_z)$
∇F	gradient operator: $\left(\frac{\partial F}{\partial x_1}, \ldots, \frac{\partial F}{\partial x_n}\right)$ with $F : \mathbb{C}^n \to \mathbb{C}$
$\| \cdot \|_{H^1}$	norm of function space $H^1(\Omega)$
$\| \cdot \|_{H_{\mathrm{curl}}}$	norm of function space $H_{\mathrm{curl}}(\Omega)$
$\| A \|$	arbitrary norm of matrix $A \in \mathbb{C}^{n\times m}$
$\| A \|_2$	spectral norm: $\max_{x\neq 0} \frac{\| Ax \|_2}{\| x \|_2}$ with $A \in \mathbb{C}^{n\times m}$
$\| A \|_F$	Frobenius norm: $\sum_{i,j} \| a_{i,j} \|$ with $A \in \mathbb{C}^{n\times m}$
$\| u \|_p$	p-norm of function $u : \mathcal{I} \to \mathbb{R}^n$ $(p \in \mathbb{N})$
$\| x \|_2$	$(x_1^2 + \ldots + x_n^2)^{1/2}$ with $x \in \mathbb{C}^n$
$\mathrm{curl}(F)$	abbreviation for $\nabla \times F$ with $F \equiv (F_x, F_y, F_z)$
$\mathrm{div}(F)$	abbreviation for $\nabla \cdot F$ with $F \equiv (F_1, \ldots, F_n)$
$\mathrm{grad}(F)$	abbreviation for ∇F with $F : \mathbb{C}^n \to \mathbb{C}$
$\mathrm{span}(V)$	span of the subspace V
$\partial/\partial t$	partial derivative
$\partial^k/\partial t$	k-th partial derivative
$\mathbb{R}$	field of real numbers
$\mathbb{R}^{n\times m}$	field of real $n \times m$ matrices
$\mathbb{R}^n$	vector space of dimension $n > 0$ with real entries
$\mathbb{R}_+$	positive real numbers
$\mathrm{Re}(z)$	real part of complex number $z \in \mathbb{C}$
$\sigma(A)$	spectrum of matrix A
$\sigma_{\max}(A)$	largest singular value of matrix A

$\vec{\boldsymbol{n}}$	outer unit normal vector
$\vec{\boldsymbol{\tau}}$	unit tangential vector
$A \prec (\preceq)\ 0$	negative (semi-) definite matrix A
$A \succ (\succeq)\ 0$	positive (semi-) definite matrix A
$a \times b$	vector product: $(a_2b_3 - a_3b_2, a_3b_1 - a_1b_3, a_1b_2 - a_2b_1)^{\mathrm{T}}$ with $a = (a_1, a_2, a_3)^{\mathrm{T}}$ and $b = (b_1, b_2, b_3)^{\mathrm{T}} \in \mathbb{R}^3$
A^*	complex conjugate of matrix A: $(a_{ij})^* = \bar{a}_{ji}$
A^{-1}	inverse of matrix A: $AA^{-1} = A^{-1}A = I$
A^{T}	transpose of matrix A: $(a_{ij})^{\mathrm{T}} = a_{ji}$
$C^\infty(\Omega)$	space of infinitely differentiable functions
e_i	i-th unit vector: $(0, \ldots, 0, \underbrace{1}_{i-\text{th component}}, 0, \ldots, 0)^{\mathrm{T}}$
$H(\mathrm{curl}, \Omega)$	$\left\{\boldsymbol{u} \in [\mathbb{L}_2(\Omega)]^3 : \nabla \times \boldsymbol{u} \in [\mathbb{L}_2(\Omega)]^3\right\}$
$H^1(\Omega)$	$\left\{u \in \mathbb{L}_2(\Omega) : \nabla u \in [\mathbb{L}_2(\Omega)]^3\right\}$
I	identity matrix: $(e_1, \ldots, e_n) \in \mathbb{C}^{n \times n}$, where e_i refers to the i-th unit vector
I_n	identity matrix of dimension $n \times n$
$W \perp V$	orthogonal (-orthonormal) subspaces: $w_i^* v_j = 0$ or $w_i^{\mathrm{T}} v_j = 0$ for all $v_i \in V, w_j \in W$
$W \perp_b V$	biorthogonal (-orthonormal) subspaces: $w_i^* v_j = \delta_{ij}$ or $w_i^{\mathrm{T}} v_j = \delta_{ij}$ for all $v_i \in V, w_j \in W$
$y^* x$	scalar product: $y^* x = \sum_{i=1}^n x_i \bar{y}_i$ with $x, y \in \mathbb{C}^n$
$y^{\mathrm{T}} x$	scalar product: $y^{\mathrm{T}} x = \sum_{i=1}^n x_i y_i$ with $x, y \in \mathbb{C}^n$

Symbols in model order reduction

$[0, t_*]$	time-interval of linear dynamical systems ($t_* > 0$)
$\#\,\mathrm{col}(V)$	number of columns of $V \in \mathbb{C}^{n \times p}$ in AORA-MAX method
$\bar{\mathcal{A}}, \bar{\mathcal{B}}, \bar{\mathcal{C}}$	standard state space linear dynamical system
$\bar{V}$	structure-preserving orthonormal matrix for Galerkin projection
$\bar{x}(t)$	state variable of standard state space system
$\epsilon_{\max}(f)$	relative error between full-order and reduced order model problem
$\hat{\delta}_i$	relative error between subsequent reduced order models
$\hat{\epsilon}_k$	heuristic error estimation from sequence of reduced order models
$\mathcal{E}, \mathcal{A}, \mathcal{B}, \mathcal{C}$	first-order linear dynamical system
$\mathcal{G}_{j_i}(s_i)$	second-order Krylov subspace of dimension $j_i > 0$ corresponding to $s_i \in \mathbb{C}$

$\mathcal{H}(s)$	transfer function of linear dynamical system
$\mathcal{H}_q(s)$	q-th Padé approximation of transfer function
$\mathcal{K}_{j_1,\ldots,j_l}(\mathcal{S}_l)$	$\mathcal{K}_{j_1}(s_1) + \ldots + \mathcal{K}_{j_l}(s_l)$ $(s_1, \ldots, s_l \in \mathbb{C})$
$\mathcal{K}_{j_i}(s_i)$	Krylov subspace of dimension $j_i > 0$ corresponding to $s_i \in \mathbb{C}$
$\mathcal{P}$	(proper) controllability Gramian
$\mathcal{Q}$	(proper) observability Gramian
$\mathcal{S}$	set of sampling points from frequency range $\imath[f_{\min}, f_{\max}]$
$\mathcal{S}_l$	set of expansion points $s_1, \ldots, s_l \in \mathbb{C}$
Π	(Petrov-) Galerkin projection
$\tilde{\mathcal{E}}, \tilde{\mathcal{A}}, \tilde{\mathcal{B}}, \tilde{\mathcal{C}}$	reduced first-order linear dynamical system
$\tilde{\mathcal{H}}(s)$	transfer function of reduced order linear dynamical system
$\tilde{M}, \tilde{D}, \tilde{K}, \tilde{\mathcal{B}}_*, \tilde{\mathcal{C}}_*$	reduced second-order linear dynamical system
$\tilde{m}_i \equiv \tilde{m}_i(s_0)$	moments of Taylor expansion of transfer function of reduced order model problem at $s_0 \in \mathbb{C}$
$\tilde{X}^{(j)}(s_i)$	j-th reduced order system moment corresponding to $s_i \in \mathbb{C}$
$\tilde{Y}^{(j)}(s_i)$	j-th reduced order output moment corresponding to $s_i \in \mathbb{C}$
E_{n_r}	output moment error
m	number of inputs of linear dynamical system
$M, D, K, \mathcal{B}_*, \mathcal{C}_*$	second-order linear dynamical system
$m_i \equiv m_i(s_0)$	moments of Taylor expansion of transfer function of full-order model problem at $s_0 \in \mathbb{C}$
n	dimension of full-order model problem
n_d	dimension of reduced order model problem
n_r	number of iteration steps of rational Arnoldi-type method
p	number of outputs of linear dynamical system
P_l, P_r	left and right spectral projections onto finite eigenvalues of matrix pencil $\lambda\mathcal{E} - \mathcal{A}$, $\lambda \in \mathbb{C}$
$s_\#$	number of expansion points in AORA-MAX and AORA-H2 method
$u(t)$	input variable of linear dynamical system
V	orthonormal matrix corresponding to Galerkin projection
$V^{(i)}$	orthonormal matrix corresponding to Galerkin projection w.r.t. expansion points $\mathcal{S}_i \subset \mathbb{C}$
$x(t)$	state variable of descriptor system

$X^{(j)}(s_i)$	j-th system moment corresponding to $s_i \in \mathbb{C}$
$y(t)$	output variable of linear dynamical system
$Y^{(j)}(s_i)$	j-th output moment corresponding to $s_i \in \mathbb{C}$
$z(t)$	state variable of linearization of second-order linear dynamical system

Physical symbols

$[f_{\min}, f_{\max}]$	frequency range of model problem
$\boldsymbol{B}$	magnetic flux density
$\boldsymbol{D}$	electric flux density
$\boldsymbol{E}$	electric field strength
$\boldsymbol{H}$	magnetic field strength
$\boldsymbol{j}$	current density
ϵ	electric permittivity
$\boldsymbol{j}_C$	conduction current density
$\boldsymbol{j}_i$	impressed current density
μ	magnetic permeability
ρ	charge density
σ	electric conductivity

CHAPTER 1

Introduction

The development of new semiconductor structures is mainly guided by the law from G. E. Moore, which states that the number of transistors of an integrated circuit doubles approximately every two years, see [86]. Hence, an accurate design of the electric circuit under consideration becomes indispensable in order to obtain a reliable and sensible usage in practical applications. In particular, the design should minimize the appearance of parasitic effects, e.g. crosstalk or signal delay, such that the employment of the electric circuit guarantees a cost-efficient deployment in the field of nanotechnology.

Due to the fact that the production of a prototype in the nano-scale range is rather infeasible with respect to the high costs of the development, the application of numerical simulations during the advancement of integrated circuits has become of great importance in many years. Here, the accurate knowledge of the electromagnetic field of each single component of the electric circuit allows for an appropriate analysis of the parasitic effects of the neighbouring ingredients. Since the description of the electromagnetic field is based on Maxwell's equations [80], the discretization of the three-dimensional model problem yields a linear dynamical system with several millions of degrees of freedom. The limitations of the numerical simulation are obvious as far as we require the efficient simulation of the model problem for different material parameters within a varying geometric framework of the computational domain.

For the efficient numerical simulation of a high-dimensional linear dynamical system, the application of model order reduction represents an important technique in order to significantly reduce the dimension of the model problem, see [4]. Since the application of model order reduction has to ensure the preservation of the input-output behaviour of a linear dynamical system within a given accuracy, the numerical simulation with the corresponding reduced order model allows for a considerable decreasing of the computational costs. The choice of the

accuracy in the reduced order model mainly depends on the model problem under consideration.

Although the application of model order reduction results in a significant improvement of the computational effort for the numerical simulation, the computational costs required for the construction of the reduced order model may lead to a significant limitation. In the following, this phase will be referred to as the *offline-stage* of model order reduction. For example, the importance of the offline-stage arises from the application of model order reduction within a simulation tool on a standard desktop computer.

Another important observation is that the application of model order reduction typically requires solving a sequence of shifted linear systems corresponding to the high-dimensional full-order model problem. Since the three-dimensional Maxwell's equations lead to a linear dynamical system of high dimension, the increasing memory requirement limits the employment of a direct solver from this point of view. Hence, the application of an efficient iterative solution technique, e.g. iterative Krylov subspace methods [104], becomes indispensable in order to limit the increasing memory requirement and computational costs.

In the following, we will briefly review the current state of the art of the application of moment matching methods in model order reduction of linear dynamical systems. Thereafter, we discuss the main contribution of the thesis at hand for the application of moment matching methods in the field of computational electromagnetism. Finally, we outline the thesis with a short description of each chapter.

1.1 The state of the art

Moment matching methods in model order reduction are based on the Padé approximation [11] of the transfer function. For a long time, the asymptotic waveform evaluation (AWE) was referred to the method of choice for efficiently analysing electric circuits, see [95]. Due to the numerical limitations of the AWE, Freund and Feldmann have shown that the Padé approximation of the transfer function may be also computed by means of the (unsymmetric) Lanczos method, see [41]. In addition, Freund introduced the structure-preserving reduced order interconnect macromodeling (SPRIM) method for the application of moment matching methods with a single expansion point to electric circuits, see [46]. The major advantage of the SPRIM method consists of the preservation of the specific block-structure of the linear dynamical system in the reduced order model. An overview about structure-preserving Arnoldi methods for linear dynamical systems has been provided by Bai [8].

Moreover, an extensive discussion on the application of moment matching methods to Maxwell's equations in model order reduction has been given recently in [114]. In this con-

text, the two-step Lanczos method from Wittig et al. [128] has been applied to linear dynamical systems of first-order Maxwell's equations.

Nevertheless, the limitations of moment matching methods with a single expansion point in model order reduction are apparent from the fact that an accurate reduced order model primarily occurs in the vicinity of the given expansion point $s_0 \in \mathbb{C}$. Therefore, an extension to moment matching methods with multiple expansion points on the basis of a rational Arnoldi-type method has been introduced [74, 90]. Since moment matching methods do not offer an a-priori error estimation for the accuracy of the reduced order model, we will introduce an efficient and suitable greedy-type technique for the adaptive selection of a nested set of expansion points.

Typically, the literature features two common approaches for the computation of a sequence of expansion points. On the one hand, Antoulas et al. [56] have introduced the computation of a set of expansion points in order to obtain a quasi-optimal reduced order model with respect to the $\mathbb{H}_2$-norm. For example, the iterative rational Krylov algorithm (IRKA) refers to as a tangential interpolation method fulfilling the first-order necessary conditions of optimal $\mathbb{H}_2$ model order reduction. On the other hand, an adaptive greedy-type expansion point selection strategy allows for the matching of higher-order derivatives of the transfer function at a given set of expansion points, see [19, 40, 70, 113]. Nevertheless, each adaptive expansion point selection for moment matching methods requires the employment of a heuristic error estimation, e.g. based on a sequence of reduced order models, see [55].

The application of iterative Krylov subspace methods for the solution to a sparse and high-dimensional linear system has been widely discussed in the literature, see [104]. Since the application of model order reduction requires solving a sequence of shifted linear systems with several right hand sides, recycling Krylov subspace methods are typically the preferred approach, see [2, 18, 91]. The improvement of the convergence behaviour of a recycling Krylov subspace method is mainly achieved by the incorporation of a recycling subspace during the iterative solution to each linear system.

The appropriate application of an iterative Krylov subspace method mainly depends on the application of a reliable preconditioning technique. For example, Hiptmair has given an approach for the application of a geometric multigrid method in [61], while Beck proposed an algebraic multigrid approach on the basis of splitting the degrees of freedom with respect to the potential and edge element space, respectively, see [15]. For Helmholtz-type model problems, which are closely related to second-order Maxwell's equations, Erlangga et al. have given a preconditioning technique by means of a complex-shifted mass matrix, see [38]. Another preconditioning technique for Helmholtz equations with a moving PML boundary condition was introduced by Engquist et al. [36]. The latter technique allows for a straightforward extension

to the time-harmonic second-order Maxwell's equations, see [118].

1.2 The main contribution of the thesis

The content of the thesis mainly consists of the research work summarised in [19] and [18]. This thesis will give a comprehensive discussion on the key ingredients of the different aspects of moment matching methods in model order reduction of the first- and second-order Maxwell's equations.

In [19], structure-preserving rational Arnoldi-type methods for moment matching based model order reduction of the Maxwell's equations have been discussed. Thereby, we have shown that the specific block-structure of Maxwell's equations allows for an extension of the SPRIM algorithm developed by Freund to a given set of expansion points based on the rational Arnoldi method. Structure-preserving model order reduction techniques feature the advantage of an increasing accuracy in the reduced order model. The extension of the SPRIM algorithm to Maxwell's equations is justified by the fact that linear dynamical systems corresponding to electric circuits maintain a comparable block-structure.

Moreover, we will introduce a novel adaptive greedy-type expansion point selection strategy, which we refer to as the AORA-RK method, based on the output moment error of the adaptive-order rational Arnoldi (AORA) method and the rational Krylov residual, see [19]. The advantage of the AORA-RK method is that we compute a sequence of expansion points by means of an adequate approximation of an upper bound of the output moment error. Apart from that the output moment error will be employed for the computation of the Galerkin projection in order to adaptively determine the dimensions of the different input Krylov subspaces for a given size of the reduced order model, see [74]. The computation of the subsequent expansion point does not require solving a shifted linear system of high dimension but only a matrix-vector multiplication with the corresponding matrix pencil.

As we have already mentioned in the motivation of the thesis, several applications need an efficient offline-phase for the computation of a reduced order model with moment matching methods, see [18]. Since a Greedy-type expansion point selection strategy requires the subsequent calls of a rational Arnoldi-type method with a sequence of expansion points $\mathcal{S}_{i+1} = \mathcal{S}_i \cup \{s_{i+1}\}$, $s_{i+1} \in \mathbb{C}$, $(i = 1, \ldots, l-1)$, a modification of the rational Arnoldi method as well as the adaptive-order rational Arnoldi method will be introduced in order to avoid recomputing the sequence of Krylov subspaces associated with previous expansion points. In this way, the number of solving a shifted linear system corresponding to the previous expansion points significantly decreases as compared to explicitly computing each Krylov subspace in each subsequent call.

Finally, we will give an extension of the LU decomposition for solving a shifted linear system with the help of an algebraic two-level method (ATLM), see [19]. The algebraic two-level method allows for solving a shifted linear system of Maxwell's equations by exploiting the specific block-structure of the electric and magnetic field strength. The major advantage of the ATLM stems from the fact that it mainly requires solving a linear system with the corresponding Schur complement. Since the Schur complement refers to a discrete (complex) symmetric, but highly indefinite second-order Maxwell's equation, we will present an extension of the recycling BiCG method from Ahuja et al. [2] to a recycling simplified quasi-minimal residual (rSQMR) method, see [18]. The SQMR method has the advantage that it can make use of a (complex) symmetric, but indefinite preconditioning technique for a (complex) symmetric, but indefinite coefficient matrix, see [50]. Here, the rSQMR method leads to an efficient solution technique for a sequence of high-dimensional linear systems obtained via the discretization of the three-dimensional Maxwell's equations.

The modified rational Arnoldi-type method together with the recycling SQMR method and the algebraic two-level approach allows for an improving memory requirement in the offline-stage of moment matching based model order reduction.

1.3 The outline of the thesis

The thesis at hand consists of seven different chapters. In Chapter 2, we will initially introduce the framework of first- and second-order linear dynamical systems and review the basic properties of a descriptor system, e.g. stability and passivity on the one hand and controllability and observability on the other hand. Apart from moment matching methods, we will also give a short introduction on balanced truncation and proper orthogonal decomposition for model order reduction of linear dynamical systems.

A physical interpretation of model problems in computational electromagnetism with respect to Maxwell's equations will be introduced in Chapter 3. Here, we will review the basic principle of a spatial discretization of Maxwell's equations on the basis of the finite integration technique (FIT) and the finite element method (FEM) applied to the first- and second-order formulation of Maxwell's equations.

An extensive discussion on the application of structure-preserving moment matching methods to first- and second-order model problems of Maxwell's equations is given in Chapter 4. Thereby, we will introduce the AORA-RK method, which adaptively selects a set of expansion points based on an upper bound of the output moment error. Furthermore, some results about the explicit incorporation of the projection onto the subspace of discrete, divergence-free functions during the application of model order reduction with moment matching methods will be

summarised.

In Chapter 5, we will provide an extension of the adaptive-order rational Arnoldi method, which can be used to raise the efficiency of the offline-stage in model order reduction. Moreover, we will review the common framework of (recycling) iterative Krylov subspace methods for solving a sequence of shifted linear systems and we will extend the recycling BiCG method to a recycling SQMR method. This can be used when dealing with the (complex) symmetric, but indefinite structure of the second-order Maxwell's equations. It is important to note that solving a discrete first-order Maxwell's equations by means of an algebraic two-level method is essentially based on solving the linear system corresponding to the Schur complement. Since the latter one represents a second-order Maxwell's equation, the recycling SQMR method may be also employed for first-order Maxwell's equations by means of the ATLM.

An overview about the application of moment matching methods to a selection of model problems of Maxwell's equations in semiconductor structures will be given in Chapter 6. Here, we will discuss the computational improvement during the offline-stage of model order reduction by the modified rational Arnoldi-type methods. Numerical experiments show the effectiveness of the recycling SQMR method when being used to solve a sequence of shifted linear systems of first- and second-order Maxwell's equations.

Finally, we will summarise the results on moment matching methods in model order reduction of Maxwell's equations in Chapter 7. An outlook will point out possible future directions of the development of moment matching methods in model order reduction and will conclude the thesis.

CHAPTER 2

Framework for model order reduction

Numerical simulations of model problems arising from electric circuits, mechanical systems, or computational flow dynamics often require solving high-dimensional (non-) linear dynamical systems, see [5]. For example, the increasing working frequency range in computational electromagnetism requires a small step size $h > 0$ for the discretization of the computational domain in order to maintain a reliable simulation of the model problem under consideration, e.g. $h \simeq \lambda_{\max}/10$ with the maximum wavelength $\lambda_{\max}$. Since a numerical simulation of the resulting (non-) linear dynamical system depends on the solution to high-dimensional linear systems, the application of efficient solvers for linear systems is often limited in view of the increasing memory requirement and computational effort.

Due to the significantly smaller dimension of the reduced order model in comparison with the full-order model problem, the application of model order reduction represents an appealing approach for an efficient numerical simulation of a high-dimensional linear dynamical system. The model order reduction methods under consideration should at least ensure the following properties in order to provide a reliable application for the numerical simulation based on the reduced order model.

- A-priori error estimation for the accuracy of the reduced order model.
- Structure preservation of the linear dynamical system in the reduced order model.
- Stability and passivity preservation in the reduced order model.

Typically, model problems based on Maxwell's equations lead to linear dynamical systems. The most popular methods for model order reduction of linear dynamical systems are moment matching methods on the basis of Krylov subspaces on the one hand and balanced truncation

on the other hand. In particular, the most important difference between moment matching methods and balanced truncation follows from the fact that an a-priori error estimation for the accuracy of the reduced order model is only available for balanced truncation. Nevertheless, numerical experiments in Chapter 6 will show that moment matching methods still allow for the computation of an appropriate reduced order model on the basis of a sensible greedy-type expansion point selection, see Subsection 4.2.5.

The outline of the chapter is as follows: At first glance, we will recapitulate a common framework of first- and second-order linear dynamical systems with the important interpretation of a linear dynamical system by means of the transfer function. Moreover, some essential properties of descriptor systems, e.g. stability and passivity on the one hand and controllability and observability on the other hand, are presented. In this context, various fundamental norms in the frequency domain lead to a different interpretation of the error estimation in model order reduction. Finally, we will give a short overview on the most popular methods in model order reduction, i.e. balanced truncation, moment matching methods and proper orthogonal decomposition, see [4].

2.1 Linear dynamical systems

Linear dynamical systems arise in several different applications, e.g. machine tool simulations or electric circuits [39, 88], and represent the connection between different inputs and outputs in view of the state variable of the dynamical system. The application of different kinds of model order reduction techniques to linear dynamical systems has been extensively discussed in recent years, see [4, 5, 8, 82]. Generally speaking, the computation of a reduced order model consists of the identification of the most important parts of the state variable of the high-dimensional linear dynamical system. In the following, we will give an overview on the important components of the state variable for the most popular methods in model order reduction, cf. Section 2.3.

The integral task of model order reduction is to preserve the input-output behaviour of the linear dynamical system in the reduced order model. In this context, a reliable error estimation represents an essential component for any application of model order reduction in order to ensure the achievement of a given accuracy. This paragraph will review a common framework for first- and second-order linear dynamical systems, see [4,82]. Here, the linear dynamical systems being discussed do not include any variation of given material or geometric parameters, see [29, 126].

2.1.1 First-order linear dynamical systems

Let $\mathcal{E}, \mathcal{A} \in \mathbb{R}^{n\times n}$, $\mathcal{B} \in \mathbb{R}^{n\times m}$ and $\mathcal{C} \in \mathbb{R}^{p\times n}$. A *descriptor system* represents a linear dynamical system of the form

$$\begin{aligned} \mathcal{E}\dot{x}(t) &= \mathcal{A}x(t) + \mathcal{B}u(t), \\ y(t) &= \mathcal{C}x(t), \end{aligned} \tag{2.1.1}$$

where $x(t) \in \mathbb{R}^n$, $u(t) \in \mathbb{R}^m$ and $y(t) \in \mathbb{R}^p$ refer to as the *state variable*, the *input variable* and the *output variable*, see [28, 82, 113, 116]. Moreover, $t \in [0, t_*]$, $t_* > 0$, denotes an arbitrary point of time of the time-interval of the linear dynamical system. The state variable features the given initial value $x(0) = x_0 \in \mathbb{R}^n$. For a singular matrix $\mathcal{E}$, the descriptor system is termed a *differential-algebraic equation*. In the context of computational electromagnetism on the basis of Maxwell's equations, the matrix $\mathcal{E}$ is always regular.

The special case $\mathcal{E} = I \in \mathbb{R}^{n\times n}$, where I denotes the $n \times n$ identity matrix, of the descriptor system (2.1.1) leads to the *standard state space system*

$$\begin{aligned} \dot{x}(t) &= \mathcal{A}x(t) + \mathcal{B}u(t), \\ y(t) &= \mathcal{C}x(t), \end{aligned} \tag{2.1.2}$$

Consider the case where $\mathcal{E}$ is symmetric positive definite. The transformation of a descriptor system into a standard state space system preserves the symmetric structure of the matrix pencil $\lambda\mathcal{E} - \mathcal{A}$, $\lambda \in \mathbb{C}$, using the Cholesky factorization $\mathcal{E} = LL^{\mathrm{T}}$ [53], i.e.

$$\begin{aligned} \dot{\bar{x}}(t) &= \bar{\mathcal{A}}\bar{x}(t) + \bar{\mathcal{B}}u(t), \\ y(t) &= \bar{\mathcal{C}}\bar{x}(t), \end{aligned}$$

where $\bar{\mathcal{A}} \equiv L^{-1}\mathcal{A}L^{-\mathrm{T}}$, $\bar{\mathcal{B}} \equiv L^{-1}\mathcal{B}$, and $\bar{\mathcal{C}} \equiv \mathcal{C}L^{-\mathrm{T}}$ with the transformation of the state variable $\bar{x}(t) \equiv L^{\mathrm{T}}x(t)$. Even if the computational effort for a Cholesky factorization of a (block-)diagonal matrix is comparably cheap, model order reduction techniques are preferably applied to the descriptor system (2.1.1).

The main idea of model order reduction consists of computing a *reduced order model*

$$\begin{aligned} \tilde{\mathcal{E}}\dot{\tilde{x}}(t) &= \tilde{\mathcal{A}}\tilde{x}(t) + \tilde{\mathcal{B}}u(t), \\ \tilde{y}(t) &= \tilde{\mathcal{C}}\tilde{x}(t), \end{aligned} \tag{2.1.3}$$

where $\tilde{\mathcal{E}}, \tilde{\mathcal{A}} \in \mathbb{R}^{n_d\times n_d}$, $\tilde{\mathcal{B}} \in \mathbb{R}^{n_d\times m}$ and $\tilde{\mathcal{C}} \in \mathbb{R}^{p\times n_d}$ with $n_d \ll n$. We refer to $\tilde{x}(t) \in \mathbb{R}^{n_d}$ and $u(t) \in \mathbb{R}^m$ as the state variable and input variable of the reduced order model, respectively. Moreover, the output variable of the reduced order model is denoted by $\tilde{y}(t) \in \mathbb{R}^p$ in order to emphasise that the input-output behaviour of the reduced order linear dynamical system follows from the matrix quadruplet $\left(\tilde{\mathcal{E}}, \tilde{\mathcal{A}}, \tilde{\mathcal{B}}, \tilde{\mathcal{C}}\right)$, see [82].

Assuming that the computation of the reduced order model consists of the application of the *Galerkin projection* $\Pi = VW^{\mathrm{T}}$ to the linear dynamical system (2.1.1). Then, the matrices of the reduced order model are determined by applying transformation matrices $V \in \mathbb{R}^{n \times n_d}$ and $W \in \mathbb{R}^{n \times n_d}$ of full-rank satisfying $W^{\mathrm{T}}V = I$ such that

$$\tilde{\mathcal{E}} = W^{\mathrm{T}}\mathcal{E}V, \quad \tilde{\mathcal{A}} = W^{\mathrm{T}}\mathcal{A}V, \quad \tilde{\mathcal{B}} = W^{\mathrm{T}}\mathcal{B} \quad \text{and} \quad \tilde{\mathcal{C}} = \mathcal{C}V. \tag{2.1.4}$$

Reliable simulations of a linear dynamical system on the basis of the reduced order model (2.1.3) require the preservation of the input-output behaviour of the full-order model problem. In other words, model order reduction must ensure the relation

$$\| \, y(t) - \tilde{y}(t) \, \| \; \rightarrow \; \min$$

with respect to an adequate norm, e.g. the $\mathbb{H}_2$- or $\mathbb{H}_\infty$-norm, see [4]. The measurement of the accuracy of the reduced order model for moment matching methods or balanced truncation will be primarily carried out in view of the transfer function of the full-order and reduced order linear dynamical system.

Definition 2.1.1 (Transfer function)**.** *The* transfer function *of a linear dynamical system (2.1.1) is given by*

$$\mathcal{H}(s) = \mathcal{C}\left(s\mathcal{E} - \mathcal{A}\right)^{-1}\mathcal{B}, \quad s \in \mathbb{C}. \tag{2.1.5}$$

Typically, the transfer function $\mathcal{H}(s)$ can be obtained from the Laplace transformation applied to the descriptor system (2.1.1), see [82].

For any given matrices $(\mathcal{E}, \mathcal{A}, \mathcal{B}, \mathcal{C})$ of adequate dimensions satisfying (2.1.5), we denote the stated quadruplet a *realization* of the linear dynamical system (2.1.1). If the dimension of the quadruplet is as small as possible, the realization $(\mathcal{E}, \mathcal{A}, \mathcal{B}, \mathcal{C})$ of the transfer function refers to a *minimal realization*. Minimal realizations play a major role in the computation of a reduced order model using balanced truncation, see [116].

In accordance with (2.1.5), we denote the *transfer function* of the reduced order model (2.1.3) by

$$\tilde{\mathcal{H}}(s) = \tilde{\mathcal{C}}(s\tilde{\mathcal{E}} - \tilde{\mathcal{A}})^{-1}\tilde{\mathcal{B}}.$$

The reliability of the model order reduction technique can be expressed by means of an *a-priori error estimation* of the form

$$\| \, \mathcal{H}(s) - \tilde{\mathcal{H}}(s) \, \| \leq \mathrm{tol} \tag{2.1.6}$$

with respect to an adequate norm. Since an a-priori error estimation (2.1.6) is not yet available for moment matching methods, heuristic error estimations during the computation of a

sequence of reduced order models have been employed in order to obtain a measure of the accuracy of the reduced order model, see [54]. The development of an a-priori error estimation still poses an open research problem in the field of moment matching methods in model order reduction. In contrast to this, balanced truncation offers an a-priori error estimation allowing for a direct connection to the dimension of the reduced order model, see [82].

Fundamental solution to linear dynamical systems

Throughout the section, the matrix pencil $\lambda\mathcal{E}-\mathcal{A}$ is assumed to be regular for at least one $\lambda \in \mathbb{C}$, see [82]. The fundamental solution to a linear dynamical system is based on the canonical *Weierstrass form* of a matrix pencil given by

$$\mathcal{E} = S \begin{pmatrix} I_{n_f} & 0 \\ 0 & N \end{pmatrix} T \quad \text{and} \quad \mathcal{A} = S \begin{pmatrix} J & 0 \\ 0 & I_{n_\infty} \end{pmatrix} T, \tag{2.1.7}$$

where S and T are non-singular transformation matrices, J and N denote matrices in Jordan canonical form, and I_{n_f} and I_{n_∞} refer to as identity matrices of dimension $n_f \times n_f$ and $n_\infty \times n_\infty$ [82, 115]. The matrix N is nilpotent of order $\nu \geq 0$, i.e. $N^\nu = 0$, which defines the *index* of the matrix pencil and descriptor system, respectively.

Since n_f and n_∞ denote the dimensions of the subspaces corresponding to the finite and infinite eigenvalues of $\lambda\mathcal{E} - \mathcal{A}$, the Weierstrass form (2.1.7) represents a spectral decomposition of the matrix pencil. More precisely, the left and right *spectral projections*[1]

$$P_l = S \begin{pmatrix} I_{n_f} & 0 \\ 0 & 0 \end{pmatrix} S^{-1} \quad \text{and} \quad P_r = T \begin{pmatrix} I_{n_f} & 0 \\ 0 & 0 \end{pmatrix} T^{-1}$$

corresponding to the matrix pencil $\lambda\mathcal{E} - \mathcal{A}$ refer to the projections onto the finite eigenvalues, see [82]. Similarly, the projections $I - P_l$ and $I - P_r$ denote the projections onto the infinite eigenvalues.

Let $z_1(t)$ and $z_2(t)$ be the exact solutions to the slow and fast subsystem of the descriptor system. Then, the transformation of the state variable $Tx(t) \equiv [z_1^{\mathrm{T}}(t), z_2^{\mathrm{T}}(t)]^{\mathrm{T}}$ leads to the fundamental solution of the linear dynamical system (2.1.1), see [82].

Lemma 2.1.2. *Let the matrix pencil $\lambda\mathcal{E} - \mathcal{A}$ be regular, let the input $u(t)$ be ν-times continuously differentiable, and let the initial value $x(0) = x_0$ be consistent. Then, the descriptor system (2.1.1) has a unique, continuously differentiable solution*

$$x(t) = \mathcal{F}(t)\mathcal{E}x_0 + \int_0^t \mathcal{F}(t-\tau)\mathcal{B}u(\tau)\, d\tau + \sum_{k=0}^{\nu-1} F_{-k-1}\mathcal{B}\frac{\partial^k u}{\partial t^k},$$

[1] Let V be a vector space. A projection $P : V \to V$ is an idempotent linear transformation, i.e. $P^2 = P$.

where

$$\mathcal{F}(t) = T^{-1} \begin{bmatrix} e^{tJ} & 0 \\ 0 & 0 \end{bmatrix} S^{-1} \tag{2.1.8}$$

denotes the fundamental solution *of the descriptor system. The coefficients* F_k $(k \in \mathbb{Z})$ *are obtained via the Laurent series expansion of* $(\lambda\mathcal{E} - \mathcal{A})^{-1}$.

The result of Lemma 2.1.2 indicates that the fundamental solution of a descriptor system mainly depends on the Jordan matrix J corresponding to the finite eigenvalues of the matrix pencil $\lambda\mathcal{E} - \mathcal{A}$. This observation features a key ingredient of the framework of balanced truncation based model order reduction.

Since the explicit computation of the Weierstrass form (2.1.7) is highly ill-conditioned, i.e. small perturbations in the realization of $(\mathcal{E}, \mathcal{A}, \mathcal{B}, \mathcal{C})$ will have a large impact on the canonical form, it will only be employed for theoretical considerations but not for actual computations, see [82, 116].

2.1.2 Second-order linear dynamical systems

Let $M, D, K \in \mathbb{R}^{n\times n}$, $\mathcal{B}_* \in \mathbb{R}^{n\times m}$ and $\mathcal{C}_* \in \mathbb{R}^{p\times n}$. A *second-order linear dynamical system* is of the form

$$\begin{aligned} M\ddot{x}(t) \;+\; D\dot{x}(t) \;+\; Kx(t) &= \mathcal{B}_* u(t), \\ y(t) &= \mathcal{C}_* x(t), \end{aligned} \tag{2.1.9}$$

where $x(t) \in \mathbb{R}^n$, $u(t) \in \mathbb{R}^m$ and $y(t) \in \mathbb{R}^p$ denote the *state variable*, the *input variable* and the *output variable*, respectively. Similar to first-order linear dynamical systems, it holds $t \in [0, t_*]$, $t_* > 0$, for a given time-interval. The (second-order) *transfer function* of the linear dynamical system (2.1.9) is given by

$$\mathcal{H}(s) = \mathcal{C}_* \left(s^2 M + sD + K\right)^{-1} \mathcal{B}_* \quad \text{with} \quad s \in \mathbb{C}. \tag{2.1.10}$$

Similar to first-order linear dynamical systems, the reduced order model arises out of the transformation matrices $V \in \mathbb{R}^{n\times n_d}$ and $W \in \mathbb{R}^{n\times n_d}$ of full-rank with $W^{\mathrm{T}}V = I$, i.e.

$$\begin{aligned} \tilde{M}\ddot{\tilde{x}}(t) \;+\; \tilde{D}\dot{\tilde{x}}(t) \;+\; \tilde{K}\tilde{x}(t) &= \tilde{\mathcal{B}}_* u(t), \\ \tilde{y}(t) &= \tilde{\mathcal{C}}_* \tilde{x}(t), \end{aligned}$$

where $\tilde{M}, \tilde{D}, \tilde{K} \in \mathbb{R}^{n_d\times n_d}$, $\tilde{\mathcal{B}}_* \in \mathbb{R}^{n_d\times m}$ and $\tilde{\mathcal{C}}_* \in \mathbb{R}^{p\times n_d}$ with $n_d \ll n$. More precisely, each matrix of the reduced order model follows from

$$\tilde{M} = W^{\mathrm{T}} M V, \quad \tilde{D} = W^{\mathrm{T}} D V, \quad \tilde{K} = W^{\mathrm{T}} K V, \quad \tilde{\mathcal{B}}_* = W^{\mathrm{T}} \mathcal{B}_* \quad \text{and} \quad \tilde{\mathcal{C}}_* = \mathcal{C}_* V$$

such that the computation of the reduced order model is obtained via the application of the *Galerkin projection* $\Pi = VW^{\mathrm{T}}$ to the second-order linear dynamical system (2.1.9). Finally, we refer to

$$\tilde{\mathcal{H}}(s) = \tilde{\mathcal{C}}_*(s^2\tilde{M} + s\tilde{D} + \tilde{K})^{-1}\tilde{\mathcal{B}}_* \quad \text{with} \quad s \in \mathbb{C}$$

as the corresponding (second-order) *transfer function* of the reduced order model.

The development of different kinds of model order reduction methods has been initially carried out for first-order linear dynamical systems. A common approach for second-order linear dynamical systems is the *linearization* of the descriptor system (2.1.9). Defining the state variable $z(t) = (x^{\mathrm{T}}(t), \dot{x}^{\mathrm{T}}(t))^{\mathrm{T}}$, a second-order dynamical system may be transformed to a first-order descriptor system in two different ways, see [113]. On the one hand, a linearization offers the form

$$\mathcal{E} = \begin{pmatrix} I & 0 \\ 0 & M \end{pmatrix}, \quad \mathcal{A} = \begin{pmatrix} 0 & I \\ -K & -D \end{pmatrix}, \quad \mathcal{B} = \begin{pmatrix} 0 \\ \mathcal{B}_* \end{pmatrix}, \quad \mathcal{C} = \begin{pmatrix} 0 & \mathcal{C}_* \end{pmatrix}, \tag{2.1.11}$$

while on the other hand

$$\mathcal{E} = \begin{pmatrix} D & M \\ I & 0 \end{pmatrix}, \quad \mathcal{A} = \begin{pmatrix} -K & 0 \\ 0 & I \end{pmatrix}, \quad \mathcal{B} = \begin{pmatrix} \mathcal{B}_* \\ 0 \end{pmatrix}, \quad \mathcal{C} = \begin{pmatrix} \mathcal{C}_* & 0 \end{pmatrix}. \tag{2.1.12}$$

In view of the special block-structure of each linearization (2.1.11) and (2.1.12), existing approaches for moment matching methods and balanced truncation discuss the computation of a structure-preserving reduced order model, see [8, 97]. Since a linearization doubles the dimension of the corresponding state variable $z(t) \in \mathbb{R}^{2n}$, the computation of a reduced order model is highly recommended by means of the second-order linear dynamical system (2.1.9). Both linearizations will be only employed for theoretical considerations in the following.

2.2 Characteristics of linear dynamical systems

The application of model order reduction to linear dynamical systems given in the first- and second-order formulation requires the preservation of important properties like stability and passivity. In this paragraph, we will also review a characterization of the linear dynamical system in view of controllability and observability allowing for the identification of state components which are difficult to reach and to observe. Finally, we will give an overview on different norms for the error estimation (2.1.6) in model order reduction.

2.2.1 Stability and passivity

A descriptor system (2.1.1) is called *stable* if all solutions $x(t) \in \mathbb{R}^n$ to the initial value problem

$$\mathcal{E}\dot{x}(t) = \mathcal{A}x(t) \tag{2.2.1}$$

are bounded for every feasible initial value condition $x(0) = x_0$. Furthermore, a descriptor system is called *asymptotically stable* if $\lim_{t\to\infty} x(t) = 0$ holds for all solutions $x(t)$ to the initial value problem (2.2.1) with an appropriate initial value $x_0 \in \mathbb{R}^n$, see [82]. From the literature [28, 82, 116], the following necessary and sufficient conditions for a descriptor system (2.1.1) being asymptotically stable are known.

Theorem 2.2.1 ([82, Theorem 3.2.6])**.** *Let a descriptor system (2.1.1) with a regular matrix pencil $\lambda\mathcal{E} - \mathcal{A}$ be given. Then, the following statements are equivalent:*

- *The descriptor system (2.1.1) is asymptotically stable.*
- *All finite eigenvalues of the matrix pencil $\lambda\mathcal{E} - \mathcal{A}$ lie in the open left half of the complex plane.*
- *The projected generalized continuous-time Lyapunov equation*

$$\mathcal{E}^{\mathrm{T}} X \mathcal{A} + \mathcal{A}^{\mathrm{T}} X \mathcal{E} = -P_r^{\mathrm{T}} Q P_r, \quad X = P_l^{\mathrm{T}} X P_l$$

  has a unique hermitian, positive semidefinite solution X for every hermitian, positive definite matrix Q.

Since the linearization of a second-order model problem (2.1.9) results in a first-order descriptor system of the form (2.1.11) or (2.1.12), the previous remarks about stability remain valid for the second-order eigenvalue problem

$$(\lambda^2 M + \lambda D + K)x = 0, \quad \lambda \in \mathbb{C}, \quad \text{for all} \quad x \in \mathbb{R}^n \backslash \{0\}.$$

In general, the application of model order reduction does not guarantee that the reduced order model remains stable. Therefore, the additional application of Krylov subspace methods, e.g. the Arnoldi method or the Lanczos method, becomes indispensable for the extraction of the unstable part, see [107]. An extensive analysis on the stability of descriptor systems has been given in [116].

Apart from the conservation of the stability in the reduced order model, another important task is the preservation of the passivity of the linear dynamical system, see [79, 113]. Let $\mathbb{L}_2([0,t],\mathbb{R}^m)$ denote the space of all square integrable and Lebesgue measurable functions

$u : [0, t] \to \mathbb{R}^m$, see [4]. For the same number of inputs and outputs of the linear dynamical system (2.1.1), a descriptor system is called *passive* if

$$\int_0^{t_*} u(t)^{\mathrm{T}} y(t)\ dt \geq 0$$

holds for all $t_* \in \mathbb{R}_+$ and all $u(t) \in \mathbb{L}_2([0, t_*], \mathbb{R}^m)$ consistent with $x(0) = 0$, see [99]. The definition states that a dynamical system can not produce more energy than it gains from the input. A characterization of passive systems can be obtained via the positive realness of the transfer function.

Definition 2.2.2 (Positive realness)**.** *A square transfer function $\mathcal{H}(s) \in \mathbb{C}^{p\times m}$ with $p = m$ is called* positive real *if*

- *$\mathcal{H}(s)$ is analytic in $\mathbb{C}_+$,*
- *$\mathcal{H}(\bar{s}) = \overline{\mathcal{H}(s)}$ for all $s \in \mathbb{C}$,*
- *$\mathcal{H}(s) + \mathcal{H}(s)^* \geq 0$ for all $s \in \mathbb{C}_+$.*

The previous definition leads to an important equivalence for the passivity of a descriptor system: A descriptor system (2.1.1) is passive if and only if the corresponding transfer function $\mathcal{H}(s)$ is positive real, see [3].

2.2.2 Controllability and observability

For the computation of a reduced order model, the principal idea of balanced truncation is based on the analysis of the state components in view of controllability and observability, see [28, 82, 116]. In comparison to standard state space systems, a common terminology for controllability and observability does not exist for descriptor systems [116].

A standard state space system (2.1.2) is called *controllable* if any given initial state $x(0) = x_0$ and an arbitrary point of time $t_c \in [0, t_*]$ with $x(t_c) = x_c$ ensure the existence of a piecewise continuous input $u(t)$ such that the solution to the linear dynamical system implies $x(t_c) = x_c$, see [132].

For descriptor systems, different kinds of characterizations for controllability are given in [116]. In general, a descriptor system (2.1.1) is called *completely controllable* if

$$\operatorname{rank}\left[\ \alpha\mathcal{E} - \beta\mathcal{A},\ \mathcal{B}\ \right] = n \quad \text{for all} \quad (\alpha, \beta) \in \mathbb{C}^2 \backslash \{(0, 0)\}.$$

There exist several different necessary and sufficient conditions for a descriptor systems being completely controllable. Here, we will only summarize a choice selection of [116].

Theorem 2.2.3 ([116, Theorem 3.24]). *The following statements are equivalent.*

- *The triplet* $(\mathcal{E}, \mathcal{A}, \mathcal{B})$ *is completely controllable.*
- *The relation* $\operatorname{rank}[\ \lambda\mathcal{E} - \mathcal{A},\ \mathcal{B}\ ] = n$ *holds for all* $\lambda \in \mathbb{C}$ *and* $\operatorname{rank}[\ \mathcal{E},\ \mathcal{B}\ ] = n$.
- $\operatorname{rank}[\ \mathcal{B}_1,\ J\mathcal{B}_1,\ \ldots,\ J^{n_f-1}\mathcal{B}_1\ ] = n_f$ *and* $\operatorname{rank}[\ \mathcal{B}_2,\ N\mathcal{B}_2,\ \ldots,\ N^{\nu-1}\mathcal{B}_2\ ] = n_\infty$, *where* $\mathcal{B} = [\mathcal{B}_1^{\mathrm{T}}, \mathcal{B}_2^{\mathrm{T}}]^{\mathrm{T}}$, $\mathcal{B}_1 \in \mathbb{R}^{n_f}$ *and* $\mathcal{B}_2 \in \mathbb{R}^{n_\infty}$, *are transformed according to the canonical Weierstrass form (2.1.7).*

Furthermore, the standard state space system (2.1.2) is called *observable* if for any point of time $t_o \in [0, t_*]$ the initial state $x(0) = x_0$ and the input variable $u(t)$ allows for the computation of the state variable $x(t_o) = x_{t_o}$ directly from the output variable $y(t)$, see [132].

Since observability refers to the dual concept of controllability, a descriptor system is termed *completely observable*, if

$$\operatorname{rank}\left[\ \alpha\mathcal{E}^{\mathrm{T}} - \beta\mathcal{A}^{\mathrm{T}},\ \mathcal{C}^{\mathrm{T}}\ \right] = n \quad \text{for all} \quad (\alpha, \beta) \in \mathbb{C}^2 \backslash \{(0,0)\},$$

see [116]. Again, we review different equivalent conditions for a descriptor system being completely observable, see [116].

Theorem 2.2.4 ([116, Theorem 3.27]). *The following statements are equivalent.*

- *The triplet* $(\mathcal{E}, \mathcal{A}, \mathcal{C})$ *is completely observable.*
- *The relation* $\operatorname{rank}[\ \lambda\mathcal{E}^* - \mathcal{A}^*,\ \mathcal{C}^*\ ] = n$ *holds for all* $\lambda \in \mathbb{C}$ *and* $\operatorname{rank}[\ \mathcal{E}^*,\ \mathcal{C}^*\ ] = n$.
- $\operatorname{rank}[\ \mathcal{C}_1^*,\ J^*\mathcal{C}_1^*,\ \ldots,\ (J^{n_f-1})^*\mathcal{C}_1^*\ ] = n_f$ *and* $\operatorname{rank}[\ \mathcal{C}_2^*,\ N^*\mathcal{C}_2^*,\ \ldots,\ (N^{\nu-1})^*\mathcal{C}_2^*\ ] = n_\infty$, *where* $\mathcal{C} = [\mathcal{C}_1, \mathcal{C}_2]$, $\mathcal{C}_1 \in \mathbb{R}^{n_f}$ *and* $\mathcal{C}_2 \in \mathbb{R}^{n_\infty}$, *are transformed according to the canonical Weierstrass form (2.1.7).*

The controllability and observability of dynamical systems may be also characterized with the help of the proper Gramians, see [82, 116]. For example, the proper *controllability* and *observability Gramians* $\mathcal{P}$ and $\mathcal{Q}$ corresponding to first-order descriptor systems (2.1.1) are defined by

$$\mathcal{P} = \int_0^\infty \mathcal{F}(t)\mathcal{B}\mathcal{B}^{\mathrm{T}}\mathcal{F}(t)^{\mathrm{T}}\ dt \qquad \text{and} \qquad \mathcal{Q} = \int_0^\infty \mathcal{F}(t)^{\mathrm{T}}\mathcal{C}^{\mathrm{T}}\mathcal{C}\mathcal{F}(t)\ dt,$$

where $\mathcal{F}(t)$ refers to as the fundamental solution (2.1.8). The controllability and observability Gramians may be obtained via the solutions to the *generalized Lyapunov equations*

$$\mathcal{E}\mathcal{P}\mathcal{A}^{\mathrm{T}} + \mathcal{A}\mathcal{P}\mathcal{E}^{\mathrm{T}} = -P_l\mathcal{B}\mathcal{B}^{\mathrm{T}}P_l^{\mathrm{T}}, \qquad \mathcal{P} = P_r\mathcal{P}P_r^{\mathrm{T}}, \tag{2.2.2}$$

$$\mathcal{E}^{\mathrm{T}}\mathcal{Q}\mathcal{A} + \mathcal{A}^{\mathrm{T}}\mathcal{Q}\mathcal{E} = -P_r^{\mathrm{T}}\mathcal{C}^{\mathrm{T}}\mathcal{C}P_r, \qquad \mathcal{Q} = P_l^{\mathrm{T}}\mathcal{Q}P_l. \tag{2.2.3}$$

We leave out the introduction of the *improper Gramians*, since they become only important when the matrix $\mathcal{E} \in \mathbb{R}^{n\times n}$ is singular, see [116].

2.2.3 Norms in the frequency domain

The framework of model order reduction for linear dynamical systems requires the introduction of an adequate norm in order to determine an appropriate (a-priori) error estimation (2.1.6) for the accuracy of the reduced order model.

As a first step, we will briefly review the *Hardy spaces*, which are often associated as frequency domain spaces and have been previously studied in [4,7,33,68,132]. Unless otherwise stated, the dimensions of the state variable $x(t) \in \mathbb{R}^n$, input variable $u(t) \in \mathbb{R}^m$ and output variable $y(t) \in \mathbb{R}^p$ are in no way related to the symbols used in this section.

We denote the *p-norm* ($p \in \mathbb{N}$) of a vector $x = (x_1, \ldots, x_n) \in \mathbb{C}^n$ by

$$\| x \|_p = \begin{cases} (\sum_{i=1}^n | x_i |^p)^{1/p}, & 1 \leq p < \infty \\ \max_{i=1,\ldots,n} | x_i |, & p = \infty \end{cases}$$

and the p-norm of an arbitrary function $u : \mathcal{I} \to \mathbb{R}^n$, $\mathcal{I} = [a, b]$, by

$$\| u \|_p = \begin{cases} \left(\int\limits_{t \in \mathcal{I}} \| u(t) \|_p^p \, dt \right)^{1/p}, & 1 \leq p < \infty \\ \operatorname{ess\,sup}\limits_{t \in \mathcal{I}} \| u(t) \|_p, & p = \infty \end{cases} .$$

Hence, the space of Lebesgue measurable n-dimensional functions is referred to as

$$[\mathbb{L}_p(\mathcal{I})]^n = \{ u : \mathcal{I} \to \mathbb{R}^n, \ \| u \|_p < \infty \} .$$

The definition of the $[\mathbb{L}_p(\mathcal{I})]^n$ spaces may be also extended to the frequency domain. Let $F : \mathbb{C} \to \mathbb{C}^{r \times m}$ be a function, which does not have any singularities on the imaginary axis, but does not need to be analytic in the left or right half of the complex plane, see [4]. If $\sigma_{\max}(F(\imath\omega))$, $\omega \in \mathbb{R}$, denotes the largest singular value of the complex matrix-valued function $F : \mathbb{C} \to \mathbb{C}^{r \times m}$, the frequency domain $\mathcal{L}_p$-norm is given by

$$\| F \|_{\mathcal{L}_p} = \begin{cases} \left(\sup\limits_{\omega \in \mathbb{R}} \int\limits_{-\infty}^{\infty} \| F(\imath\omega) \|_p^p \, d\omega \right)^{1/p}, & 1 \leq p < \infty \\ \sup\limits_{\omega \in \mathbb{R}} \sigma_{\max}(F(\imath\omega)), & p = \infty \end{cases} .$$

Similar to the space of Lebesgue measurable n-dimensional functions $[\mathbb{L}_p(\mathcal{I})]^n$, the corresponding frequency domain space follows from

$$\mathcal{L}_p(\imath\mathbb{R}) = \left\{ F : \mathbb{C} \to \mathbb{C}^{r \times m} : \| F \|_{\mathcal{L}_p} < \infty \right\} .$$

The special case of a matrix-valued function $F : \mathbb{C} \to \mathbb{C}^{r \times m}$ which is analytic in the right half of the complex plane leads to the definition of the Hardy space

$$\mathbb{H}_p \equiv \mathbb{H}_p^{r \times m} = \left\{ F : \mathbb{C} \to \mathbb{C}^{r \times m} : \| F \|_{\mathbb{H}_p} < \infty \right\}$$

with the corresponding norm

$$\| F \|_{\mathbb{H}_p} = \begin{cases} \left(\sup\limits_{z \in \mathbb{C}_+} \int\limits_{-\infty}^{\infty} \| F(z) \|_p^p \, dy \right)^{1/p}, & 1 \leq p < \infty \\ \sup\limits_{z \in \mathbb{C}_+} \| F(z) \|_p, & p = \infty \end{cases}.$$

More precisely, $\mathbb{H}_\infty$ denotes the space of all proper rational transfer functions which are analytic in the right half of the complex plane, see [82]. The definition of the $\mathbb{H}_\infty$-norm of the transfer function $\mathcal{H}(s) \in \mathbb{H}_\infty$ is given by

$$\| \mathcal{H}(s) \|_{\mathbb{H}_\infty} = \sup_{u \neq 0} \frac{\| \mathcal{H}u \|_{[\mathbb{L}_2(\imath\mathbb{R})]^p}}{\| u \|_{[\mathbb{L}_2(\imath\mathbb{R})]^m}} = \sup_{\omega \in \mathbb{R}} \| \mathcal{H}(\imath\omega) \|_2. \tag{2.2.4}$$

For this reason, the application of *Parseval's identity* [7] to relation (2.2.4) leads to $\| \mathcal{H}(s) \|_{\mathbb{H}_\infty} = \sup_{u \neq 0} \| y \|_{[\mathbb{L}_2(\mathbb{R})]^p} / \| u \|_{[\mathbb{L}_2(\mathbb{R})]^m}$, see [82]. In other words, the $\mathbb{H}_\infty$-norm of a transfer function $\mathcal{H}(s)$ provides a relation between the output and the input energy of the descriptor system.

2.3 Survey on suitable methods for model order reduction

This section provides a survey on the most important methods in model order reduction of linear dynamical systems. For example, the Gramian-based balanced truncation method allows for a precise energy interpretation for the computation of a reduced order model. Moreover, moment matching methods are essentially based on appropriate Krylov subspaces for a given set of expansion points. Finally, the proper orthogonal decomposition employs a principal component analysis for a given set of snapshots in order to characterize the impact of each snapshot for the computation of the reduced order model. The literature comprises several references to different methods and applications in model order reduction, see [4, 5, 8, 60, 82] and the references therein.

2.3.1 Balanced truncation

Balanced truncation based model order reduction represents a fundamental technique for model order reduction incorporating the controllability and observability Gramians $\mathcal{P}$ and $\mathcal{Q}$ of a linear dynamical system, see [28, 43, 82, 116]. During a period of several decades, a major drawback of balanced truncation was often associated with the requirement of solving the high-dimensional generalized Lyapunov equations (2.2.2) and (2.2.3).

An important progress in solving large-scale Lyapunov equations has been achieved by the low-rank alternating direct implicit (LR-ADI) method [76, 94]. The main idea of the LR-ADI

method consists of the computation of a low-rank factor for each Gramian within a prescribed accuracy, i.e. $\mathcal{P} \approx L_p L_p^{\mathrm{T}}$ and $\mathcal{Q} \approx R_p R_p^{\mathrm{T}}$, see [17,76]. An important requirement for a reliable convergence behaviour of the LR-ADI method depends on the choice of suitable shift parameters. If the matrix $\mathcal{A}$ is symmetric, positive definite, the shift parameters are obtained via the ADI min-max problem, see [121, 122]. For solving the ADI min-max problem, the heuristic approach given by Penzl is often considered as a favourable approach, see [94].

In comparison with other methods, e.g. the generalized Schur-Hammarling method, the LR-ADI method has been proven its effectiveness for different applications, see [106,116]. Since each iteration step of the LR-ADI method requires solving a sequence of high-dimensional, shifted linear system of the form $(\tau_i \mathcal{E} - \mathcal{A})x = f$, $\tau_i \in \mathbb{C}$, $(i = 1, \ldots, k)$ the application of iterative Krylov subspace methods for solving large-scale Lyapunov equations has been studied recently, see [37,69,110].

However, the key ingredient of balanced truncation based model order reduction arises from the identification of state components which are difficult to reach and to observe at the same time. A *balanced realization* of the descriptor system (2.1.1), i.e.

$$\mathcal{P} = \mathcal{E}^{\mathrm{T}} \mathcal{Q} \mathcal{E} = \begin{bmatrix} \Sigma & 0 \\ 0 & 0 \end{bmatrix},$$

allows for the truncation of state components with a small impact on the behaviour of the linear dynamical system based on the singular value decomposition

$$L_p^{\mathrm{T}} \mathcal{E} R_p = U \begin{bmatrix} \Sigma_1 & 0 \\ 0 & \Sigma_2 \end{bmatrix} V^{\mathrm{T}}.$$

Here, U and V are orthonormal matrices consisting of the left- and right singular vectors as columns, while Σ_1 and Σ_2 contain the Hankel singular values of the descriptor system, see [82]. For the negligibly small Hankel singular values $\Sigma_2 = \mathrm{diag}(\sigma_{l_f+1}, \ldots, \sigma_{n_f})$, the a-priori error estimation for model order reduction with respect to the $\mathbb{H}_\infty$-norm is given by

$$\| \mathcal{H}(s) - \tilde{\mathcal{H}}(s) \|_{\mathbb{H}_\infty} \leq 2 \left(\sigma_{l_f+1} + \ldots + \sigma_{n_f} \right).$$

Whenever the dimension of the reduced order model remains large in contrast to the number of columns of the low-rank factor, an adaptation of the accuracy during the LR-ADI method becomes indispensable.

The previous framework for first-order descriptor systems has been also discussed for second-order linear dynamical systems, see [97]. An extension of balanced truncation allowing for the preservation of the passivity in the reduced order model has been given in [98]. Moreover, the application of balanced truncation based model order reduction to unstable dynamical systems was discussed recently in [20].

2.3.2 Moment matching methods

Apart from balanced truncation based methods, model order reduction techniques on the basis of Krylov subspace methods represent another appealing approach for the computation of reduced order models [4, 8, 45]. Since the main part of the thesis at hand deals with the application of moment matching methods to Maxwell's equations, a comprehensive overview will be given in Chapter 4.

Moment matching methods are based on the Taylor expansion of the transfer function at different expansion points, where the systems moments of each Taylor expansion refer to a suitable Krylov subspace. Generally speaking, the application of multiple expansion points requires the incorporation of rational Arnoldi- and Lanczos-type methods, see [101]. In this context, rational Krylov subspace methods have been developed in order to adaptively select the number of system moments on the basis of an output moment error [72,74].

For moment matching methods in model order reduction, an adaptive expansion point selection has been carried out in view of optimal $\mathbb{H}_2$ model order reduction [56] and a greedy-type expansion point selection on the basis of the multiple expansion of the transfer function [19, 40, 71, 113]. Apart from the appropriate expansion point selection, a major drawback of moment matching methods is still the lack of an a-priori error estimation for model order reduction. A heuristic error estimation on the basis of a sequence of reduced order models has been introduced by Grimme et al. in [54].

2.3.3 Proper orthogonal decomposition

The application of model order reduction based on the *proper orthogonal decomposition* (POD) has been mainly developed with the help of the principal component analysis (PCA), see [67]. For a given set of observations, the PCA employs an orthogonal transformation for the extraction of the linearly uncorrelated principal components, see [92]. In the sense of signal processing, the PCA is sometimes associated with the Karhunen-Loève decomposition.

In view of model order reduction with the POD, the set of observations refers to a collection of snapshots

$$x_i \equiv x_i(t_i) \in \mathbb{R}^n \quad \text{for all} \quad i = 1, \ldots, m,$$

where $t_i \in \mathbb{R}$ is an arbitrary point in the time interval of the descriptor system (2.1.1), see [4,63]. The so-called *snapshot matrix* collects the set of snapshots such that

$$X = [x_1, \ldots, x_m] \in \mathbb{R}^{n \times m}.$$

The basic principle of the proper orthogonal decomposition consists of choosing the most relevant snapshots by projecting the snapshot matrix $X \in \mathbb{R}^{n \times m}$ onto a d-dimensional sub-

space [120]. An adequate d-dimensional subspace $U_d = [u_1, \ldots, u_d]$ is obtained by means of the optimization problem

$$\max_{u_1,\ldots,u_d \in \mathbb{R}^n} \quad \sum_{i=1}^{d} \sum_{j=1}^{m} | \, x_j^{\mathrm{T}} u_i \, |^2 \quad \text{subject to} \quad U_d^{\mathrm{T}} U_d = I. \tag{2.3.1}$$

It has been shown in [120] that the solution to the optimization problem (2.3.1) can be reformulated as symmetric eigenvalue problem

$$X X^{\mathrm{T}} u_i = \lambda_i u_i, \quad \lambda_i \in \mathbb{R}, \tag{2.3.2}$$

using the largest d eigenvalues and their associated eigenvectors. This leads to the singular value decomposition of the snapshot matrix

$$X = \sum_{i=1}^{\min\{m,n\}} \sigma_i u_i v_i^{\mathrm{T}}, \tag{2.3.3}$$

where $u_i \in \mathbb{R}^n$ and $v_i \in \mathbb{R}^m$ denote the left and right singular vectors with the singular values $\sigma_1 \geq \ldots \geq \sigma_{\min\{m,n\}}$, see [53].

Let $U_d = [u_1, \ldots, u_d]$ denote the d-dimensional subspace corresponding to the singular values $\sigma_1 \geq \ldots \geq \sigma_d > 0$. The application of the full-rank reduction $V = U_d$ and $W = U_d$ leads to the reduced order model (2.1.4) with the well-known error estimation

$$\| \, X - X_d \, \|_F^2 = \sum_{i=d+1}^{\min\{m,n\}} \sigma_i^2$$

where X_d refers to the truncated singular value decomposition (2.3.3) with the singular values $\sigma_1 \geq \ldots \geq \sigma_d > 0$ and $\| \cdot \|_F$ denotes the Frobenius norm.

The POD has been primarily applied to non-linear dynamical systems, e.g. aerodynamic applications, see [60, 127]. In this context, previous results have indicated the usage of an averaged covariance matrix instead of employing the snapshot matrix $X \in \mathbb{R}^{n \times m}$, see [67].

A possible extension of the POD yields the important class of *reduced basis methods*, see [100]. Here, the snapshots corresponding to the subspace $U_d \in \mathbb{R}^{n \times d}$ are collected with a greedy-type sampling strategy in view of an adequate a posteriori error estimation. The advantage of the reduced basis methods is that the computation of the reduced order model is decomposed in offline-online stages. However, the evaluations of the posteriori error estimations are typically expensive, due to repeatedly solving high-dimensional eigenvalue problems. Therefore, the computational costs during the offline stage of the reduced basis methods may be quite expensive for a specific class of practical applications, e.g. the application of model order reduction within a toolbox on a standard desktop computer. An overview on the application of the reduced basis methods to parametric linear dynamical systems in semiconductor structures has been given recently in [58].

CHAPTER 3

Spatial discretization of Maxwell's equations

This chapter will briefly review the discretization of the Maxwell's equations with the finite integration technique (FIT) and the finite element method (FEM) leading to first- and second-order linear dynamical systems (2.1.1) and (2.1.9). In doing so, we define the state variable of a first-order linear dynamical system of Maxwell's equations by $x(t) = [\boldsymbol{E}(t)^{\mathrm{T}}, \boldsymbol{H}(t)^{\mathrm{T}}]^{\mathrm{T}}$, where $\boldsymbol{E}(t)$ and $\boldsymbol{H}(t)$ denote the electric and magnetic field strength, respectively. As we shall see later, the discretization of Faraday's and Ampère's law yields a linear dynamical system of the form

$$\begin{aligned} \begin{pmatrix} M_\epsilon & 0 \\ 0 & M_\mu \end{pmatrix} \dot{x}(t) &= \begin{pmatrix} -M_\sigma & C_H \\ -C_E & 0 \end{pmatrix} x(t) + \mathcal{B}u(t), \\ y(t) &= \mathcal{C}x(t), \end{aligned} \tag{3.0.1}$$

where C_E and C_H denote the *discrete curl operators* of the electric and magnetic field strength, respectively. Due to the large nullspace of the curl-operator, C_E and C_H are positive semidefinite. The symmetric, positive (semi-) definite mass matrices M_ϵ, M_μ and M_σ refer to the material parameters $\epsilon, \mu > 0$ and $\sigma \geq 0$, which are diagonal for the FIT, while they are block-tridiagonal for the FEM.

Gauss's law for electric and magnetic fields leads to the *discrete divergence operators* D_E and D_H corresponding to the divergence conditions $D_E\,(M_\epsilon \boldsymbol{E}) = 0$ and $D_H\,(M_\mu \boldsymbol{H}) = 0$. In addition, the discrete divergence operators lead to the well-known left and right nullspace properties, i.e.

$$D_E C_H = 0, \quad D_H C_E = 0, \quad C_H D_H^{\mathrm{T}} = 0 \quad \text{and} \quad C_E D_E^{\mathrm{T}} = 0. \tag{3.0.2}$$

The FIT and the FEM already implies $C_E = C_H^{\mathrm{T}}$ offering a J-symmetric property of the matrix pencil $\lambda\mathcal{E} - \mathcal{A}$ corresponding to the linear dynamical system (3.0.1), i.e. $(\lambda\mathcal{E} - \mathcal{A})^{\mathrm{T}} J =$

$J(\lambda\mathcal{E} - \mathcal{A})$ with a non-singular $J \in \mathbb{C}^{n\times n}$. In Section 5.3, we will introduce a structure-preserving recycling Krylov subspace solver – the recycling SQMR method – based on the J-symmetric property of the matrix pencil.

Model order reduction of Maxwell's equations will be primarily applied to the discrete formulation of Faraday's and Ampère's law. Typically, the appropriate application of the discrete divergence conditions is achieved by the explicit projection onto the subspace of discrete, divergence-free functions, see [19].

A discretization of the second-order formulation of Maxwell's equations obtained via the first-order Maxwell's equations eliminating either the electric or magnetic field strength leads to the second-order descriptor system. The choice of the field strength of interest usually depends on the analysis of the model problem, e.g. employing the electric field strength $\boldsymbol{E}(t)$ focus on the second-order linear dynamical system

$$\begin{aligned} M_\epsilon \ddot{\boldsymbol{E}}(t) \;+\; M_\sigma \dot{\boldsymbol{E}}(t) \;+\; K_\mu \boldsymbol{E}(t) &= \mathcal{B}_* u(t), \\ y(t) &= \mathcal{C}_* \boldsymbol{E}(t). \end{aligned} \tag{3.0.3}$$

where the symmetric positive semi-definite matrix K_μ refers to the discretization of the curl-curl operator involving the inverse magnetic permeability $1/\mu > 0$. By comparison with the first-order linear dynamical system (3.0.1), M_ϵ and M_σ refer to as the symmetric, positive (semi-) definite mass matrices corresponding to $\epsilon > 0$ and $\sigma \geq 0$.

Remember that the FIT leads to diagonal mass matrices M_ϵ, M_μ and M_σ, where each entry corresponds to an average value related to the material parameters ϵ, μ and σ in each grid point. For this reason, the FIT allows for a cheap construction of $K_\mu \equiv C_H M_\mu^{-1} C_E$ by means of the first-order linear dynamical system (3.0.1). Instead, the FEM employs a Galerkin approach with a suitable finite element space to the weak formulation of the first- or second-order Maxwell's equations in order to obtain the corresponding linear dynamical system. By comparison with the FIT, an explicit construction of K_μ by means of the first-order linear dynamical system does not exist because the mass matrices are block-tridiagonal.

We will leave out an explicit description of the construction of the control input matrix $\mathcal{B} \in \mathbb{R}^{n\times m}$ and the control output matrix $\mathcal{C} \in \mathbb{R}^{n\times p}$, respectively. For example, a proper incorporation of the control input and control output matrix on the basis of the FIT for model problems appearing in the context of semiconductor structures has been given in [88].

This chapter firstly recapitulates the physical interpretation of Maxwell's equations. For the FIT, Maxwell's grid equations allow for the formulation of Maxwell's equations on the discretization of the computational domain. The discretization error of the FIT follows from the approximation of the material parameters with respect to the underlying grid. In contrast, the FEM requires the introduction of an adequate functional space and a weak formulation of

the first- and second-order formulation of Maxwell's equations. Typically, an adequate ansatz space in computational electromagnetism is based on the Nédélec element, see [89].

3.1 Physical interpretation of Maxwell's equations

Electromagnetic fields are essentially governed by *Maxwell's equations*, which have been discovered by the Scottish mathematician and physicist James Clerk Maxwell in 1862. The Maxwell's equations establish a connection between the interaction of time-varying electric and magnetic fields. The presentation will primarily follow the introduction to classical electromagnetism by Zaglmayr [131].

The formulation of Maxwell's equations requires the introduction of the following space- and time-dependent vector fields:

- *Electric field strength*: $\boldsymbol{E} \equiv \boldsymbol{E}(x,t)\ [V/m]$,
- *Magnetic field strength*: $\boldsymbol{H} \equiv \boldsymbol{H}(x,t)\ [A/m]$,
- *Electric flux density*: $\boldsymbol{D} \equiv \boldsymbol{D}(x,t)\ [As/m^2]$,
- *Magnetic flux density*: $\boldsymbol{B} \equiv \boldsymbol{B}(x,t)\ [Vs/m^2]$,

where the units voltage (V), ampere (A), seconds (s) and meters (m) have been used, see [25]. Moreover, the unit siemens (S) is constituted by $S \equiv A/V$. Additionally, we make use of the *electric charge density* $\rho \equiv \rho(x,t)\ [As/m^3]$ and the *electric current density* $\boldsymbol{j} \equiv \boldsymbol{j}(x,t)\ [A/m^2]$. The current density is usually written as $\boldsymbol{j} = \boldsymbol{j}_C + \boldsymbol{j}_i$, where $\boldsymbol{j}_C$ and $\boldsymbol{j}_i$ denote the *conduction current density* and the *impressed current density*, respectively, see [131].

Let $V \subset \mathbb{R}^3$ and $A \subset V$ denote an arbitrary volume and a corresponding surface of the volume, where the boundary of the volume and the surface are given by ∂V and ∂A, respectively. For an arbitrary vector field $\boldsymbol{F} : \mathbb{R}^n \to \mathbb{R}^n$, we state the well-known *Gauss'* and *Stokes' integral laws*, i.e.

$$\int_V \operatorname{div} \boldsymbol{F}\ d\boldsymbol{x} = \int_{\partial V} \boldsymbol{F} \cdot \vec{\boldsymbol{n}}\ dA \quad \text{and} \quad \int_A \operatorname{curl} \boldsymbol{F} \cdot \vec{\boldsymbol{n}}\ dA = \int_{\partial A} \boldsymbol{F} \cdot \vec{\boldsymbol{\tau}}\ ds,$$

where $\vec{\boldsymbol{n}}$ and $\vec{\boldsymbol{\tau}}$ refer to as the outer unit normal vector of V and the unit tangential vector of A. In the following, we will briefly review the physical interpretation of the integral and differential formulation of *Faraday's* and *Ampère's law* on the one hand and *Gauss'* and *Stokes' law* on the other hand, see [131].

1. **Faraday's law** refers to the time-dependent change of the magnetic flux density $\boldsymbol{B}$ through a surface A such that

$$\int_{\partial A} \boldsymbol{E} \cdot \vec{\boldsymbol{\tau}}\ ds = -\int_A \frac{\partial \boldsymbol{B}}{\partial t} \cdot \vec{\boldsymbol{n}}\ dA. \tag{3.1.1}$$

Here, the application of Stokes' integral law leads to the differential form

$$\frac{\partial \boldsymbol{B}}{\partial t} = -\operatorname{curl} \boldsymbol{E}. \tag{3.1.2}$$

2. **Ampère's law** provides a measure of the magnetic field on the boundary of an arbitrary surface $\partial A \subset A$ caused by the changing electric flux density $\boldsymbol{D}$ through the surface, i.e.

$$\int_{\partial A} \boldsymbol{H} \cdot \vec{\boldsymbol{\tau}}\, ds = \int_A \frac{\partial \boldsymbol{D}}{\partial t} \cdot \vec{\boldsymbol{n}}\, dA - \int_A \boldsymbol{j} \cdot \vec{\boldsymbol{n}}\, dA. \tag{3.1.3}$$

Again, Stokes' theorem yields the differential form

$$\frac{\partial \boldsymbol{D}}{\partial t} = \operatorname{curl} \boldsymbol{H} - \boldsymbol{j}. \tag{3.1.4}$$

3. **Gauss's law for electric fields** indicates that the electric flux density $\boldsymbol{D}$ through a surface $A \subset V$ coincides with the electric charge density inside the volume, i.e.

$$\int_{\partial V} \boldsymbol{D} \cdot \vec{\boldsymbol{n}}\, dA = \int_V \rho\, d\boldsymbol{x}. \tag{3.1.5}$$

Here, Gauss' integral law allows for the differential form

$$\operatorname{div} \boldsymbol{D} = \rho. \tag{3.1.6}$$

4. **Gauss's law for magnetic fields** implies that the magnetic flux density $\boldsymbol{B}$ through the surface of a volume equals zero since magnetic field lines are solenoidal and closed, i.e.

$$\int_{\partial V} \boldsymbol{B} \cdot \vec{\boldsymbol{n}}\, dA = 0. \tag{3.1.7}$$

Again, Gauss' integral law leads to the differential form

$$\operatorname{div} \boldsymbol{B} = 0. \tag{3.1.8}$$

The connection between the electric and magnetic field strength $\boldsymbol{E}$ and $\boldsymbol{H}$ and the electric and magnetic flux density $\boldsymbol{D}$ and $\boldsymbol{B}$ arises out of the *constitutive laws*. Therefore, we introduce the following material parameters:

- *Electric permittivity* ϵ $[As/Vm]$,
- *Magnetic permeability* μ $[Vs/Am]$,
- *Electric conductivity* σ $[S/m]$.

The material parameters reduce to scalar values for isotropic media, while in case of linear materials, they are independent of the electromagnetic field, see [131]. More importantly, the material parameters ϵ, μ and σ lead to the formulation of the constitutive laws, i.e.

$$\boldsymbol{D} = \epsilon \boldsymbol{E}, \quad \boldsymbol{B} = \mu \boldsymbol{H} \quad \text{and} \quad \boldsymbol{j}_C = \sigma \boldsymbol{E}. \tag{3.1.9}$$

For first-order model problems of Maxwell's equations, we typically incorporate the electric and magnetic field strength $\boldsymbol{E}$ and $\boldsymbol{H}$. Hence, the differential forms of Faraday's and Ampère's law (3.1.2) and (3.1.4) lead to the first-order formulation of Maxwell's equations

$$\begin{array}{rcl} \frac{\partial(\epsilon \boldsymbol{E})}{\partial t} & = & -\sigma \boldsymbol{E} \quad + \quad \nabla \times \boldsymbol{H}, \\ \frac{\partial(\mu \boldsymbol{H})}{\partial t} & = & -\nabla \times \boldsymbol{E}, \end{array} \tag{3.1.10}$$

where the constitutive laws (3.1.9) have been employed. For simplicity, we have assumed that the impressed current density $\boldsymbol{j}_i$ equals zero, which yields the simplified divergence conditions from Gauss' law for electric and magnetic fields

$$\nabla \cdot (\epsilon \boldsymbol{E}) = 0 \quad \text{and} \quad \nabla \cdot (\mu \boldsymbol{H}) = 0.$$

The first-order Maxwell equations (3.1.10) immediately allow for a second-order formulation of Maxwell's equations on the basis of the electric field strength $\boldsymbol{E} \equiv \boldsymbol{E}(x,t)$ such that

$$\frac{\partial^2 (\epsilon \boldsymbol{E})}{\partial t^2} = -\frac{\partial (\sigma \boldsymbol{E})}{\partial t} - \nabla \times \left(\frac{1}{\mu} \nabla \times \boldsymbol{E} \right). \tag{3.1.11}$$

Additionally, the simplified divergence condition follows from $\operatorname{div}(\epsilon \boldsymbol{E}) = 0$.

As seen in the first-order formulation, a discretization of the second-order Maxwell's equations (3.1.11) offers the structure of a second-order descriptor system (3.0.3). Again, the incorporation of the discrete divergence condition follows from the application of the projection onto the subspace of discrete, divergence-free functions, see [19].

The definition of appropriate model problems of Maxwell's equations requires the incorporation of Dirichlet- and Neumann-type boundary conditions, see [131].

1. **Perfect electric conductors (*PEC*).** Assuming that the electric conductivity behaves similarly to $\sigma \to \infty$ for highly conducting materials. Then, Ohm's law $\boldsymbol{j}_C = \sigma \boldsymbol{E}$ already implies that $\boldsymbol{E} \to 0$ in order to ensure that the conduction current density $\boldsymbol{j}_C$ remains bounded. Hence, the Dirichlet-type boundary conditions are given by

$$\boldsymbol{E} \times \vec{\boldsymbol{n}} = 0 \quad \text{on} \quad \Gamma_{\text{PEC}}. \tag{3.1.12}$$

2. **Perfect magnetic conductors (*PMC*).** Employing the assumption $\mu \to \infty$ for a perfect magnetic conductor, a similar argument to the PEC boundary condition leads to the Neumann-type boundary condition for Maxwell's equations, i.e.

$$\boldsymbol{H} \times \vec{\boldsymbol{n}} = 0 \quad \text{on} \quad \Gamma_{\text{PMC}}. \tag{3.1.13}$$

3.2 The finite integration technique

The *finite integration technique* (FIT) represents an efficient technique for the discretization of the (time-harmonic) first- and second-order Maxwell's equations (3.1.10) and (3.1.11). It has been initially developed by Weiland in 1977, see [124]. This paragraph summarises the key ingredients of the FIT, see [16, 114, 125].

Assuming that the computational domain $\Omega = [x_1, x_1] \times [y_0, y_1] \times [z_0, z_1] \subset \mathbb{R}^3$ has been discretized using the grid

$$\mathcal{G} = \{(x_0 + ih_x, y_0 + jh_y, z_0 + kh_z) \in \Omega : \\ i = 0, \ldots, n_x - 1,\ j = 0, \ldots, n_y - 1,\ k = 0, \ldots, n_z - 1\},$$

where $h_x = (x_1 - x_0)/(n_x - 1), h_y = (y_1 - y_0)/(n_y - 1)$ and $h_z = (z_1 - z_0)/(n_z - 1)$. Following a lexicographical ordering of the grid points, the n-th grid point may be accessed by

$$n = 1 + (i - 1)m_x + (j - 1)m_y + (k - 1)m_z,$$

where $m_x = 1, m_y = n_x$ and $m_z = n_x n_y$, see [16]. Moreover, the corresponding dual grid $\tilde{\mathcal{G}}$ consists of the grid points $(\tilde{x}_0 + ih_x, \tilde{y}_0 + jh_y, \tilde{z}_0 + kh_z)$, where $\tilde{x}_0 = x_0 + h_x/2, \tilde{y}_0 = y_0 + h_y/2$ and $\tilde{z}_0 = z_0 + h_z/2$. An illustration of the grid doublet $\{\mathcal{G}, \tilde{\mathcal{G}}\}$ is given in Figure 3.1.

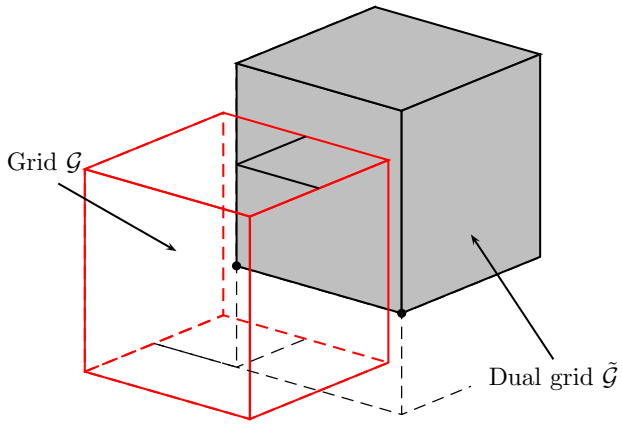

Figure 3.1: FIT: Staggered grid.

The principal idea of the grid doublet is given by the discretization of the pair $(\boldsymbol{E}, \boldsymbol{B})$ on the grid $\mathcal{G}$ and consequently $(\boldsymbol{H}, \boldsymbol{D})$ on the dual grid $\tilde{\mathcal{G}}$. In this way, the discrete set of Maxwell's grid equations are obtained representing the structure of the grid with respect to the orientation at hand. Here, we only briefly review the discretization of the pair $(\boldsymbol{E}, \boldsymbol{B})$.

Let us define the electrical grid voltage along an edge $L_{\{x,y,z\}}(n)$ and the magnetic grid flux through a face $A_{\{x,y,z\}}(n)$ by

$$\widehat{e}_{\{x,y,z\}}(n) \equiv \int_{L_{\{x,y,z\}}(n)} \boldsymbol{E} \cdot \vec{\boldsymbol{\tau}}\, ds \quad \text{and} \quad \widehat{\widehat{b}}_{\{x,y,z\}}(n) \equiv \int_{A_{\{x,y,z\}}(n)} \boldsymbol{B} \cdot \vec{\boldsymbol{n}}\, dA.$$

Hence, the integral form of Faraday's law (3.1.1) corresponding to an arbitrary grid face $A_z(n)$ follows from

$$\widehat{e}_x(n) - \widehat{e}_x(n+m_y) - \widehat{e}_y(n) + \widehat{e}_y(n+m_x) = -\frac{\partial}{\partial t}\widehat{\widehat{b}}_z(n). \tag{3.2.1}$$

An interpretation of the discrete formulation of Faraday's law (3.2.1) involving the orientation of the electrical grid voltage and the magnetic grid flux is given by Figure 3.2.

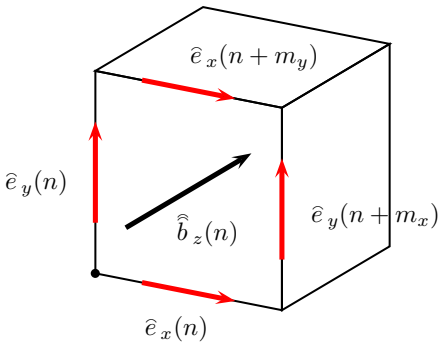

Figure 3.2: FIT: Electrical grid voltage and magnetic grid flux.

Since magnetic fields are solenoidal, cf. (3.1.7), the magnetic flux through an arbitrary volume V immediately yields Gauss's law for magnetic fields in integral form

$$-\widehat{\widehat{b}}_x(n) + \widehat{\widehat{b}}_x(n+m_x) - \widehat{\widehat{b}}_y(n) + \widehat{\widehat{b}}_y(n+m_y) - \widehat{\widehat{b}}_z(n) + \widehat{\widehat{b}}_z(n+m_z) = 0.$$

Following the lexicographical ordering of the grid points, a collection of the electrical grid voltage $\widehat{e}_{\{x,y,z\}}(n)$ and the magnetic grid flux $\widehat{\widehat{b}}_{\{x,y,z\}}(n)$ in each coordinate direction allows for a linear system of equations corresponding to Faraday's law and Gauss's law for magnetic fields, i.e.

$$C\,\widehat{\mathbf{e}} = -\frac{\partial}{\partial t}\widehat{\widehat{\mathbf{b}}} \quad \text{and} \quad D\,\widehat{\widehat{\mathbf{b}}} = 0. \tag{3.2.2}$$

On the dual grid $\tilde{\mathcal{G}}$ the magnetic grid voltage $\widehat{h}_{\{x,y,z\}}(n)$, the electrical grid flux $\widehat{\widehat{d}}_{\{x,y,z\}}(n)$ and the electrical current density $\widehat{\widehat{j}}_{\{x,y,z\}}(n)$ are defined in a similar way. In doing so, the integral formulations of Ampère's law (3.1.3) and Gauss's law for electric fields (3.1.5) lead to the linear systems on the dual grid, i.e.

$$\tilde{C}\,\widehat{\mathbf{h}} = \frac{\partial}{\partial t}\widehat{\widehat{\mathbf{d}}} + \widehat{\widehat{\mathbf{j}}} \quad \text{and} \quad \tilde{D}\,\widehat{\widehat{\mathbf{d}}} = 0. \tag{3.2.3}$$

For simplicity, we have assumed that the electric charge density equals zero.

Since the linear systems (3.2.2) and (3.2.3) are obtained via the topology of the grid doublet, Maxwell's grid equations do not involve a discretization error. The discretization error arises from the appropriate incorporation of the constitutive laws (3.1.9) leading to the diagonal mass matrices M_ϵ, M_μ and M_σ. In the following, we will omit the index set $\{x, y, z\}$ of the grid fluxes and grid voltages whenever an arbitrary coordinate direction may be applied. Then, each entry of the diagonal permittivity matrix $M_\epsilon \in \mathbb{R}^{3n_\# \times 3n_\#}$ is constituted by

$$\frac{\int\limits_{\tilde{A}(n)} \boldsymbol{D} \cdot \vec{\boldsymbol{n}}\, dA}{\int\limits_{L(n)} \boldsymbol{E} \cdot \vec{\boldsymbol{\tau}}\, ds} = \frac{\bar{\epsilon}(n) \int\limits_{\tilde{A}(n)} dA}{\int\limits_{L(n)} ds} + \mathcal{O}\left(h^{k+1}\right) \approx \frac{\bar{\epsilon}(n) |\, \tilde{A}(n)\,|}{|\, L(n)\,|}$$

where $|\, L(n)\,|$ and $|\, \tilde{A}(n)\,|$ denote the length of an edge and the area of a face, respectively, see [16]. Furthermore, $\bar{\epsilon}(n) = \int_{\tilde{A}(n)} \epsilon(n)\ dA / \int_{\tilde{A}(n)}\ dA$ refers to as the mean value of the electric permittivity of the four neighbouring volumes of the n-th grid point. These results are spread in a similar way to the mass matrices $M_\sigma \in \mathbb{R}^{3n_\# \times 3n_\#}$ and $M_\mu \in \mathbb{R}^{3n_\# \times 3n_\#}$ using the averaged electric conductivity $\bar{\sigma}(n) = \int_{\tilde{A}(n)} \sigma(n)\ dA / \int_{\tilde{A}(n)}\ dA$ and the averaged inverse magnetic permeability $\bar{\mu}^{-1}(n) = \int_{\tilde{L}(n)} (1/\mu(n))\ ds / \int_{\tilde{L}(n)}\ ds$.

For the second-order formulation of Maxwell's equations (3.0.3), the mass matrices M_ϵ and M_σ on the one hand and $K_\mu \equiv \tilde{C} M_{\mu^{-1}} C = C^{\mathrm{T}} M_{\mu^{-1}} C$ on the other hand are needed. Since C refers to a sparse matrix and $M_{\mu^{-1}}$ to a diagonal matrix, the computational effort for the matrix-matrix multiplication is rather inexpensive. In contrast to the FEM, the FIT allows for the discretization of a second-order model problem of the Maxwell's equations by means of the corresponding first-order formulation.

The special correspondence between the grid $\mathcal{G}$ and the dual grid $\tilde{\mathcal{G}}$ already implies $C = \tilde{C}^{\mathrm{T}}$. Moreover, the discrete operators feature the advantage that the construction of the discrete divergence operators D and $\tilde{D}$ depends on the same block matrices as the discrete curl operators C and $\tilde{C}$, see [16]. The algebraic nullspace properties of the curl-operator (3.0.2) remain valid, whenever the boundary conditions are not applied to the discrete operators.

The incorporation of the PEC boundary condition $\boldsymbol{E} \times \vec{\boldsymbol{n}} = 0$ requires the elimination of the corresponding degrees of freedom by cancelling out the associated rows and columns of the discrete curl and divergence operators, respectively, see [16].

3.3 The finite element method

An initial approach to the basic principle of the *finite element method* (FEM) has been introduced by R. L. Courant in 1941, see [93]. Up to the present day, the FEM has been widely anal-

ysed and successfully employed to a large variety of applications, see [7, 22, 23]. Since the application of the FEM in computational electromagnetism was discussed recently, see [62,85,96], the description of the finite element method summarises results given by Zaglmayr [131]. Throughout the thesis, the discretization of the different model problems of Maxwell's equations by means of the FEM has been achieved with *FEniCS*, see [78].

In the following, we restrict the discussion to the discretization of the time-harmonic second-order Maxwell's equations

$$-\omega^2 (\epsilon \boldsymbol{E}) \quad + \quad \imath\omega (\sigma \boldsymbol{E}) \quad + \quad \nabla \times \left(\tfrac{1}{\mu} (\nabla \times \boldsymbol{E}) \right) \quad = \quad 0, \tag{3.3.1}$$

where $\omega = 2\pi f$ and $f \in [f_{\min}, f_{\max}]$. In this way, we obtain a time-independent formulation of the FEM leading to a simplification of the notation. It is important to note that the explicit construction of the second-order linear dynamical system (3.0.3) by means of the discretized first-order formulation does not exist.

The principal idea of the FEM makes use of a *triangulation* Ω_h of the computational domain $\Omega \subset \mathbb{R}^3$. Let $\mathcal{T}_i \in \Omega_h$ denote an arbitrary element of the triangulation and $\mathcal{T}_i^o \equiv \mathcal{T}_i \backslash \partial \mathcal{T}_i$ the interior domain of the element. Throughout the section, the triangulation of the computational domain is assumed to be *regular*, i.e. $\bar{\Omega} = \bigcup \mathcal{T}_i$, where $\mathcal{T}_i^o \cap \mathcal{T}_j^o = \emptyset$ holds for all $i \neq j$ and $\mathcal{T}_i \cap \mathcal{T}_j$, $i \neq j$, represents either an empty set, or a vertex, or an edge, or a face, see [23].

Since the FEM requires a weak formulation of the second-order Maxwell's equations (3.1.11), we initially review two common functional spaces, see [131].

Definition 3.3.1 ([131, Definition 3.2]). *Let* $(\boldsymbol{u}, \boldsymbol{v})_0 = \int_\Omega \boldsymbol{u} \cdot \boldsymbol{v} \, d\boldsymbol{x}$ *denote a scalar product with* $\boldsymbol{u}, \boldsymbol{v} \in [\mathbb{L}_2(\Omega)]^3$, *where* $\Omega \subset \mathbb{R}^3$ *refers to as a Lipschitz domain.*

- $H^1(\Omega) := \left\{ u \in \mathbb{L}_2(\Omega) : \nabla u \in [\mathbb{L}_2(\Omega)]^3 \right\}$ *with the scalar product*

$$(u, v)_{H^1} := (\nabla u, \nabla v)_0 + (u, v)_0.$$

- $H(\mathrm{curl}, \Omega) := \left\{ \boldsymbol{u} \in [\mathbb{L}_2(\Omega)]^3 : \nabla \times \boldsymbol{u} \in [\mathbb{L}_2(\Omega)]^3 \right\}$ *with the scalar product*

$$(\boldsymbol{u}, \boldsymbol{v})_{H(\mathrm{curl})} := (\nabla \times \boldsymbol{u}, \nabla \times \boldsymbol{v})_0 + (\boldsymbol{u}, \boldsymbol{v})_0.$$

The corresponding induced norms are denoted by $\| \cdot \|_{H^1}$ *and* $\| \cdot \|_{H(\mathrm{curl})}$.

The appropriate treatment of the boundary of the computational domain requires the definition of the *trace* of a function. Generally speaking, the trace of a function refers to as the value of the function on the boundary $\partial\Omega$ of the computational domain $\Omega \subset \mathbb{R}^3$. For example, the tangential trace of an arbitrary function $\boldsymbol{u} \in \left[C^\infty(\bar{\Omega}) \right]^3$ is defined by

$$\mathrm{tr}_T(\boldsymbol{u})(x) = (\boldsymbol{u}(x) \times \vec{\boldsymbol{n}}) \times \vec{\boldsymbol{n}} \quad \text{for all} \quad x \in \partial\Omega,$$

see [131]. In this way, the explicit incorporation of the PEC boundary condition $\boldsymbol{E} \times \vec{\boldsymbol{n}} = 0$ in the $H(\mathrm{curl}, \Omega)$ space can be directly realised using the space

$$H_0(\mathrm{curl}, \Omega) = \{\boldsymbol{u} \in H(\mathrm{curl}, \Omega) : \mathrm{tr}_T(\boldsymbol{u}) \equiv 0\} \subset H(\mathrm{curl}, \Omega).$$

The weak formulation of the time-harmonic second-order formulation of Maxwell's equations follows from multiplying (3.3.1) with the test function $\boldsymbol{\psi} \in H(\mathrm{curl}, \Omega)$, see [62]. Applying a well-known partial integration formula [131], the variational formulation is given by: Seek $\boldsymbol{E} \in H_0(\mathrm{curl}, \Omega)$ subject to

$$-\omega^2 (\epsilon \boldsymbol{E}, \boldsymbol{\psi})_0 \quad + \quad \imath\omega (\sigma \boldsymbol{E}, \boldsymbol{\psi})_0 \quad + \quad \left(\tfrac{1}{\mu} (\nabla \times \boldsymbol{E}), \nabla \times \boldsymbol{\psi}\right)_0 \quad = \quad 0 \quad \text{for all} \quad \boldsymbol{\psi} \in H_0(\mathrm{curl}, \Omega).$$

The matrices of the second-order linear dynamical system (3.0.3) are obtained via the assembly of each bilinear form by means of the Galerkin approach of the weak formulation. The Galerkin approach is based on an appropriate finite dimensional subspace of the $H_0(\mathrm{curl}, \Omega)$ space. A finite-dimensional subspace arises from the definition of the local basis functions corresponding to a finite element on a single element $\mathcal{T} \in \Omega_h$, where a continuity argument allows for the extension of the basis functions to the whole triangulation.

Hence, we initially review a definition of a finite element, which has been originally formulated by Ciarlet.

Definition 3.3.2 ([23, Definition 3.1.1])**.** *Let*

- $\Omega_\mathcal{T} \subseteq \mathbb{R}^n$ *be a bounded and closed set with a non-empty interior and a piecewise smooth boundary,* (element domain)
- $\mathcal{P}_\mathcal{T}$ *be a finite-dimensional space of functions on* $\Omega_\mathcal{T}$*,* (shape functions)
- $\mathcal{N}_\mathcal{T} = \{N_1, \ldots, N_k\}$ *be a basis of the dual space* $\mathcal{P}'_\mathcal{T}$*.* (nodal variables)

Then, the triplet $(\Omega_\mathcal{T}, \mathcal{P}_\mathcal{T}, \mathcal{N}_\mathcal{T})$ *is referred to as* finite element*.*

Typically, the *nodal basis* of a finite element will be employed, i.e. an arbitrary shape function $\phi_j \in \mathcal{P}_\mathcal{T}$ implies $N_i(\phi_j) = \delta_{ij}$ for all $N_i \in \mathcal{N}_\mathcal{T}$, where δ_{ij} denotes the Kronecker symbol, see [7]. The discretization of the electric field strength by means of the FEM makes use of an approximation along the edges of the triangulation. Therefore, an appropriate ansatz space for the finite element consists of the *edge elements* of a tetrahedron, see [131].

Definition 3.3.3 ([131, Definition 4.11])**.** *The lowest-order edge elements of a tetrahedron* $\mathcal{T} \in \Omega_h$ *are obtained via the local space*

$$\mathcal{N}_0^I(\mathcal{T}) = \left\{a + b \times \boldsymbol{x} \ : \ a, b \in \mathbb{R}^3\right\}$$

with the dimension $\dim(\mathcal{N}_0^I(\mathcal{T})) = 6$. *Furthermore, the corresponding degrees of freedom follow from the tangential components of each edge* $E_\alpha \in \mathcal{E}_\mathcal{T}$, *i.e.*

$$N_\alpha^{\mathcal{N}_0} \; : \; \boldsymbol{v} \longmapsto \int_{E_\alpha} \boldsymbol{v} \cdot \vec{\boldsymbol{\tau}} \; d\boldsymbol{x} \quad \textit{for all} \quad \alpha = 1, \ldots, |\, \mathcal{E}_\mathcal{T} \,|,$$

where $|\, \mathcal{E}_\mathcal{T} \,|$ *refers to as the number of edges of a tetrahedron.*

Let $\lambda_i \equiv \lambda_i(x)$ denote the *barycentric coordinates* corresponding to the vertices of the triangulation. Then, the nodal basis functions of the local space $\mathcal{N}_0^I(\mathcal{T})$ are given by the shape functions $\boldsymbol{\phi}_\alpha^{\mathcal{N}_0} = \nabla\lambda_{\alpha_1}\lambda_{\alpha_2} - \lambda_{\alpha_1}\nabla\lambda_{\alpha_2}$, where $E_\alpha = [V_{\alpha_1}, V_{\alpha_2}] \in \mathcal{E}_\mathcal{T}$, $V_{\alpha_1}, V_{\alpha_2} \in \mathcal{V}$ $(\alpha_1, \alpha_2 > 0)$, refers to as an arbitrary edge of the triangulation, see [131].

If $\boldsymbol{E} = \sum_{i=1}^{\mathcal{E}_\#} E_i \, \boldsymbol{\phi}_i^{\mathcal{N}_0}$ denotes the expansion of the electric field strength corresponding to the number of edges of the triangulation $\mathcal{E}_\# > 0$, the *assembly* of the matrix K_μ follows from the corresponding bilinear form, i.e.

$$\left(\frac{1}{\mu}\left(\nabla \times \boldsymbol{E}\right), \nabla \times \boldsymbol{\psi}\right)_0 \quad = \quad \sum_{\mathcal{T} \in \Omega_h} \int_\mathcal{T} \frac{1}{\mu} \left(\sum_{i=1}^{\mathcal{E}_\#} E_i \left(\nabla \times \phi_i^{\mathcal{N}_0} \right) \right) \cdot \left(\nabla \times \boldsymbol{\psi} \right) \; dx, \qquad (3.3.2)$$

where $\boldsymbol{\psi} \in V_{h,0}$ represents an arbitrary test function of the global finite element space

$$V_{h,0} = \left\{ \boldsymbol{v} \in H_0(\mathrm{curl}, \Omega) \; : \; \boldsymbol{v}_{|\mathcal{T}} \in \mathcal{N}_0^I(\mathcal{T}) \quad \forall \, \mathcal{T} \in \Omega_h \right\}.$$

The global finite element space $V_{h,0} \subset H_0(\mathrm{curl}, \Omega)$ already ensures the continuity across interface elements. For efficiently computing (3.3.2), a transformation of each tetrahedron $\mathcal{T} \in \Omega_h$ to a common reference tetrahedron is employed, see [131].

While the matrices of the curl-operator as well as the curl-curl operator in the FIT represent the structure of the grid topology, the FEM requires the evaluation of the curl-operator with respect to a set of basis functions on a tetrahedron involving the impact on the neighbouring tetrahedrons of the triangulation. For this reason, the assembly of the bilinear forms $(\epsilon \boldsymbol{E}, \boldsymbol{\psi})_0$ and $(\sigma \boldsymbol{E}, \boldsymbol{\psi})_0$ typically lead to block-tridiagonal mass matrices.

In [62], Hiptmair has given an approach for the construction of the discrete divergence operator leading to the left and right nullspace of the discretized curl-curl operator.

CHAPTER 4

Moment matching based model order reduction for Maxwell's equations

Over the last decades, efficient and reliable methods for solving high-dimensional sparse linear systems of the form $Ax = b$, where $A \in \mathbb{C}^{n\times n}$, $x \in \mathbb{C}^n$ and $b \in \mathbb{C}^n$, have been developed on the basis of Krylov subspace methods, see [104]. In principle, these methods are based on computing an approximate solution to the linear system by means of the *Krylov subspace*

$$\mathcal{K}_k(A, r_0) = \operatorname{span}\left\{r_0, Ar_0, \ldots, A^{k-1}r_0\right\},$$

where $r_0 = b - Ax_0$ and $x_0 \in \mathbb{C}$, see [104]. Here, $k > 0$ denotes the number of iteration steps of the Krylov subspace method. We will provide an overview on Krylov subspace methods for solving sparse linear systems in Chapter 5. Another important field of application of Krylov subspace methods is solving generalized eigenvalue problems $Ax = \lambda Ex$, $x \neq 0$, with $E \in \mathbb{C}^{n\times n}$, $A \in \mathbb{C}^{n\times n}$ and $\lambda \in \mathbb{C}$, see [123].

Apart from sparse linear systems and generalized eigenvalue problems, Krylov subspace methods have also been applied in model order reduction of linear dynamical systems, see [4, 8,9,45,51]. The model order reduction technique known as moment matching method requires the computation of a sequence of Krylov subspaces using rational Arnoldi- or Lanczos-type methods based on a set of expansion points [52,74,102,103]. In the following, we will primarily restrict the discussion to rational Arnoldi-type methods.

In comparison to other model order reduction methods, a major drawback of moment matching methods arises from the missing a-priori error estimation for the accuracy of the reduced order model. The computation of a reliable set of expansion points has often been considered as another disadvantage. Nevertheless, accurate and reliable reduced order models may be obtained via rational Arnoldi-type methods with a Greedy-type expansion point

selection strategy, see [19,70,113].

For simplicity, we will only consider single-input, single-output linear dynamical systems, i.e. $p = 1$ and $m = 1$. Further details on moment matching based model order reduction of multiple-input, multiple-output linear dynamical systems have been given in [65,113].

The outline of the chapter is as follows: At first, we will review the principal idea of moment matching methods on the basis of the Padé approximation. Thereafter, an overview on structure- and passivity-preserving Arnoldi-type moment matching methods is given. In this context, we apply the SPRIM algorithm, which has been initially introduced by Freund for RCL circuits [46], to linear dynamical systems of the first-order Maxwell's equations.

Since the application of moment matching methods with a single expansion point is rather limited for practical applications, we will recapitulate moment matching methods with multiple expansion points using rational Arnoldi-type methods. Here, the adaptive-order, rational Arnoldi (AORA) method represents the method of choice for the adaptive computation of each dimension of the different Krylov subspaces leading to the Galerkin projection $\Pi = VV^{\mathrm{T}}$, see [74].

Due to the missing a-priori error estimation, a common way for moment matching methods is the computation of a sequence of reduced order models from nested sets of expansion points $\mathcal{S}_{i+1} = \mathcal{S}_i \cup \{s_{i+1}\}$, $s_{i+1} \in \mathbb{C}$, $(i = 0, \ldots, l-1)$. In this context, we will introduce a suitable adaptive expansion point selection – the AORA-RK method – on the basis of an upper bound of the output moment error, see [19].

In Section 4.3, moment matching methods are applied to second-order linear dynamical systems of Maxwell's equations (3.0.3). The key ingredient for second-order descriptor systems follows from the efficient computation of a structure-preserving reduced order model using a second-order rational Arnoldi-type method, see [9]. Here, a specific framework for the second-order linear dynamical system is required in order to properly benefit from the application of the modified Gram-Schmidt procedure, see [14,107].

In the context of the Maxwell's equations, we will also present some results for the explicit incorporation of the discrete, divergence conditions during the computation of reduced order models with moment matching methods. Thereby, we will show that under certain conditions the system moments of the expansion of the transfer function are already divergence-free, see [19].

4.1 Moment matching with Arnoldi-type methods

The Arnoldi method has been initially introduced by W. E. Arnoldi in 1951 and provides an efficient way for the computation of an orthonormal basis of the Krylov subspace $\mathcal{K}_k(A, b)$, see

[6]. Although the first popular results for moment matching methods were based on Lanczos-type methods, e.g. the PVL method [41], Arnoldi-type methods for model order reduction have become of great importance due to the introduction of the SPRIM algorithm at the latest, see [45].

4.1.1 The Arnoldi method

The application of $k \in \mathbb{N}$ iteration steps of the *Arnoldi method* to $A \in \mathbb{C}^{n\times n}$ and $b \in \mathbb{C}^n$ leads to the computation of an orthonormal basis $V_k \in \mathbb{C}^{n\times k}$ of the Krylov subspace $\mathcal{K}_k(A, b)$, see [104]. More precisely, the algorithm offers the decomposition $AV_{k+1} = \underline{H}_k V_k$, where $\underline{H}_k \in \mathbb{C}^{(k+1)\times k}$ and $V_k \in \mathbb{C}^{n\times k}$ denote an upper Hessenberg matrix and an orthonormal matrix, respectively, cf. Algorithm 1. The initial vector of the Krylov subspace will be usually chosen as $v_1 = b/\| b \|_2$. An Arnoldi method with implicit restarts has been previously discussed in [75, 87].

Algorithm 1 The Arnoldi method [104]

Input: Matrix $A \in \mathbb{C}^{n\times n}$; initial vector $v_1 \in \mathbb{C}^n$ with $\| v_1 \|_2 = 1$; number of iteration steps $k \in \mathbb{N}$.

Output: $AV_{k+1} = \underline{H}_k V_k$ with an orthonormal matrix $V_k \in \mathbb{C}^{n\times k}$ and an upper Hessenberg matrix $\underline{H}_k \in \mathbb{C}^{(k+1)\times k}$.

Initialize $V_1 = [v_1]$.
for $j = 1, \ldots, k$ **do**
  for $i = 1, \ldots, j$ **do**
    $h_{ij} = v_i^{\mathrm{T}} A v_j$
  end for
  $w_j = Av_j - \sum_{i=1}^{j} h_{ij} v_i$ % Modified Gram-Schmidt procedure
  $h_{j+1,j} = \| w_j \|_2$
  if $h_{j+1,j} \neq 0$ **then**
    $v_{j+1} = w_j / h_{j+1,j}$
    $V_{j+1} = [V_j,\ v_{j+1}]$
  end if
end for

In contrast to the Arnoldi method, the *unsymmetric Lanczos method* computes two biorthogonal matrices $V_k \in \mathbb{C}^{n\times k}$ and $W_k \in \mathbb{C}^{n\times k}$ satisfying $W_k^{\mathrm{T}} V_k = I$ such that $W_{k+1}^{\mathrm{T}} A V_k = \underline{T}_k$ where $\underline{T}_k \in \mathbb{C}^{(k+1)\times k}$ denotes a tridiagonal matrix [104]. Moreover, the (unsymmetric) Lanczos method offers the advantage computing the biorthogonal vector sequence V_k and W_k using a three-term recurrence. Although Lanczos-type methods have been also employed for moment

matching based model order reduction, see [4, 72], the contribution of the thesis at hand primarily deals with Arnoldi-type methods. In the following, we simply recall some well-known differences of Lanczos-type methods in model order reduction.

4.1.2 The Padé approximation for moment matching

The first results on model order reduction with moment matching methods have been developed on the basis of the *Padé approximation* of the transfer function, see [41]. For $p, q \in \mathbb{N}$, the rational representation

$$\mathcal{H}_{p,q}(s_0 + \sigma) = \frac{b_p \sigma^p + \ldots + b_1 \sigma + b_0}{a_q \sigma^q + \ldots + a_1 \sigma + 1}$$

represents a Padé approximation of the transfer function $\mathcal{H}(s_0 + \sigma)$, where both Taylor series at $\sigma = 0$ coincide, i.e. $\mathcal{H}_{p,q}(s_0 + \sigma) = \mathcal{H}(s_0 + \sigma) + \mathcal{O}(\sigma^{p+q+1})$. Typically, the rational representation of $\mathcal{H}(s_0 + \sigma)$ holds a numerator and denominator of degree at most $n - 1$ and n leading to $p = q - 1$.

Moreover, the coefficients of the q-th Padé approximant $\mathcal{H}_q(s) \equiv \mathcal{H}_{q-1,q}(s)$ are obtained via the Taylor expansion of the transfer function at the expansion point $s_0 \in \mathbb{C}$, i.e.

$$\mathcal{H}(s_0 + \sigma) = \sum_{j=0}^{\infty} m_j(s_0)\sigma^j \quad \text{with} \quad m_j(s_0) = \mathcal{C}\left[-(s_0\mathcal{E} - \mathcal{A})^{-1}\mathcal{E}\right]^j (s_0\mathcal{E} - \mathcal{A})^{-1}\mathcal{B} \in \mathbb{C}^{p\times m}.$$

In terms of the explicit computation of the moments $m_j \equiv m_j(s_0)$ $(j = 0, 1, \ldots, n_r - 1)$, the expansion of the transfer function leads to the moment matching property

$$\mathcal{H}^{(j)}(s_0) = \tilde{\mathcal{H}}^{(j)}(s_0) \quad \text{for all} \quad j = 0, 1, \ldots, n_r - 1, \tag{4.1.1}$$

where $\mathcal{H}^{(j)}(s_0)$ refers to as the j-th derivative of the transfer function at the expansion point $s_0 \in \mathbb{C}$. In other words, the moments $m_j(s_0)$ of the full-order model problem and the moments of the reduced order linear dynamical system

$$\tilde{m}_j \equiv \tilde{m}_j(s_0) = \tilde{\mathcal{C}}\left[-(s_0\tilde{\mathcal{E}} - \tilde{\mathcal{A}})^{-1}\tilde{\mathcal{E}}\right]^j (s_0\tilde{\mathcal{E}} - \tilde{\mathcal{A}})^{-1}\tilde{\mathcal{B}} \in \mathbb{C}^{p\times m}$$

coincide up to a given order $n_r > 0$ [41].

For example, the *asymptotic waveform evaluation* (AWE) algorithm introduced in [95] seeks the reduced order model from the explicit computation of the moments $m_j \in \mathbb{C}^{p\times m}$ following a recursive formula. Since the explicit computation of the moments $m_j \in \mathbb{C}^{p\times m}$ $(j = 0, 1, \ldots, n_r - 1)$ represents a highly ill-conditioned problem, the application of the AWE algorithm is only possible for small dimensions of the full-order linear dynamical system.

Indeed, Feldmann and Freund have shown in [41] that the Padé approximation of the transfer function may be directly established from the (unsymmetric) Lanczos method based on the

Padé-via-Lanczos (PVL) method. In this way, the PVL method avoids the explicit computation of the moments of the transfer function leading to a more reliable model order reduction technique.

An extension of the idea by Feldmann and Freund for Arnoldi-type methods follows from the Taylor series of the transfer function at the expansion point $s_0 \in \mathbb{C}$, i.e.

$$\mathcal{H}(s) = \sum_{j=0}^{\infty} \mathcal{C}X^{(j)}(s_0)(s-s_0)^j \equiv \sum_{j=0}^{\infty} Y^{(j)}(s_0)(s-s_0)^j,$$

where $X^{(j)}(s_0) = \left[-(s_0\mathcal{E}-\mathcal{A})^{-1}\mathcal{E}\right]^j (s_0\mathcal{E}-\mathcal{A})^{-1}\mathcal{B}$ and $Y^{(j)}(s_0) = \mathcal{C}X^{(j)}(s_0)$ denote the j-th *system moment* and the j-th *output moment*, respectively, see [74]. The system moments $X^{(j)}(s_0)$ $(j = 0, 1, \ldots, n_r - 1)$ lead to the definition of the *input Krylov subspace*[1]

$$\mathcal{K}_{n_r}\left(-(s_0\mathcal{E}-\mathcal{A})^{-1}\mathcal{E}, (s_0\mathcal{E}-\mathcal{A})^{-1}\mathcal{B}\right) \tag{4.1.2}$$

and the *output Krylov subspace*

$$\mathcal{K}_{n_r}\left(-(s_0\mathcal{E}-\mathcal{A})^{-\mathrm{T}}\mathcal{E}^{\mathrm{T}}, (s_0\mathcal{E}-\mathcal{A})^{-\mathrm{T}}\mathcal{C}^{\mathrm{T}}\right). \tag{4.1.3}$$

As seen in Section 2.1, the reduced order model of the high-dimensional linear dynamical system arises out of the application of the *Petrov-Galerkin projection* $\Pi = VW^{\mathrm{T}}$, where the columns of the biorthonormal matrices $V \in \mathbb{C}^{n\times n_r}$ and $W \in \mathbb{C}^{n\times n_r}$ span the input and output Krylov subspace (4.1.2) and (4.1.3), respectively. The state variable of the reduced order model is referred to as $\tilde{x}(t) \equiv W^{\mathrm{T}}x(t) \in \mathbb{C}^{n_r}$, see [4].

An important approximation result of moment matching methods in model order reduction is based on the number of matched moments in the reduced order model depending on the choice of the Petrov-Galerkin projection. Remember that $m > 0$ and $p > 0$ denote the number of inputs and outputs of the linear dynamical system (2.1.1), where we have assumed that $m = 1$ and $p = 1$. The following approximation results for model order reduction with moment matching methods have been shown in [55, 117].

Lemma 4.1.1 ([55, Lemma 3.2])**.** *Let* $\mathcal{K}_{n_r}(-(s_0\mathcal{E}-\mathcal{A})^{-1}\mathcal{E}, (s_0\mathcal{E}-\mathcal{A})^{-1}\mathcal{B}) \subseteq \mathrm{colspan}(V)$. *The application of the Galerkin projection* $\Pi = VV^{\mathrm{T}}$ *to a linear dynamical system (2.1.1) leads to the moment matching property*

$$m_j(s_0) = \tilde{m}_j(s_0) \quad \textit{for all} \quad j = 0, 1, \ldots, n_r - 1$$

in the reduced order model (2.1.3).

[1] Initially, the relation $n_d = n_r$ remains valid. Later, we introduce some adaptations for the orthonormal matrix $V \in \mathbb{C}^{n\times n_r}$ affecting the dimension of the reduced order model.

A similar moment matching property will be achieved for the Galerkin projection $\Pi = WW^{\mathrm{T}}$, where $\mathcal{K}_{n_r}(-(s_0\mathcal{E}-\mathcal{A})^{-\mathrm{T}}\mathcal{E}^{\mathrm{T}}, (s_0\mathcal{E}-\mathcal{A})^{-\mathrm{T}}\mathcal{C}^{\mathrm{T}}) \subseteq \mathrm{colspan}(W)$, see [55, Lemma 3.3]. The combination of both moment matching properties allows for the well-known approximation property of a Petrov-Galerkin projection $\Pi = VW^{\mathrm{T}}$.

Theorem 4.1.2 ([55, Theorem 3.1]). *Let $\mathcal{K}_{n_r}(-(s_0\mathcal{E}-\mathcal{A})^{-1}\mathcal{E}, (s_0\mathcal{E}-\mathcal{A})^{-1}\mathcal{B}) \subseteq \mathrm{colspan}(V)$ and $\mathcal{K}_{n_r}(-(s_0\mathcal{E}-\mathcal{A})^{-\mathrm{T}}\mathcal{E}^{\mathrm{T}}, (s_0\mathcal{E}-\mathcal{A})^{-\mathrm{T}}\mathcal{C}^{\mathrm{T}}) \subseteq \mathrm{colspan}(W)$. The application of the Galerkin projection $\Pi = VW^{\mathrm{T}}$ to a linear dynamical system (2.1.1) leads to the moment matching property*

$$m_j(s_0) = \tilde{m}_j(s_0) \quad \textit{for all} \quad j = 0, 1, \ldots, 2n_r - 2$$

in the reduced order model (2.1.3).

Numerical experiments have indicated that the one-sided Arnoldi method already allows for the computation of an appropriate reduced order model, cf. Chapter 6. Hence, we will mainly restrict the discussion to the application of the Galerkin projection $\Pi = VV^{\mathrm{T}}$ or $\Pi = WW^{\mathrm{T}}$ in the following.

4.1.3 Moment matching methods with real-valued Galerkin projection

For linear dynamical systems (2.1.1) with a real-valued matrix quadruplet $\mathcal{E}, \mathcal{A} \in \mathbb{R}^{n\times n}, \mathcal{B} \in \mathbb{R}^{n\times m}$ and $\mathcal{C} \in \mathbb{R}^{p\times n}$, the application of moment matching methods in model order reduction shall provide a real-valued reduced order model (2.1.3). A common approach for the computation of a *real-valued Galerkin projection* based on a complex-valued expansion point $s_0 \in \mathbb{C}$ was previously given in [45,74].

Let the columns of the orthonormal matrix $V \in \mathbb{C}^{n\times n_r}$ span the input Krylov subspace (4.1.2). Computing a *QR decomposition* [53] of the block matrix consisting of the real and imaginary part of the orthonormal matrix $V \in \mathbb{C}^{n\times n_r}$, it follows that

$$\Big[\mathrm{real}(V), \quad \mathrm{imag}(V)\Big] = \Big[Q_{V,1}, \quad Q_{V,2}\Big] \begin{bmatrix} R \\ 0 \end{bmatrix} = Q_{V,1}R, \tag{4.1.4}$$

where $Q_{V,1} \in \mathbb{R}^{n\times 2n_r}$ and $Q_{V,2} \in \mathbb{R}^{n\times(n-2n_r)}$ denote orthonormal matrices and $R \in \mathbb{R}^{2n_r\times 2n_r}$ represents an upper-triangular matrix of full rank. Due to the fact that

$$\mathrm{colspan}\left(\Big[\mathrm{real}(V), \quad \mathrm{imag}(V)\Big]\right) \subseteq \mathrm{colspan}\left(Q_{V,1}\right)$$

holds, the employment of the real-valued Galerkin projection $\Pi = Q_{V,1}Q_{V,1}^{\mathrm{T}}$ leads to the computation of a reduced order model corresponding to the input Krylov subspace (4.1.2).

The application of the Galerkin projection resulting from the QR decomposition (4.1.4) ensures the Padé approximation of the transfer function at an expansion point $s_0 \in \mathbb{C}$ and the

corresponding complex conjugate expansion point $\bar{s}_0 \in \mathbb{C}$, see [66]. A reduced order model of dimension $2n_r \times 2n_r$ obtained via the real-valued Galerkin projection offers a notably increasing accuracy as compared to the corresponding complex-valued reduced order models.

The computation of a real-valued Petrov-Galerkin projection $\Pi = VW^{\mathrm{T}}$ requires a QR decomposition of each matrix $V \in \mathbb{C}^{n\times n_r}$ and $W \in \mathbb{C}^{n\times n_r}$ such that $\mathrm{colspan}(V) \subseteq \mathrm{colspan}\,(Q_{V,1})$ and $\mathrm{colspan}(W) \subseteq \mathrm{colspan}\,(Q_{W,1})$. In order to ensure the moment matching approximation property of a two-sided Krylov subspace method, an explicit biorthogonalization of $Q_{V,1} \in \mathbb{R}^{n\times 2n_r}$ and $Q_{W,1} \in \mathbb{R}^{n\times 2n_r}$ becomes necessary.

An efficient implementation of the Arnoldi method depends on the subsequent application of the modified Gram-Schmidt procedure to the real and imaginary part of each system moment $X^{(j)}(s_0)$ $(j = 0, 1, \ldots, n_r - 1)$ separately, see [74].

4.1.4 Structure- and passivity-preserving moment matching methods

An important requirement for model order reduction is the computation of a structure-preserving reduced order model whenever the linear dynamical system offers a special block-structure. For example, in view of first-order descriptor systems of Maxwell's equations (3.0.1), the reduced order model shall preserve the block-structure of the electric and magnetic field strength. A general framework of structure-preserving moment matching methods of first-order descriptor systems has been discussed by Bai and Li [77].

Here, we review the SPRIM algorithm allowing for the computation of a structure-preserving reduced order model for RCL circuits, see [46]. Moreover, we discuss the connection between RCL circuits and Maxwell's equations and present a common application of the SPRIM algorithm to first-order linear dynamical systems of the Maxwell's equations.

A comparison between linear dynamical systems of an RCL circuit on the one hand and Maxwell's equations on the other hand shows that both applications lead to the same block-structure, i.e.

$$\begin{aligned} \begin{bmatrix} \mathcal{E}_{11} & 0 \\ 0 & \mathcal{E}_{22} \end{bmatrix} \begin{pmatrix} \dot{x}_1(t) \\ \dot{x}_2(t) \end{pmatrix} &= \begin{bmatrix} -\mathcal{A}_{11} & \mathcal{A}_{12} \\ -\mathcal{A}_{12}^{\mathrm{T}} & 0 \end{bmatrix} \begin{pmatrix} x_1(t) \\ x_2(t) \end{pmatrix} + \mathcal{B}u(t), \\ y(t) &= \mathcal{C} \begin{pmatrix} x_1(t) \\ x_2(t) \end{pmatrix}, \end{aligned} \tag{4.1.5}$$

where $x_1(t) \in \mathbb{R}^{n_1}$ and $x_2(t) \in \mathbb{R}^{n_2}$ with $n = n_1 + n_2$ and $n_1, n_2 > 0$. Furthermore, it holds $\mathcal{E}_{11} \in \mathbb{R}^{n_1\times n_1}$ and $\mathcal{E}_{22} \in \mathbb{R}^{n_2\times n_2}$, while $\mathcal{A}_{11} \in \mathbb{R}^{n_1\times n_1}$ and $\mathcal{A}_{12} \in \mathbb{R}^{n_1\times n_2}$.

A linear dynamical system of an *RCL circuit* features the descriptor system (4.1.5) with a singular matrix $\mathcal{E}_{22}$, see [98]. The state variable $x(t) = \left[x_1^{\mathrm{T}}(t), x_2^{\mathrm{T}}(t)\right]^{\mathrm{T}} \in \mathbb{R}^n$ consists of node

potentials on the one hand and voltage and current sources on the other hand. More importantly, the relation $\mathcal{B} = \mathcal{C}^{\mathrm{T}}$ holds, which does usually not appear for linear dynamical systems of Maxwell's equations in semiconductor structures.

The principal idea of the SPRIM algorithm for the computation of a structure-preserving reduced order model is as follows: After the computation of an n_r-dimensional orthonormal vector sequence of the input Krylov subspace (4.1.2) with the help of the Arnoldi method, an appropriate decomposition of the orthonormal matrix $V \in \mathbb{C}^{n \times n_r}$ follows from

$$V = \begin{bmatrix} V_1 \\ V_2 \end{bmatrix} \in \mathbb{C}^{n \times n_r}, \tag{4.1.6}$$

where $V_1 \in \mathbb{C}^{n_1 \times n_r}$ and $V_2 \in \mathbb{C}^{n_2 \times n_r}$ with $n_1 + n_2 = n$ and $n_1, n_2 > 0$. Due to the fact that the decomposition (4.1.6) does not necessarily result in a matrix pair $V_1 \in \mathbb{C}^{n_1 \times n_r}$ and $V_2 \in \mathbb{C}^{n_2 \times n_r}$ each of full column rank, a QR decomposition to each matrix block $V_1 = Q_1 R_1$ and $V_2 = Q_2 R_2$ is required, where Q_1 and Q_2 are orthonormal matrices and R_1 and R_2 are upper-triangular matrices. The Galerkin projection $\Pi = \bar{V}\bar{V}^{\mathrm{T}}$ with

$$\bar{V} = \begin{bmatrix} Q_1 & 0 \\ 0 & Q_2 \end{bmatrix} \in \mathbb{C}^{n \times 2n_r} \tag{4.1.7}$$

results in a *structure-preserving* reduced order model, where $\tilde{x}_1(t) \equiv Q_1^{\mathrm{T}} x_1(t) \in \mathbb{C}^{n_r}$ and $\tilde{x}_2(t) \equiv Q_2^{\mathrm{T}} x_2(t) \in \mathbb{C}^{n_r}$ denote the components of the state variable of the reduced order model. Due to the fact that $\mathrm{colspan}(V) \subseteq \mathrm{colspan}(\bar{V})$ holds, the application of the Galerkin projection $\Pi = \bar{V}\bar{V}^{\mathrm{T}}$ ensures the projection onto the input Krylov subspace (4.1.2), see [46].

Finally, we give an overview on the SPRIM algorithm for Maxwell's equations in Algorithm 2. The structure-preserving property of the SPRIM algorithm based on the orthonormal matrix $\bar{V} \in \mathbb{C}^{n \times 2n_r}$ doubles the number of matched moments in comparison to the application of the orthonormal matrix $V \in \mathbb{C}^{n \times n_r}$, see [46].

The SPRIM algorithm preserves the passivity in the reduced order model at least for the special case $\mathcal{B} = \mathcal{C}^{\mathrm{T}}$. Since the passivity of a linear dynamical system is equivalent to the positive realness of the corresponding transfer function [3], Freund has shown the following necessary condition for a transfer function being positive-real, see [45].

Theorem 4.1.3 ([45, Theorem 13]). *Let $\mathcal{E}, \mathcal{A} \in \mathbb{R}^{n \times n}$ and $\mathcal{B} \in \mathbb{R}^{n \times m}$. Assume that*

$$\mathcal{E} = \mathcal{E}^{\mathrm{T}} \succcurlyeq 0 \qquad \textit{and} \qquad \mathcal{A} + \mathcal{A}^{\mathrm{T}} \preccurlyeq 0$$

hold and that the matrix pencil $\lambda\mathcal{E} - \mathcal{A}$ is regular. Then, the transfer function $\mathcal{H}(s) = \mathcal{C}(s\mathcal{E} - \mathcal{A})^{-1}\mathcal{B}$ is positive real.

Algorithm 2 The SPRIM algorithm [46] for Maxwell's equations

Input: Descriptor system $(\mathcal{E}, \mathcal{A}, \mathcal{B}, \mathcal{C})$ of first-order Maxwell's equations (3.0.1); number of iteration steps of Arnoldi method $n_r > 0$; arbitrary expansion point $s_0 \in \mathbb{C}$.

Output: Structure-preserving and real-valued reduced order model $(\tilde{\mathcal{E}}, \tilde{\mathcal{A}}, \tilde{\mathcal{B}}, \tilde{\mathcal{C}})$ of dimension $n_d = 4n_r$.

1: Apply $n_r > 0$ iteration steps of the Arnoldi method with $A \equiv -(s_0\mathcal{E} - \mathcal{A})^{-1}\mathcal{E}$ and $b \equiv (s_0\mathcal{E} - \mathcal{A})^{-1}\mathcal{B}$ and denote the resulting matrix by $V \in \mathbb{C}^{n \times n_r}$.

2: Decompose $V = [V_E^{\mathrm{T}}, V_H^{\mathrm{T}}]^{\mathrm{T}}$ with $V_E \in \mathbb{C}^{n_E \times n_r}$ and $V_H \in \mathbb{C}^{n_H \times n_r}$, $n = n_E + n_H$, in accordance with the dimensions of the electric and magnetic field strength.

3: Compute a QR decomposition of each block V_E and V_H, i.e.

$$V_E = \begin{bmatrix} Q_{E,1}, & Q_{E,2} \end{bmatrix} \begin{bmatrix} R_{E,1} \\ 0 \end{bmatrix} = Q_{E,1} R_{E,1} \text{ and } V_H = \begin{bmatrix} Q_{H,1}, & Q_{H,2} \end{bmatrix} \begin{bmatrix} R_{H,1} \\ 0 \end{bmatrix} = Q_{H,1} R_{H,1}.$$

4: Define the orthonormal matrix

$$\bar{V} = \begin{bmatrix} V_E & 0 \\ 0 & V_H \end{bmatrix} \in \mathbb{C}^{n \times 2n_r}.$$

5: Compute the real-valued orthonormal matrix from the QR decomposition (4.1.4) and determine the real-valued reduced order model from the corresponding Galerkin projection.

For model problems of Maxwell's equations, the first two conditions of Theorem 4.1.3 remain valid for the reduced order model due to the application of the Galerkin projection $\Pi = VV^{\mathrm{T}}$ or $\Pi = \bar{V}\bar{V}^{\mathrm{T}}$, respectively. Hence, we only have to consider the regularity of the reduced order matrix pencil $\lambda\tilde{\mathcal{E}} - \tilde{\mathcal{A}}$, $\lambda \in \mathbb{C}$.

The matrix $\mathcal{A}$ corresponding to the first-order linear dynamical system of Maxwell's equations (3.0.1) is singular due to the large nullspace of the curl-operator. Indeed, the employment of the projection onto the space of the discrete, divergence-free functions leads to a regular matrix $\mathcal{A}$. In view of model order reduction, we only have to ensure that the discrete divergence conditions are preserved for the electric and magnetic field components during the computation of a reduced order model. A divergence-free control input matrix $\mathcal{B} \in \mathbb{R}^{n \times m}$ and a divergence-free control output matrix $\mathcal{C} \in \mathbb{R}^{p \times n}$ already ensure the preservation of the discrete divergence conditions with respect to a structure-preserving reduced order model, see [19].

The reliable choice of a single expansion point represents a major disadvantage of the SPRIM algorithm. If the choice of an expansion point is obtained from a set of discrete points in the given frequency range, e.g. $\mathcal{S} \subset \imath[f_{\min}, f_{\max}]$, an accurate reduced order model may be

expected in the vicinity of the given expansion point, see [54]. For example, a natural way of choosing a single expansion point would be the geometric mean of the frequency range under consideration, see [26].

Since we mainly consider high-frequency model problems of Maxwell's equations maintaining a frequency range of several gigahertz, a reliable application of moment matching methods with single expansion points seems only possible for a small class of model problems of the Maxwell's equations.

4.2 Moment matching with adaptive expansion point selection

The natural extension of moment matching methods with a single expansion point uses the introduction of a set of expansion points, see [56, 74, 90]. Moment matching methods with multiple expansion points require a reliable expansion point selection strategy in order to benefit from the multiple expansion of the transfer function. Here, a distinction is usually made between two different concepts of an adaptive expansion point selection. On the one hand, a greedy-type expansion point selection strategy subsequently selects the different sets of expansion points based on a heuristic error estimation [39, 40, 71], while on the other hand expansion points may be chosen optimally in the sense of a given norm, e.g. the optimal $\mathbb{H}_2$ model order reduction [56].

In the following, we will present a greedy-type expansion point selection strategy on the basis of an approximation of the upper bound of the output moment error. Since moment matching methods with multiple expansion points are primarily based on rational Krylov subspace methods, the advantage of the proposed strategy is the connection between the rational Arnoldi-type method and a heuristic error estimation with respect to the output moment error, see [19].

4.2.1 The adaptive-order rational Arnoldi method

Rational Arnoldi-type methods allow for the computation of a reduced order model for a given set of expansion points $\mathcal{S}_l = \{s_1, \ldots, s_l\}$, $s_i \in \mathbb{C}$, $(i = 1, \ldots, l)$. The advantage of the adaptive-order rational Arnoldi (AORA) method follows from the adaptive selection of the dimension of each Krylov subspace corresponding to the maximum output moment error, see [74].

To begin with, the Taylor expansion of the transfer function $\mathcal{H}(s)$ at each expansion point $s_i \in \mathcal{S}_l = \{s_1, \ldots, s_l\}$ is constituted by

$$\mathcal{H}(s) = \sum_{j=0}^{\infty} \mathcal{C}X^{(j)}(s_i)(s - s_i)^j \equiv \sum_{j=0}^{\infty} Y^{(j)}(s_i)(s - s_i)^j,$$

where

$$X^{(j)}(s_i) = \left[-(s_i\mathcal{E} - \mathcal{A})^{-1}\mathcal{E}\right]^j (s_i\mathcal{E} - \mathcal{A})^{-1}\mathcal{B} \quad \text{and} \quad Y^{(j)}(s_i) = \mathcal{C}X^{(j)}(s_i) \tag{4.2.1}$$

for all $i = 1, \ldots, l$, see [74]. The state and output moments of the reduced order model are denoted by

$$\tilde{X}^{(j)}(s_i) = \left[-(s_i\tilde{\mathcal{E}} - \tilde{\mathcal{A}})^{-1}\tilde{\mathcal{E}}\right]^j (s_i\tilde{\mathcal{E}} - \tilde{\mathcal{A}})^{-1}\tilde{\mathcal{B}} \quad \text{and} \quad \tilde{Y}^{(j)}(s_i) = \tilde{\mathcal{C}}\tilde{X}^{(j)}(s_i), \tag{4.2.2}$$

respectively. The expansion of the transfer function at each expansion point $s_i \in \mathcal{S}_l$ yields an extension of the definition of the *input Krylov subspace* (4.1.2) such that

$$\mathcal{K}_{j_i}(s_i) \equiv \mathcal{K}_{j_i}(-(s_i\mathcal{E} - \mathcal{A})^{-1}\mathcal{E}, (s_i\mathcal{E} - \mathcal{A})^{-1}\mathcal{B}) \quad \text{for all} \quad i = 1, \ldots, l. \tag{4.2.3}$$

The Galerkin projection for the computation of the reduced order model is based on the expansion points $\mathcal{S}_l \subset \mathbb{C}$ using the subspace

$$\mathcal{K}_{j_1,\ldots,j_l}(\mathcal{S}_l) = \operatorname{colspan}\left[X^{(0)}(s_1), \ldots, X^{(j_1-1)}(s_1), \ldots, X^{(0)}(s_l), \ldots, X^{(j_l-1)}(s_l)\right], \tag{4.2.4}$$

where $j_1, \ldots, j_l > 0$ refer to the dimensions of each Krylov subspace (4.2.3). In view of the number of iteration steps $n_r = j_1 + \ldots + j_l$ of a rational Arnoldi-type method, an important task affects the selection of each single dimension $j_1, \ldots, j_l > 0$ corresponding to a given set of expansion points.

The computation of an orthonormal matrix $V \in \mathbb{C}^{n\times n_r}$ corresponding to the subspace (4.2.4) could be achieved by subsequently applying the SPRIM algorithm to each expansion point $s_i \in \mathcal{S}_l$ $(i = 1, \ldots, l)$ followed by a QR decomposition. Let

$$\operatorname{colspan}\left[X^{(0)}(s_i), \ldots, X^{(j_i-1)}(s_i)\right] \subseteq \operatorname{colspan}\left(V^{(i)}\right)$$

denote the orthonormal matrix obtained via the SPRIM algorithm applied to the expansion point $s_i \in \mathbb{C}$. In order to obtain an orthonormal matrix for the Galerkin projection, the relation $\left(V^{(i)}\right)^{\mathrm{T}} V^{(j)} = 0$ must hold for all $i, j = 1, \ldots, l$, $i \neq j$. For this reason, the Galerkin projection may be characterized by

$$\Pi = Q_{V,1}Q_{V,1}^{\mathrm{T}}, \quad \text{where} \quad \left[V^{(1)}, \ldots, V^{(l)}\right] \equiv \begin{bmatrix} Q_{V,1} & Q_{V,2} \end{bmatrix} \begin{bmatrix} R \\ 0 \end{bmatrix} = Q_{V,1}R.$$

Note that $Q_{V,1} \in \mathbb{C}^{n\times n_r}$ and $Q_{V,2} \in \mathbb{C}^{n\times(n-n_r)}$ refer to as orthonormal matrices with

$$\operatorname{colspan}\left[V^{(1)}, \ldots, V^{(l)}\right] \subseteq \operatorname{colspan}\left(Q_{V,1}\right),$$

while $R \in \mathbb{C}^{n_r\times n_r}$ denotes an upper triangular matrix. Since the explicit orthonormalization of the columns of each matrix block $V^{(i)} \in \mathbb{C}^{n\times j_i}$ is rather inefficient for practical applications,

rational Arnoldi-type methods already include the modified Gram-Schmidt procedure in each iteration step, see [102].

The details of the computation of a reduced order model with the *rational Arnoldi method* for Maxwell's equations are summarised in Algorithm 3, see [74]. Previous results on a structure-preserving Galerkin projection have also been taken into account for rational Arnoldi-type methods, see [19]. Moreover, the application of the rational Arnoldi method in model order reduction matches the system and the output moments of the full-order and reduced order model (4.2.1) and (4.2.2) as follows:

$$X^{(j)}(s_i) = V\tilde{X}^{(j)}(s_i) \qquad \text{and} \qquad Y^{(j)}(s_i) = \tilde{Y}^{(j)}(s_i), \tag{4.2.5}$$

where $i = 1, \ldots, l$ and $j = 0, \ldots, j_i - 1$, cf. Theorem 1 in [74]. The moment matching property (4.2.5) is a straightforward extension of Lemma 4.1.1 with respect to the expansion points $s_1, \ldots, s_l \in \mathbb{C}$.

The adequate behaviour of the modified Gram-Schmidt procedure in the rational Arnoldi method is implied by the following lemma given by Grimme et al. [52].

Lemma 4.2.1 ([52, Appendix, Lemma 1])**.** *If $s_1 \in \mathbb{C}$ and $s_2 \in \mathbb{C}$ denote two different expansion points, the relation*

$$(\mathcal{A} - s_2\mathcal{E})^{-1}\mathcal{E}\left[(\mathcal{A} - s_1\mathcal{E})^{-1}\mathcal{E}\right]^{j_1-1}(\mathcal{A} - s_1\mathcal{E})^{-1}\mathcal{B} \in \operatorname{span}\left\{(\mathcal{A} - s_2\mathcal{E})^{-1}\mathcal{B}\right\} \cup \mathcal{K}_{j_1}\left((\mathcal{A} - s_1\mathcal{E})^{-1}\mathcal{E}, (\mathcal{A} - s_1\mathcal{E})^{-1}\mathcal{B}\right)$$

holds for all $j_1 > 0$.

Essentially, Lemma 4.2.1 stems from the relationship

$$(s_2 - s_1)(\mathcal{A} - s_2\mathcal{E})^{-1}\mathcal{E}(\mathcal{A} - s_1\mathcal{E})^{-1} = (\mathcal{A} - s_2\mathcal{E})^{-1} - (\mathcal{A} - s_1\mathcal{E})^{-1}, \tag{4.2.6}$$

which implies that the application of the matrix $(\mathcal{A} - s_2\mathcal{E})^{-1}\mathcal{E}$ to an orthonormal vector of the Krylov subspace $\mathcal{K}_{j_1}(s_1)$ contains a component of each Krylov subspace $\mathcal{K}_{j_1}(s_1)$ and $\mathcal{K}_1(s_2)$, cf. (4.2.3), belonging to the expansion points $s_1 \in \mathbb{C}$ and $s_2 \in \mathbb{C}$. The original formulation of the rational Arnoldi method given by Ruhe [101] computes the initial residual of the subsequent Krylov subspace via $r_k = -(s_{i+1}\mathcal{E} - \mathcal{A})^{-1}\mathcal{E}v_{k-1}$, cf. line 7 in Algorithm 3. Although this approach gives the impression to lead to a better numerical stability during numerical experiments, the initialization of the subsequent Krylov subspace usually follows from $r_k = (s_{i+1}\mathcal{E} - \mathcal{A})^{-1}\mathcal{B}$ allowing for an analytical expression of the output moment error [74].

The major drawback of the rational Arnoldi method is that it requires to prescribe the expansion points and their corresponding dimensions $j_i > 0$ of each Krylov subspace $\mathcal{K}_{j_i}(s_i)$ $(i = 1, \ldots, l)$ in advance. Due to the fact that moment matching methods do not provide an

Algorithm 3 The rational Arnoldi method [74] for Maxwell's equations

Input: Descriptor system $(\mathcal{E}, \mathcal{A}, \mathcal{B}, \mathcal{C})$ of first-order Maxwell's equations (3.0.1); set of expansion points $\mathcal{S}_l = \{s_1, \ldots, s_l\} \subset \mathbb{C}$ with corresponding dimensions $j_1, \ldots, j_l > 0$.

Output: Structure-preserving and real-valued reduced order model $(\tilde{\mathcal{E}}, \tilde{\mathcal{A}}, \tilde{\mathcal{B}}, \tilde{\mathcal{C}})$ of dimension $n_d = 4n_r$.

$r_0 = (s_1\mathcal{E} - \mathcal{A})^{-1}\mathcal{B}$ % Initialize first Krylov subspace
for $i = 1, \ldots, l$ **do**
  for $j = 1, \ldots, j_i$ **do**
    $k = \sum_{c=1}^{i-1} j_c + j$
    $v_k = r_{k-1} / \| r_{k-1} \|_2$ % New orthonormal vector
    if $j = j_i$ and $i \leq l$ **then**
      $r_k = (s_{i+1}\mathcal{E} - \mathcal{A})^{-1}\mathcal{B}$ % Initialize subsequent Krylov subspace
    else
      $r_k = -(s_i\mathcal{E} - \mathcal{A})^{-1}\mathcal{E}v_k$ % New vector of Krylov subspace
    end if
    for $t = 1, \ldots, k$ **do**
      $r_k = r_k - (v_t^{\mathrm{T}} r_k) v_t$ % Modified Gram-Schmidt procedure
    end for
  end for
end for
Application of the QR decompositions (4.1.4) and (4.1.7) to the orthonormal matrix $V = [v_1, \ldots, v_{n_r}] \in \mathbb{C}^{n \times n_r}$ leading to $\bar{V} \in \mathbb{R}^{n \times 4n_r}$.
Compute the reduced order model using the Galerkin projection $\Pi = \bar{V}\bar{V}^{\mathrm{T}}$.

a-priori error estimation, an extension of the rational Arnoldi method allows for the adaptive computation of each dimension corresponding to the different Krylov subspaces.

Following the presentation of Lee et al. [74], we introduce the *output moment error*

$$E_{n_r}(s) = \mathcal{H}(s) - \tilde{\mathcal{H}}(s) \equiv Y^{(0)}(s) - \tilde{Y}^{(0)}(s), \tag{4.2.7}$$

where the reduced order transfer function is obtained via the Galerkin projection $\Pi = VV^{\mathrm{T}}$ after $n_r = j_1 + \ldots + j_l > 0$ iteration steps of the rational Arnoldi method. In addition, Lee et al. also refer to (4.2.7) as the *transfer function error*.

Assuming that the output moments $Y^{(j)}(s_i)$ and $\tilde{Y}^{(j)}(s_i)$ match for all $i = 1, \ldots, l$ and $j = 0, 1, \ldots, j_i - 1$, the output moment error may be written in the form

$$E_{n_r}(s) = \left(Y^{(j_i)}(s_i) - \tilde{Y}^{(j_i)}(s_i)\right)(s - s_i)^{j_i} + \mathcal{O}\left((s - s_i)^{j_i+1}\right).$$

The main observation by Lee et al. [74] is that the j_i-th output moment error of the expansion point $s_i \in \mathcal{S}_l$ may be computed as a by-product of the rational Arnoldi method.

Theorem 4.2.2 ([74, Theorem 2]). *Let the output moments $Y^{(j)}(s_i)$ and $\tilde{Y}^{(j)}(s_i)$ coincide for all $i = 1, \ldots, l$ and $j = 0, 1, \ldots, j_i - 1$. The computation of a reduced order model with the Galerkin projection $\Pi = VV^{\mathrm{T}}$, where the columns of the orthonormal matrix $V \in \mathbb{C}^{n \times n_r}$ span the subspace (4.2.4), leads to the j_i-th output moment error of the expansion point $s_i \in \mathcal{S}_l = \{s_1, \ldots, s_l\}$ satisfying*

$$| E_{n_r}^{(j_i)}(s_i) | \equiv | Y^{(j_i)}(s_i) - \tilde{Y}^{(j_i)}(s_i) | = | \mathcal{C}h_\pi(s_i) r^{(q)}(s_i) |, \tag{4.2.8}$$

where $h_\pi(s_i) = \prod_j \| r^{(j-1)}(s_i) \|_2$. If the i-th expansion point has been selected in the j-th iteration step of the rational Arnoldi method, then $r^{(j)}(s_i)/\| r^{(j)}(s_i) \|_2$ denotes the j-th column vector of the orthonormal matrix $V \in \mathbb{C}^{n \times n_r}$. More precisely, it follows that $r^{(j)}(s_i) \equiv -(s_i\mathcal{E} - \mathcal{A})^{-1}\mathcal{E}v_{j-1}$ and $r^{(j)}(s_k) \equiv r^{(j-1)}(s_k)$ for all $k = 1, \ldots, l$ with $k \neq i$.

Although the previous result has been initially developed for single-input, single-output descriptor systems, the relation (4.2.8) remains valid for multiple-input, multiple-output linear dynamical systems with respect to the Frobenius norm $\| \cdot \|_F$, see [39].

Note that employing (4.2.8) as a measure to select the subsequent expansion point in a rational Arnoldi-type method avoids the a-priori knowledge of the dimensions $j_1, \ldots, j_l > 0$ corresponding to each Krylov subspace $\mathcal{K}_{j_i}(s_i)$ $(i = 1, \ldots, l)$. By computing the output moment error in each iteration step, the subsequent orthonormal vector $v_{q+1} \in V$ belongs to the expansion point with the maximum output moment error

$$\max_{s_i \in \mathcal{S}_l} | Y^{(\hat{j}_i)}(s_i) - \hat{Y}^{(\hat{j}_i)}(s_i) | = \max_{s_i \in \mathcal{S}_l} | \mathcal{C}h_\pi(s_i) r^{(q)}(s_i) |.$$

In contrast to Algorithm 3, we simply require one iteration loop $j = 1, \ldots, n_r$ for the given number of iteration steps $n_r > 0$, where each step starts computing the maximum output moment error. Therefore, we require a residual vector for each expansion point, but not one subsequently updated residual vector. After updating the sequence of residual vectors $r^{(j)}(s_1)$, …, $r^{(j)}(s_l)$ according to Theorem 4.2.2, the application of the modified Gram-Schmidt procedure to each residual vector leads to the computation of the orthonormal vector sequence V corresponding to the subspace (4.2.4). The resulting algorithm is referred to as *adaptive-order rational Arnoldi* method [74].

Independent of the way selecting the different expansion points in each iteration step, a variant of the rational Arnoldi method is equivalent to the rational Arnoldi method given in Algorithm 3, as long as the dimensions of each Krylov subspace $\mathcal{K}_{j_1}(s_1), \ldots \mathcal{K}_{j_l}(s_l)$ coincide.

Corollary 4.2.3. *Let $s_1, \ldots, s_l \in \mathbb{C}$ denote a given set of expansion points. Moreover, assume that the rational Arnoldi method, cf. Algorithm 3, employs $j_1, \ldots, j_l$ iteration steps for each expansion point s_i*

$(i = 1, \ldots, l)$ such that $n_r = j_1 + \ldots + j_l$. If a variant of the rational Arnoldi method employs an expansion point selection criterion leading to the same dimensions $j_1, \ldots, j_l$, it is equal to the rational Arnoldi method.

Proof. Subsequently applying Lemma 4.2.1 to the already known orthonormal vector sequence $v_1, \ldots, v_q \in V$ $(q = 1, \ldots, n_r)$ of the rational Arnoldi and the variant of the rational Arnoldi method leads to an orthonormal basis of the subspace (4.2.4). The assumption that the dimensions $j_1, \ldots, j_l > 0$ coincide in both methods leads to the statement of the Corollary. □

As seen in the rational Arnoldi method, the Galerkin projection of every rational Arnoldi-type method already ensures the preservation of the block-structure in the reduced order model of Maxwell's equations, cf. line 16 in Algorithm 3.

In view of the output moment error, the AORA method represents the most natural choice of a rational Arnoldi-type method with multiple expansion points for model order reduction with moment matching methods. For rational Arnoldi-type methods the major problem that still has to be discussed is the adequate choice of expansion points. Due to the lack of an a-priori error bound for moment matching methods, a reliable heuristic error estimation becomes indispensable.

4.2.2 Heuristic error estimation

The accuracy of the reduced order model of a first- or second-order linear dynamical system is measured by the relative error

$$\epsilon_{\mathrm{rel}}(f) \equiv \frac{\| \mathcal{H}(\imath\omega) - \tilde{\mathcal{H}}(\imath\omega) \|}{\| \mathcal{H}(\imath\omega) \|},$$

where $\omega = 2\pi f$ with $f \in [f_{\min}, f_{\max}]$ and $\imath = \sqrt{-1}$. Here, we employ the absolute value $|\cdot|$ for single-input, single-output (SISO) descriptor systems, while the relative error of multiple-input, multiple-output linear dynamical systems makes use of the Frobenius norm $\|\cdot\|_F$.

Independent of the given norm, the relative error $\epsilon_{\mathrm{rel}}(f)$ is typically not available during practical applications, because the computation of the transfer function $\mathcal{H}(s)$ becomes necessary for several discrete points in the frequency range $\mathcal{S} \subset \imath[f_{\min}, f_{\max}]$. In this case, we would require solving a sequence of high-dimensional shifted linear system

$$\mathcal{H}(s) = \mathcal{C}(s\mathcal{E} - \mathcal{A})^{-1}\mathcal{B}, \quad s \in \mathcal{S}.$$

Since an important aim of the thesis at hand is to establish an efficient offline-phase in moment matching methods, e.g. keeping the number of solving shifted linear systems as small as possible, the explicit computation of the transfer function corresponding to the full-order model problem is rather infeasible.

Nevertheless, a well-known approach for moment matching methods emerges from the computation of a sequence of reduced order models within an iterative approach, see [54]. More precisely, the rationale behind the application of moment matching methods with multiple expansion points is as follows:

$$\text{Compute a sequence of reduced order models } \tilde{\mathcal{H}}_1(s), \ldots, \tilde{\mathcal{H}}_k(s) \tag{4.2.9}$$

for a nested sequence of sets of expansion points $\mathcal{S}_{i+1} = \mathcal{S}_i \cup \{s_{i+1}\}$, $s_{i+1} \in \mathbb{C}$, $(i = 0, \ldots, k-1)$, where $\mathcal{S}_0 \subset \mathbb{C}$ refers to as the initial set of expansion points. The initial set of expansion points is typically chosen in a heuristic way, see [19].

Due to the fact that $n_r \ll n$, the computational costs of evaluating each transfer function $\tilde{\mathcal{H}}_i(s)$ $(i = 1, \ldots, k)$ are small for a given set of sampling points in the frequency range. Hence, Grimme et al. have introduced the relative error[2] between two subsequent reduced order models

$$\hat{\delta}_i \equiv \hat{\delta}_i(s) = \frac{\| \tilde{\mathcal{H}}_i(s) - \tilde{\mathcal{H}}_{i-1}(s) \|}{\| \tilde{\mathcal{H}}_i(s) \|}$$

and provided an extension for a heuristic measurement[2] of the relative error $\epsilon_{\text{rel}}(f) > 0$ in the following way:

$$\hat{\epsilon}_k \equiv \hat{\epsilon}_k(s) = \sum_{i=1}^{k-1} 2^{i-(k-1)} \hat{\delta}_{i+1}(s). \tag{4.2.10}$$

A major drawback of the heuristic error estimation (4.2.10) is that a small value of $\hat{\epsilon}_k > 0$ does not indicate whether convergence or stagnation of the relative error $\epsilon_{\text{rel}}(f) > 0$ has occurred, see [54].

Typically, a significant improvement of the accuracy of the reduced order model may be expected in the vicinity of an expansion point $s_i \in \mathbb{C}$, which has not been considered during the previous iteration steps $\tilde{\mathcal{H}}_1(s), \ldots, \tilde{\mathcal{H}}_{i-1}(s)$. This leads to a large relative error $\hat{\delta}_i > 0$ and consequently $\hat{\epsilon}_k > 0$ in the environment of the latest expansion point $s_i \in \mathbb{C}$. For example, the employment of the discrete frequency point $s_{i+1} \equiv s_* = \imath(2\pi f_*)$ such that

$$s_* = \arg\max_{s \in \mathcal{S}} \hat{\epsilon}_k(s)$$

might lead to the same expansion point as in the previous iteration step of the adaptive expansion point selection. Hence, a careful employment of the heuristic error estimation becomes indispensable in order to avoid a misleading interpretation of $\hat{\epsilon}_k > 0$ or $\hat{\delta}_i > 0$, respectively, see [54, 113].

[2] The norm $\| \cdot \|$ refers either to the absolute value $| \cdot |$ or to the Frobenius norm $\| \cdot \|_F$ depending on the number of inputs and outputs of the linear dynamical system.

4.2.3 Moment matching methods with rational Krylov subspaces

The application of rational Arnoldi-type methods in the context of *optimal* $\mathbb{H}_2$ *model order reduction* has been recently discussed, see [56]. Here, the computation of the transfer function of a reduced order model $\tilde{\mathcal{H}}(s)$ is based on the optimization problem

$$\min_{\tilde{\mathcal{H}}(s)\in\mathbb{C}^{p\times m}} \| \mathcal{H}(s) - \tilde{\mathcal{H}}(s) \|_{\mathbb{H}_2}.$$

Solving the optimization problem in optimal $\mathbb{H}_2$ model order reduction leads to the first-order necessity conditions of $\mathbb{H}_2$-optimality, i.e.

$$\mathcal{H}\left(-\tilde{\lambda}_i\right) = \tilde{\mathcal{H}}\left(-\tilde{\lambda}_i\right) \quad \text{and} \quad \mathcal{H}'\left(-\tilde{\lambda}_i\right) = \tilde{\mathcal{H}}'\left(-\tilde{\lambda}_i\right) \quad \forall\, i = 1, \ldots, n_r,$$

where $\tilde{\lambda}_1, \ldots, \tilde{\lambda}_{n_r} \in \mathbb{C}$ denote the simple poles of the transfer function of the reduced order model, see [83].

The work of Gugercin et al. [56] suggests an efficient numerical algorithm for the computation of a reduced order model satisfying the first-order necessity conditions of optimal $\mathbb{H}_2$ model order reduction. Here, the subsequent iteration steps of the *iterative rational Krylov algorithm* (IRKA) compute the Petrov-Galerkin projection $\Pi = VW^{\mathrm{T}}$ from the *rational input Krylov subspace*

$$V = \operatorname{span}\left\{ (\mathcal{A} + s_1 I)^{-1}\mathcal{B}, \ldots, \prod_{j=1}^{n_r} (\mathcal{A} + s_j I)^{-1}\mathcal{B} \right\} \tag{4.2.11}$$

and the *rational output Krylov subspace*

$$W = \operatorname{span}\left\{ (\mathcal{A} + s_1 I)^{-\mathrm{T}}\mathcal{C}^{\mathrm{T}}, \ldots, \prod_{j=1}^{n_r} (\mathcal{A} + s_j I)^{-\mathrm{T}}\mathcal{C}^{\mathrm{T}} \right\} \tag{4.2.12}$$

such that $W^{\mathrm{T}}V = I$. The expansion points of each iteration step are selected based on the relation $s_i = -\lambda_i$ where $\lambda_i \in \mathbb{C}$ $(i = 1, \ldots, n_r)$ denote the Ritz values of the generalized eigenvalue problem $\tilde{\mathcal{A}}x = \lambda_i \tilde{\mathcal{E}} x$, $x \neq 0$, with $\tilde{\mathcal{E}} = W^{\mathrm{T}}\mathcal{E}V$ and $\tilde{\mathcal{A}} = W^{\mathrm{T}}\mathcal{A}V$. A major drawback of IRKA is that only the latest rational Krylov subspaces $V \in \mathbb{C}^{n\times n_r}$ and $W \in \mathbb{C}^{n\times n_r}$ are used for model order reduction.

In contrast to previous algorithms satisfying the first-order necessity conditions of $\mathbb{H}_2$-optimality, IRKA does not require solving (generalized) Lyapunov equations, see [129]. The idea behind the choice of the expansion points from the Ritz values of the reduced matrix pencil $\lambda\tilde{\mathcal{E}} - \tilde{\mathcal{A}}$, $\lambda \in \mathbb{C}$, has been previously discussed in [56]. Moreover, a Newton-type method of the iterative rational Krylov algorithm leads to a more reliable convergence behaviour [56]. An extension of optimal $\mathbb{H}_2$ model order reduction to multiple-input, multiple-output linear dynamical systems has been given in [24].

Based on the rational Krylov subspace (4.2.11), an adaptive greedy-type expansion point selection for standard space systems has been introduced by Druskin et al., see [31, 32]. In contrast to IRKA, the expansion points are determined by

$$\mathcal{S}_{i+1} = \mathcal{S}_i \cup \{s_{i+1}\} \text{ with } s_{i+1} \in \mathbb{C}. \tag{4.2.13}$$

Since the computation of an orthonormal basis of the rational input Krylov subspace requires solving a sequence of shifted linear systems $(\mathcal{A} - s_i I)x = \mathcal{B}$, an appropriate approach to compute the approximate solution $x \in \mathbb{C}^n$ is based on the *rational Krylov subspace residual*

$$\gamma_{n_r}(s) = \mathcal{B} - (\mathcal{A} - sI)v_{n_r},$$

where $v_{n_r} = V(\tilde{\mathcal{A}} - sI)^{-1}V^{\mathrm{T}}\mathcal{B}$ and $\tilde{\mathcal{A}} = V^{\mathrm{T}}\mathcal{A}V$, see [31]. Then, the rational Krylov subspace residual may be written as the skeleton approximation

$$\gamma_{n_r}(s) = \frac{r_{n_r}(\mathcal{A})\mathcal{B}}{r_{n_r}(-s)}, \quad \text{where} \quad r_{n_r}(z) = \prod_{j=1}^{n_r} \frac{z - \lambda_j}{z + s_j}.$$

Here, $\lambda_j \in \mathbb{C}$ $(j = 1, \ldots, n_r)$ refer to the Ritz values of the matrix $\tilde{\mathcal{A}} \equiv V^{\mathrm{T}}\mathcal{A}V$, where the columns of the orthonormal matrix $V \in \mathbb{C}^{n \times n_r}$ span the rational input Krylov subspace (4.2.11). Finally, the greedy-type expansion point selection determines the subsequent expansion point $s_{i+1} \in \mathbb{C}$ solving the optimization problem

$$s_{i+1} = \arg\left(\max_{s \in \partial S_i} \frac{1}{|\, r_i(s)\,|} \right),$$

where ∂S_i denotes an approximation of the border of the mirrored spectral region of the matrix $\mathcal{A} \in \mathbb{R}^{n \times n}$, see [32].

4.2.4 A survey on greedy-type expansion point selection

We have seen in the previous subsection that the rational Krylov subspaces (4.2.11) and (4.2.12) with an adequate choice of the expansion points $s_1, \ldots, s_{n_r} \in \mathbb{C}$ lead to the computation of a reduced order model in the sense of optimal $\mathbb{H}_2$ model order reduction, see [56]. Apart from the results on optimal $\mathbb{H}_2$ model order reduction, the literature features different greedy-type algorithms leading to an adaptive moment matching method in model order reduction, see [19, 32, 39, 40, 70]. It is important to note that greedy-type algorithms in moment matching methods are usually not employed in order to compute an optimal reduced order model with respect to a given norm.

For the iterative rational Krylov algorithm and the Greedy-type expansion point selection by Druskin et al., the computation of the Petrov-Galerkin projection $\Pi = VW^{\mathrm{T}}$ is obtained via

the unsymmetric rational Lanczos method, see [56]. Additionally, greedy-type adaptive expansion point selection strategies may also allow for the multiple expansion of the transfer function at different expansion points. In this context, the AORA method represents the favourable approach for the computation of the Galerkin projection, because the dimension of each Krylov subspace $\mathcal{K}_{j_i}(s_i)$ $(i = 1, \ldots, l)$ is determined adaptively by means of the output moment error, cf. Theorem 4.2.2.

As opposed to optimal $\mathbb{H}_2$ model order reduction, we will typically select complex-valued expansion points with a real part equal to zero. An extensive analysis by Grimme has shown that the multiple expansion of the transfer function at a real-valued expansion point results in an accurate reduced order model in a large vicinity of the expansion point, see [55]. Instead, purely imaginary-valued expansion points lead to a small relative error for the reduced order model near the vicinity of the expansion point. Practical applications have indicated that the increasing accuracy of complex-valued expansion points offers the favourable approach for a greedy-type expansion point selection strategy, see [19, 55, 113].

In Subsection 4.2.5, we will provide a greedy-type expansion point selection which adaptively selects the subsequent expansion points by an upper bound of the output moment error of the adaptive-order rational Arnoldi method. In order to allow for an appropriate comparison during the numerical experiments in Chapter 6, two different adaptive greedy-type moment matching methods from the literature are briefly reviewed, see [70, 113].

For second-order descriptor systems of machine tool simulations, an adaptive greedy-type expansion point selection for moment matching methods has been presented in [113]. Since a given number of expansion points are selected in a similar way to the iterative rational Krylov algorithm, we refer to the greedy-type expansion point selection as AORA-H2 method, cf. Algorithm 4. The adaptive expansion point selection of the AORA-H2 method may be interpreted as a distance-based expansion point selection with respect to the tolerance $\eta > 0$.

Due to the fact that the AORA-H2 method selects $s_\# > 0$ expansion points in each iteration step, the preferable approach for model order reduction follows from the subsequent computation of an expansion point set by means of $\mathcal{S}_{i+1} = \mathcal{S}_i \cup \{s_{i+1}\}$, $s_{i+1} \in \mathbb{C}$. A major disadvantage of the AORA-H2 method emerges from the following fact: While the latter approach consists of $|\,\mathcal{S}_k\,|$ different shifted linear systems, the AORA-H2 method needs approximately $|\,\mathcal{S}_1\,| + \ldots + |\,\mathcal{S}_k\,|$ different shifted linear systems. Remember that rational Arnoldi-type methods require repeatedly solving the different shifted linear systems depending on the number of selecting each expansion point. Moreover, the AORA-H2 method does not allow for the reuse of an already known orthonormal vector sequence because the expansion points may be completely interchanged between two subsequent iteration steps.

Another drawback of the AORA-H2 method is due to the restriction of the computed Ritz

values in terms of $f_{\min} \leq |\operatorname{Im}(\lambda_i)| \leq f_{\max}$. Since the expansion points are defined by $\sigma_i \equiv \imath|\operatorname{Im}(\lambda_i)|$, cf. line 6 in Algorithm 4, the restriction of the Ritz values might lead to an insufficient number of possible expansion points. In other words, neglecting the restriction of the Ritz values to the frequency range $[f_{\min}, f_{\max}]$ at hand, the accuracy of the reduced order model is increased beyond the frequency range of interest. Nevertheless, numerical experiments have shown that this case rarely occurs, see [39, 113].

Algorithm 4 Adaptive expansion point selection: *AORA-H2 method* [113]

Input: Descriptor system $(\mathcal{E}, \mathcal{A}, \mathcal{B}, \mathcal{C})$; set of expansion points $\mathcal{S}_1 \subset \mathbb{C}$; frequency range $[f_{\min}, f_{\max}]$; dimension of reduced order model n_r; stopping tolerance $\epsilon > 0$; expansion point selection criterion $\eta > 0$; upper bound for number of expansion points $s_{\#} > 0$.

Output: Descriptor system of reduced order model $(\tilde{\mathcal{E}}, \tilde{\mathcal{A}}, \tilde{\mathcal{B}}, \tilde{\mathcal{C}})$.

1: $[\tilde{\mathcal{E}}, \tilde{\mathcal{A}}, \tilde{\mathcal{B}}, \tilde{\mathcal{C}}] = \text{AORA}(\mathcal{E}, \mathcal{A}, \mathcal{B}, \mathcal{C}, n, \mathcal{S}_1)$ with $\tilde{\mathcal{H}}_1(s)$
2: Define $l = 1$ and $\hat{\epsilon} = 1$
3: **while** $\hat{\epsilon} > \epsilon$ **do**
4: Compute Ritz values $\lambda_1, \ldots, \lambda_k$ of matrix pencil $\lambda\tilde{\mathcal{E}} - \tilde{\mathcal{A}}$ with $f_{\min} \leq |\operatorname{Im}(\lambda_i)| \leq f_{\max}$.
5: Reorder the Ritz values: $|\lambda_1| \leq \ldots \leq |\lambda_k|$.
6: Define $\sigma_i \equiv \imath|\operatorname{Im}(\lambda_i)|$ for all $i = 1, \ldots, k$ with $\imath = \sqrt{-1}$.
7: **while** $|\mathcal{S}_{l+1}| < s_{\#}$ **do**
8: Define $s_1 \equiv \sigma_1$ and $s_2 \equiv \sigma_k$ such that $s_1, s_2 \in \mathcal{S}_{l+1} = \{s_1, \ldots, s_{s_{\#}}\}$.
9: Determine expansion points $s_{i+1} \in \mathcal{S}_{l+1}$ by means of $|s_{i+1} - s_i| > \eta$ for all $i = 2, \ldots, s_{\#} - 1$, where $s_{i+1} \in \{\sigma_2, \ldots, \sigma_{k-1}\}$.
10: Adopt expansion point selection tolerance $\eta \equiv \eta/2$.
11: **end while**
12: $[\tilde{\mathcal{E}}, \tilde{\mathcal{A}}, \tilde{\mathcal{B}}, \tilde{\mathcal{C}}] = \text{AORA}(\mathcal{E}, \mathcal{A}, \mathcal{B}, \mathcal{C}, n, \mathcal{S}_{l+1})$ with $\tilde{\mathcal{H}}_{l+1}(s)$
13: Error estimation $\hat{\epsilon} = \frac{1}{2}\hat{\epsilon} + |\tilde{\mathcal{H}}_{l+1}(s) - \tilde{\mathcal{H}}_l(s)|/|\tilde{\mathcal{H}}_{l+1}(s)|$
14: Define $l = l + 1$
15: **end while**

The key ingredient of the adaptive expansion point selection given by Koehler et al. [70] consists of choosing the subsequent expansion point $s_i \in \mathbb{C}$ as the maximum value of the heuristic error expression $\hat{\delta}_i > 0$ and the bisection method. Thereby, the Krylov subspace corresponding to the i-th expansion point is increased by means of the *well-conditioned asymptotic wave evaluation* (WCAWE) method [112] step-by-step, until the heuristic error estimation between two subsequent reduced order models reaches a given tolerance. The bisection method computes the new expansion point either as the midpoint of the two closest previous expansion points or as the lower and upper bound of the expansion points, e.g. $s_{\min} \in \mathbb{C}$ and $s_{\max} \in \mathbb{C}$, see [70]. We refer to the resulting algorithm as AORA-MAX method, cf. Algorithm 5.

Algorithm 5 Adaptive expansion point selection: *AORA-MAX method* [71]

Input: Descriptor system $(\mathcal{E}, \mathcal{A}, \mathcal{B}, \mathcal{C})$; initial expansion points $s_{\min} \in \mathbb{C}$ and $s_{\max} \in \mathbb{C}$; frequency range $[f_{\min}, f_{\max}]$; dimension of reduced order model n_r; stopping tolerance $\epsilon > 0$; local stopping tolerance $\epsilon_0 > 0$; expansion point selection criterion $\eta > 0$.

Output: Descriptor system of reduced order model $(\tilde{\mathcal{E}}, \tilde{\mathcal{A}}, \tilde{\mathcal{B}}, \tilde{\mathcal{C}})$.

1: Compute initial expansion point $\mathcal{S}_1 = \{s_1\}$ with $s_1 = (s_{\max} - s_{\min})/2$.
2: Initialize orthonormal matrix $V = []$.
3: Define $\delta = 1$ and $i = 1$.
4: **while** $(\#\,\mathrm{col}(V) < n_r)$ or $(\delta < \epsilon)$ **do**
5: Define $l = 1$.
6: **while** $\delta < \epsilon_0$ **do**
7: $Q_i = \mathrm{WCAWE}(l, s_i, \mathcal{E}, \mathcal{A}, \mathcal{B})$
8: Orthonormalization of $V = [V, Q_i]$ such that $V^{\mathrm{T}}V = I$.
9: Determine reduced order model $\tilde{\mathcal{E}} = V^{\mathrm{T}}\mathcal{E}V, \tilde{\mathcal{A}} = V^{\mathrm{T}}\mathcal{A}V, \tilde{\mathcal{B}} = V^{\mathrm{T}}\mathcal{B}, \tilde{\mathcal{C}} = \mathcal{C}V$ with the corresponding transfer function $\tilde{\mathcal{H}}(s)$.
10: Heuristic error estimation $\delta(s) = |\,\tilde{\mathcal{H}}(s) - \tilde{\mathcal{H}}_{\mathrm{old}}(s)\,|/|\,\tilde{\mathcal{H}}(s)\,|$.
11: Define $\tilde{\mathcal{H}}_{\mathrm{old}}(s) \equiv \tilde{\mathcal{H}}(s)$ and $l = l + 1$.
12: **end while**
13: Compute $s_\star = \arg\max_s \delta(s)$.
14: Determine new expansion point $s_{i+1} \in \mathbb{C}$ via the bisection method between $(s_{\min}, s_1, \ldots, s_{i-1}, s_{\max})$ and $s_\star \in \mathbb{C}$.
15: Define $i = i + 1$.
16: **end while**

Remark 4.2.4. *Since the adaptive-order rational Arnoldi method represents the key ingredient of the proposed Greedy-type adaptive expansion point selection in Subsection 4.2.5, we do not have employed the WCAWE method in line 7 of Algorithm 5, but rather the AORA method for the expansion points $s_1, \ldots, s_i \in \mathbb{C}$. For this reason, we leave out the reinitialization of $l = 1$, cf. line 5 of Algorithm 5, and the orthonormalization step in line 8 of Algorithm 5.*

Nevertheless, numerical experiments with linear dynamical systems of Maxwell's equations have shown that the expansion point selection strategy by means of the bisection method, cf. line 14 of Algorithm 5, may lead to a poor convergence behaviour. For example, applying a simple sampling strategy with evenly distributed expansion points in the frequency range may already lead to an improving accuracy of the reduced order model. Be aware that the latter case does not necessarily refer to as an adaptive expansion point selection via $\mathcal{S}_{i+1} = \mathcal{S}_i \cup \{s_{i+1}\}$, $s_{i+1} \in \mathbb{C}$, but still makes use of the relative error between subsequently computed reduced order models.

Any expansion point selection strategy based on the heuristic error estimation by Grimme et al. offers a major disadvantage in the case of a misleading interpretation of $\hat{\delta}_i > 0$ or $\hat{\epsilon}_k > 0$ has not been recognized, see [54]. Nevertheless, numerical experiments have shown that the expansion points of the AORA-MAX method are typically evenly distributed in the interval $\imath[f_{\min}, f_{\max}]$ as observed for the AORA-H2 method, see [70].

The literature features other moment matching methods with an adaptive greedy-type expansion point selection, see [40,109]. For example, Fehr et al. have given an adaptive expansion point selection based on the output moment error $E_{n_r}(s) > 0$, see [40]. More precisely, the subsequent expansion point is selected subject to the maximum of $E_{n_r}(s) > 0$ for a given discrete set of points in the frequency range $[f_{\min}, f_{\max}]$. Remember that an explicit expression of the output moment error can be obtained as a by-product of the rational Arnoldi method, cf. (4.2.8). In Subsection 4.2.5, we employ an appropriate approximation of an upper bound of the output moment error for the adaptive greedy-type expansion point selection.

Each greedy-type expansion point selection might make use of the heuristic error estimation (4.2.10) leading to an approximation of the relative error $\epsilon_{\mathrm{rel}}(f) > 0$. For the AORA-RK method, we will additionally employ an upper bound of the number of expansion points corresponding to the given iteration steps $n_r > 0$ in order to properly benefit from the multiple expansion of the transfer function at different expansion points. Moreover, the application of the adaptive-order rational Arnoldi method in the AORA-H2 and AORA-MAX method ensures the computation of a structure-preserving reduced order model with a real-valued matrix quadruplet.

4.2.5 Adaptive expansion point selection with rational Krylov residuals

In the following, we introduce a new greedy-type expansion point selection strategy on the basis of an approximation of an upper bound of the output moment error (4.2.8), see [19]. To begin with, the key ingredient of the greedy-type expansion point selection is reviewed in the following lemma.

Lemma 4.2.5. *Let $\mathcal{S}_m = \{s_1, \ldots, s_m\} \subset \mathbb{C}$ denote a given set of expansion points with the corresponding orthonormal basis $V \in \mathbb{C}^{n \times n_r}$ computed by the AORA method, cf. (4.2.4). Moreover, the matrix pencils of the full- and reduced-order model problem are given by $\mathcal{P}(s) = s\mathcal{E} - \mathcal{A}$ and $\tilde{\mathcal{P}}(s) = s\tilde{\mathcal{E}} - \tilde{\mathcal{A}}$, where $\tilde{\mathcal{E}} = V^{\mathrm{T}}\mathcal{E}V$ and $\tilde{\mathcal{A}} = V^{\mathrm{T}}\mathcal{A}V$. Then, the following relation holds*

$$|\, Y^{(0)}(s) - \tilde{Y}^{(0)}(s)\,| \leq |\, \mathcal{C}\mathcal{P}(s)^{-1}\,|\,|\, h_n(s)\,| \;\approx\; |\, \tilde{\mathcal{C}}\tilde{\mathcal{P}}(s)^{-1}\,|\,|\, h_n(s)\,|, \tag{4.2.14}$$

where $h_n(s) = \mathcal{B} - \mathcal{P}(s)V\tilde{\mathcal{P}}(s)^{-1}\tilde{\mathcal{B}}$ and $\tilde{\mathcal{B}} = V^{\mathrm{T}}\mathcal{B}$.

Proof. A straightforward computation leads to the first part of the statement of the lemma

$$\begin{aligned} |\, Y^{(0)}(s) - \tilde{Y}^{(0)}(s)\,| &= |\, \mathcal{C}\left[\mathcal{P}(s)^{-1}\mathcal{B} - V_n\tilde{\mathcal{P}}(s)^{-1}V_n^{\mathrm{T}}\mathcal{B}\right]| \\ &= |\, \mathcal{C}\mathcal{P}(s)^{-1}\left[\mathcal{B} - \mathcal{P}(s)V_n\tilde{\mathcal{P}}(s)^{-1}V_n^{\mathrm{T}}\mathcal{B}\right]| \\ &\leq |\, \mathcal{C}\mathcal{P}(s)^{-1}\,||\, h_n(s)\,|. \end{aligned}$$

An approximation of the upper bound is given by employing the reduced order matrix quadruplet $(\tilde{\mathcal{E}}, \tilde{\mathcal{A}}, \tilde{\mathcal{B}}, \tilde{\mathcal{C}})$ for the linear system $\mathcal{C}\mathcal{P}(s)^{-1}$, which completes the proof. □

The previous lemma paves the way for an adaptive greedy-type expansion point selection (4.2.13) on the basis of the relation

$$s_{m+1} = \arg\max_{s\in\mathcal{S}} |\, \tilde{\mathcal{C}}\tilde{\mathcal{P}}(s)^{-1}\,||\, h_n(s)\,|, \tag{4.2.15}$$

where $\mathcal{S} \subset \imath[f_{\min}, f_{\max}]$ represents a set of sampling points in the frequency range. We refer to the expansion point selection strategy as AORA-RK method.

The motivation of the AORA-RK method mainly arises out of the rational Krylov residual $\gamma_n(s)$ and the extension to the adaptive-order rational Arnoldi method by $h_n(s) = \mathcal{B} - \mathcal{P}(s_{m+1})V\tilde{\mathcal{P}}(s_{m+1})^{-1}\tilde{\mathcal{B}}$, cf. Lemma 4.2.5. More precisely, the extension of the rational Krylov residual allows for a suitable measure of the reliability of the orthonormal matrix $V \in \mathbb{C}^{n\times n_r}$ with respect to the control input matrix pair $(\mathcal{B}, \tilde{\mathcal{B}})$ in model order reduction.

Algorithm 6 Adaptive expansion point selection: *AORA-RK method* [19]

Input: Descriptor system $(\mathcal{E}, \mathcal{A}, \mathcal{B}, \mathcal{C})$; initial expansion points $s_0 \in \mathbb{C}$ and $s_1 \in \mathbb{C}$; frequency range $[f_{\min}, f_{\max}]$; dimension of reduced order model n; stopping tolerance ϵ; maximum number of expansion points $s_{\#} > 0$.

Output: Descriptor system of reduced order model $(\tilde{\mathcal{E}}, \tilde{\mathcal{A}}, \tilde{\mathcal{B}}, \tilde{\mathcal{C}})$.

1: Set $\mathcal{S}_1 = \{s_0, s_1\}$
2: $[\tilde{\mathcal{E}}, \tilde{\mathcal{A}}, \tilde{\mathcal{B}}, \tilde{\mathcal{C}}] = \mathrm{AORA}(\mathcal{E}, \mathcal{A}, \mathcal{B}, \mathcal{C}, n, \mathcal{S}_1)$ with $\tilde{\mathcal{H}}_1(s)$
3: Define $\hat{\epsilon} = 1$ and $k = 1$
4: **while** $(\hat{\epsilon} > \epsilon)$ or $(|S_k| < s_{\#})$ **do**
5: Compute the subsequent expansion point $s_{k+1} \in \mathbb{C}$ by means of (4.2.15) on the basis of a set of sampling points $\mathcal{S} \subset \imath[f_{\min}, f_{\max}]$ from the frequency range.
6: Set $\mathcal{S}_{k+1} = \mathcal{S}_k \cup \{s_{k+1}\}$
7: $[\tilde{\mathcal{E}}, \tilde{\mathcal{A}}, \tilde{\mathcal{B}}, \tilde{\mathcal{C}}] = \mathrm{AORA}(\mathcal{E}, \mathcal{A}, \mathcal{B}, \mathcal{C}, n, \mathcal{S}_{k+1})$ with $\tilde{\mathcal{H}}_{k+1}(s)$
8: Error estimation $\hat{\epsilon} = \frac{1}{2}\hat{\epsilon} + |\, \tilde{\mathcal{H}}_{k+1}(s) - \tilde{\mathcal{H}}_k(s)\,|/|\, \tilde{\mathcal{H}}_{k+1}(s)\,|$
9: $k = k + 1$
10: **end while**

We do not claim to achieve an exact representation of the relative error $\epsilon_{\mathrm{rel}}(f) > 0$ by means of the upper bound of the output moment error in moment matching based model order reduction. At least, a proper subset out of the set of sampling points $\mathcal{S} \subset \mathbb{C}$ corresponding to the largest relative error components $\epsilon_{\mathrm{rel}}(f) > 0$ may be obtained. Since the employment of purely imaginary expansion points in a greedy-type expansion point selection ensures a small relative error in a large vicinity of the expansion point, an adequate approximation of the frequency range corresponding to the largest relative error components $\epsilon_{\mathrm{rel}}(f) > 0$ is already sufficient in many cases.

As an extension of the AORA-RK method, we may think about the computation of (4.2.15) belonging to different regions of the set of sampling points, e.g. $\mathcal{S} \equiv \tilde{\mathcal{S}}_1 \cup \ldots \cup \tilde{\mathcal{S}}_k$ with $\tilde{\mathcal{S}}_i \subset \imath[f_{\min}, f_{\max}]$ and $\tilde{\mathcal{S}}_i \cap \tilde{\mathcal{S}}_j = \emptyset$ for all $i, j = 1, \ldots, k$ $(i \neq j)$. In this way, we would obtain the possibility to select the subsequent expansion point from a carefully chosen set of sampling points with a reasonable approximation of the largest relative error components. Moreover, the given extension allows for a more convenient distribution of the expansion points, e.g. with respect to a given tolerance, and a careful interpretation of the upper bound (4.2.14) for the different regions $\tilde{\mathcal{S}}_j$ $(j = 1, \ldots, k)$ with $s_i \in \tilde{\mathcal{S}}_j$ $(i = 1, \ldots, m)$.

4.3 Moment matching for second-order descriptor systems

We have already seen that the linearization of a second-order linear dynamical system (2.1.9) leads to a first-order linear dynamical system of the form (2.1.11) and (2.1.12), respectively. Although any application of model order reduction may be already employed to the linearization of the second-order model problem, a linearization represents a linear dynamical system of dimension $2n \times 2n$. For this reason, the computational costs solving a sequence of shifted linear systems $(s_i\mathcal{E} - \mathcal{A})x = f$ $(i = 1, \ldots, l)$ would remarkably increase in the offline-stage of moment matching based model order reduction. Hence, the application of a Arnoldi- or Lanczos-type method to the second-order linear dynamical system is required, which allows for the preservation of the second-order structure in the reduced order model.

At first glance, the *second-order Krylov subspace* is defined by

$$\mathcal{G}_j(A, B, u) = \mathrm{span}\{r_0, r_1, \ldots, r_{j-1}\}, \tag{4.3.1}$$

where $A \in \mathbb{C}^{n\times n}$, $B \in \mathbb{C}^{n\times n}$ and $b \in \mathbb{C}^n$ with

$$r_0 = u, \quad r_1 = Ar_0 \quad \text{and} \quad r_k = Ar_{k-1} + Br_{k-2} \quad \forall\, k > 1, \tag{4.3.2}$$

see [10]. The application of the Arnoldi method, cf. Algorithm 1, to the pair

$$H = \begin{pmatrix} 0 & I \\ -M^{-1}K & -M^{-1}D \end{pmatrix} \quad \text{and} \quad b = \begin{pmatrix} 0 \\ M^{-1}\mathcal{B}_\star \end{pmatrix}$$

corresponding to the linearization (2.1.11) of the second-order linear dynamical system leads to

$$\begin{bmatrix} r_{k-1} \\ r_k \end{bmatrix} = H^k b \quad \forall\, k > 0.$$

Moreover, the first-order Krylov subspace $\mathcal{K}_j(H, b)$ allows for an embedding into the second-order Krylov subspace $\mathcal{G}_j(A, B, r_0)$, where $A \equiv -M^{-1}D$ and $B \equiv -M^{-1}K$, i.e.

$$\mathcal{K}_j(H, b) \subset \operatorname{span}\{Q_{[j]}\} \quad \text{with} \quad Q_{[j]} = \begin{bmatrix} Q_j & 0 \\ 0 & Q_j \end{bmatrix},$$

where the span of the columns of the orthonormal matrix $Q_j \in \mathbb{C}^{n\times j}$ refer to the vector sequence $r_0, \ldots, r_{j-1} \in \mathbb{C}^n$ of the second-order Krylov subspace (4.3.1), see [10].

In the following, we will review the principal idea of the second-order Arnoldi (SOAR) method based on the three-term recurrence (4.3.2) and its efficient implementation in order to avoid the increasing memory requirement for an auxiliary vector sequence, see [10]. Moment matching methods in model order reduction of second-order linear dynamical systems require the expansion of the second-order transfer function (2.1.10) at an expansion point $s_0 \in \mathbb{C}$, see [9]. In this way, the transfer of the adaptive-order rational Arnoldi (AORA) method with an adaptive greedy-type expansion point selection to a second-order linear dynamical systems is straightforward. Nevertheless, a specific framework of the second-order descriptor system becomes necessary in order to make an efficient computation of the Galerkin projection possible, see [107, 113].

4.3.1 The second-order Arnoldi method

The *second-order Arnoldi (SOAR) method* has been initially introduced by Bai and Su in [10]. Their main observation follows from the application of the Arnoldi method to the pair (H, b) allowing for an efficient implementation of the matrix-vector product, while maintaining the specific block-structure of the linearization. By introducing an auxiliary vector sequence $P_j = [p_1, \ldots, p_j] \in \mathbb{C}^{n\times j}$, the short recurrence of the second-order Krylov subspace (4.3.1), cf. Algorithm 7, reads as

$$AQ_j + BP_j = Q_{j+1}\underline{T}_j, \tag{4.3.3}$$

$$Q_j = P_{j+1}\underline{T}_j, \tag{4.3.4}$$

where $Q_j \in \mathbb{C}^{n\times j}$ and $\underline{T}_j \in \mathbb{C}^{(j+1)\times j}$ refer to as the orthonormal vector sequence of the second-order Krylov subspace and an upper Hessenberg matrix, respectively.

Algorithm 7 The second-order Arnoldi (SOAR) method [10]

Input: Matrix pair $A \in \mathbb{C}^{n\times n}$ and $B \in \mathbb{C}^{n\times n}$; initial vector $u \in \mathbb{C}^n$; number of iteration steps $m \in \mathbb{N}$.

Output: Orthonormal vector sequence $q_1, \ldots, q_m \in \mathbb{C}^n$ of second-order Krylov subspace $\mathcal{G}_m(A, B, u)$ fulfilling the three-term recurrence (4.3.2).

Initialize $q_1 = u/\| u \|_2$ and $p_1 = 0$.
for $j = 1, \ldots, m$ **do**
  $r = Aq_j + Bp_j$
  $s = q_j$
  for $i = 1, \ldots, j$ **do**
    $t_{ij} = q_i^{\mathrm{T}} r$
    $r = r - t_{ij} q_i$
    $s = s - t_{ij} p_i$
  end for
  $t_{j+1,j} = \| r \|_2$
  if $t_{j+1,j} \neq 0$ **then**
    $q_{j+1} = r/t_{j+1,j}$
    $p_{j+1} = s/t_{j+1,j}$
  end if
end for

The drawback of the implementation of the SOAR method using the relations (4.3.3) and (4.3.4) is that the algorithm requires the orthonormal vector sequence $Q_j \in \mathbb{C}^{n\times j}$ and the auxiliary vector sequence $P_j \in \mathbb{C}^{n\times j}$ simultaneously. In order to avoid the additional memory requirement for the auxiliary vector sequence, a more convenient implementation of the second-order Arnoldi method becomes indispensable, see [10]. Due to the fact the initialization of the auxiliary vector sequence follows from $p_1 \equiv 0$, a combination of (4.3.3) and (4.3.4) leads to

$$AQ_j + BQ_jS_j = Q_{j+1}\underline{T}_j \quad \text{with} \quad S_j = \begin{bmatrix} 0 & \underline{T}_j(2:j, 1:j-1)^{-1} \\ 0 & 0 \end{bmatrix}.$$

Hence, an efficient implementation of a second-order Arnoldi method does not require the auxiliary vector sequence $P_j \in \mathbb{C}^{n\times j}$ but only an additional vector $f \in \mathbb{C}^n$ obtained via the linear system

$$f = Q_j\underline{T}_j(2:j, 1:j-1)^{-1}e_j, \tag{4.3.5}$$

where e_j denotes the j-th unit vector. For the second-order rational Arnoldi method, the simplification (4.3.5) leads to an efficient computation of an orthonormal basis of a sequence of

second-order Krylov subspaces with respect to memory requirement. Moreover, Bai and Su have given an extensive discussion on the identification and reliable treatment of deflation and breakdown situations in [10].

We note that the quadratic Arnoldi (Q-Arnoldi) method given by Meerbergen in [81] represents an important alternative to the second-order Arnoldi method. Apart from the preservation of the structure of the second-order quadratic eigenvalue problem, the Q-Arnoldi method also allows for the preservation of the structure of the Schur vectors while solving the quadratic eigenvalue problem. In contrast to the SOAR method, it makes an implicit restart with a set of converged Schur vectors possible.

4.3.2 A second- and adaptive-order rational Arnoldi method

Let $\mathcal{S}_l = \{s_1, \ldots, s_l\} \subset \mathbb{C}$ denote a given set of expansion points and define $\bar{K}_i \equiv s_i^2 M + s_i D + K$ and $\bar{D}_i \equiv 2s_i M + D$. The Taylor expansion of the second-order transfer function (2.1.10) at each expansion point $s_i \in \mathcal{S}_l$ $(i = 1, \ldots, l)$ is given by

$$\mathcal{H}(s) = \sum_{j=0}^{\infty} \mathcal{C} X^{(j)}(s_i)(s - s_i)^j \equiv \sum_{j=0}^{\infty} Y^{(j)}(s_i)(s - s_i)^j,$$

where each *system moment* $X^{(j)}(s_i)$ satisfies the recurrence relation (4.3.2) of the second-order Krylov subspace $\mathcal{G}_{j_i}(s_i) \equiv \mathcal{G}_{j_i}(A_i, B_i, u_i)$ $(i = 1, \ldots, l)$ with

$$A_i \equiv -\bar{K}_i^{-1} \bar{D}_i, \quad B_i \equiv -\bar{K}_i^{-1} M \quad \text{and} \quad u_i \equiv \bar{K}_i^{-1} \mathcal{B}_*,$$

see [9,107,113]. Similar to first-order linear dynamical systems, it holds $n_r = j_1 + \ldots + j_l$, $j_i > 0$ $(i = 1, \ldots, l)$, for a given number of iteration steps $n_r > 0$ of the second-order Krylov subspace method.

For moment matching methods in model order reduction, the computation of an orthonormal vector sequence $V \in \mathbb{C}^{n \times n_r}$ follows from the subspace

$$\mathcal{G}_{j_1,\ldots,j_l}(\mathcal{S}_l) = \operatorname{span}\left[X^{(0)}(s_1), \ldots, X^{(j_1-1)}(s_1), \ldots, X^{(0)}(s_l), \ldots, X^{(j_l-1)}(s_l)\right] \tag{4.3.6}$$

in order to obtain the reduced order model by means of the Galerkin projection $\Pi = VV^{\mathrm{T}}$. This approach allows for the preservation of the structure of the second-order linear dynamical system in the reduced order model due to the application of a sequence of second-order Krylov subspaces $\mathcal{G}_{j_1}(s_1), \ldots, \mathcal{G}_{j_l}(s_l)$. Moreover, a moment matching property for the state moments of the full-order and the reduced order model follows in a similar way to the approximation result (4.2.5) of first-order linear dynamical systems.

In accordance with (4.1.4), the computation of a real-valued reduced order model is obtained via the application of a QR decomposition to the block matrix consisting of the real and

imaginary part of the orthonormal matrix $V \in \mathbb{C}^{n\times n_r}$, i.e.

$$\Big[\mathrm{Re}(V),\ \ \mathrm{Im}(V)\Big] = Q_V R, \tag{4.3.7}$$

where $Q_V \in \mathbb{R}^{n\times 2n_r}$ and $R \in \mathbb{R}^{2n_r\times 2n_r}$ denote an orthonormal matrix and an upper triangular matrix of full rank, respectively. Due to the fact that $\mathrm{colspan}\left(\Big[\mathrm{Re}(V),\ \ \mathrm{Im}(V)\Big]\right) \subseteq \mathrm{colspan}(Q_V)$, the application of the Galerkin projection $\Pi = V_Q V_Q^{\mathrm{T}}$ leads to a real-valued reduced order model of dimension $n_d = 2n_r$.

In the following, we will provide an extension of the rational Arnoldi method, cf. Algorithm 3, to second-order descriptor systems of the Maxwell's equations (3.0.3). Thereby, a review on the requirements of the reorthogonalization with the modified Gram-Schmidt procedure will be given in order to provide an efficient computation of an orthonormal vector sequence $V \in \mathbb{C}^{n\times n_r}$ according to the subspace (4.3.6), see [90].

Remember that the suitable application of the modified Gram-Schmidt procedure in the adaptive-order rational Arnoldi method for first-order linear dynamical systems is based on Lemma 4.2.1. Here, the principal idea was given by (4.2.6) leading to the computation of an orthonormal vector sequence of the subspace $\mathcal{K}_{j_1}(s_1) + \ldots + \mathcal{K}_{j_l}(s_l)$, where $n_r = j_1 + \ldots + j_l$ and $j_i > 0$ $(i = 1, \ldots, l)$. Unfortunately, the sequence of second-order Krylov subspaces $\mathcal{G}_{j_1}(s_1), \ldots, \mathcal{G}_{j_l}(s_l)$ does not provide a relation of the form

$$(s_2^2M + s_2D + K)^{-1}(2s_2M + D)(s_1^2M + s_1D + K)^{-1} = \\ \xi_2(s_2^2M + s_2D + K)^{-1} - \xi_1(s_1^2M + s_1D + K)^{-1}$$

for suitable scalars $\xi_1, \xi_2 \in \mathbb{C}$, see [90]. Hence, the application of the modified Gram-Schmidt procedure similar to the rational Arnoldi method for first-order descriptor systems would offer an orthonormal vector sequence of a different subspace than $\mathcal{G}_{j_1}(s_1) + \ldots + \mathcal{G}_{j_l}(s_l)$. One possible alternative would require the subsequent application of a QR decomposition to the orthonormal vector sequence, i.e.

$$V \equiv \Big[V,\ V^{(i)}\Big] \quad \text{and} \quad V \equiv QR \quad \forall\, i = 1, \ldots, l,$$

where the span of the columns $V^{(i)} \in \mathbb{C}^{n\times j_i}$ refers to the second-order Krylov subspace $\mathcal{G}_{j_i}(s_i)$ $(i = 1, \ldots, l)$. For an arbitrary second-order matrix pencil $\lambda^2 M + \lambda D + K$, $\lambda \in \mathbb{C}$, the efficient orthogonalization still represents an open research problem in the development of rational Arnoldi-type methods.

Nevertheless, the special cases of *proportional damping*, i.e. $D \equiv \alpha M + \beta K$ with $\alpha > 0$ and $\beta \geq 0$, and *undamped linear dynamical systems*, i.e. $D \equiv 0$, allow for the computation of an orthonormal vector sequence (4.3.6) by means of the modified Gram-Schmidt procedure. This follows from the observation that the second-order Krylov subspace corresponding to a

proportionally damped or undamped second-order linear dynamical system simplifies to a first-order Krylov subspace, see [14, 107]. More precisely, the second-order Krylov subspace of a proportionally damped second-order linear dynamical system is given by

$$\mathcal{G}_{j_i}(-\bar{K}_i^{-1}\bar{D}_i, -\bar{K}_i^{-1}M, \bar{K}_i^{-1}\mathcal{B}_\star) \equiv \mathcal{K}_{j_i}(-\bar{K}_i^{-1}M, \bar{K}_i^{-1}\mathcal{B}_\star) \quad \forall\, i = 1, \ldots, l,$$

see [34]. In this case, the formulation of a second-order rational Arnoldi method refers to the rational Arnoldi method for first-order descriptor systems, cf. Algorithm 3. The corresponding residuals are obtained via

$$r_k = (s_i^2 M + s_i D + K)^{-1} B_\star \quad \text{and} \quad r_k = -(s_i^2 M + s_i D + K)^{-1} M v_k \tag{4.3.8}$$

for all $s_i \in \mathcal{S}_l = \{s_1, \ldots, s_l\}$, respectively. In Algorithm 8, we summarise the details on the implementation of the *second-order rational Arnoldi method*. An efficient framework for solving a sequence of shifted linear systems (4.3.8) on the basis of recycling Krylov subspace methods will be reviewed in Chapter 5.

Since the adaptive computation of each dimension of the different second-order Krylov subspaces $\mathcal{G}_{j_1}(s_1), \ldots, \mathcal{G}_{j_l}(s_l)$ follows in a similar way to the adaptive-order rational Arnoldi method, the following lemma leads to the formulation of a *second- and adaptive-order rational Arnoldi* (SAORA) method, see [113].

Lemma 4.3.1 ([113, Proposition 10.2])**.** *Let the system moments of the second-order descriptor system and the corresponding reduced order model $X^{(j)}(s_i)$ and $\tilde{X}^{(j)}(s_i)$ coincide for all $j = 0, 1, \ldots, j_i - 1$ and $i = 1, \ldots, l$. If the columns of the orthonormal matrix $V = [v_1, \ldots, v_{n_r}] \in \mathbb{C}^{n \times n_r}$, where $n_r = \sum_{i=1}^{l} j_i$, have been computed by means of the second- and adaptive-order rational Arnoldi method, the j_i-th output moment error of each expansion point $s_i \in \mathbb{C}$ satisfies*

$$|\, Y^{(j_i)}(s_i) - \tilde{Y}^{(j_i)}(s_i)\,| = |\, \mathcal{C} h_\pi(s_i) r^{(q)}(s_i)\,| \quad \textit{with} \quad h_\pi(s_i) = \prod_j \| \, r^{(j-1)}(s_i) \, \|_2.$$

The selection of the expansion point $s_i \in \mathbb{C}$ in the j-th iteration step leads to $r^{(j)}(s_i) \equiv -(s_i^2 M + s_i D + K)^{-1}(2s_i M + D) v_{j-1}$ and $r^{(j)}(s_k) \equiv r^{(j-1)}(s_k)$ for all $k = 1, \ldots, l$ $(k \neq i)$.

Any greedy-type adaptive expansion point selection strategy allows for a straightforward extension to second-order linear dynamical systems. Similar to first-order linear dynamical systems, moment matching methods for second-order linear dynamical systems with a greedy-type expansion point selection require computing a sequence of reduced order models $\tilde{\mathcal{H}}_1(s)$, $\ldots$, $\tilde{\mathcal{H}}_m(s)$. Each transfer function $\tilde{\mathcal{H}}_{i+1}(s)$ is constructed by the SAORA method for a given set of expansion points $\mathcal{S}_{i+1} = \mathcal{S}_i \cup \{s_{i+1}\}$, $s_{i+1} \in \mathbb{C}$. The heuristic error estimation $\hat{\epsilon}_k > 0$ from Grimme et al. (4.2.10) may be also employed for a sequence of reduced order models.

Algorithm 8 The second-order rational Arnoldi method [113] for Maxwell's equations

Input: Descriptor system $(M, D, K, \mathcal{B}_\star, \mathcal{C}_\star)$ of second-order Maxwell's equations (3.0.3) with proportional damping or without damping; set of expansion points $\mathcal{S}_l = \{s_1, \ldots, s_l\} \subset \mathbb{C}$ with corresponding dimensions $j_1, \ldots, j_l > 0$ such that $n_r = j_1 + \ldots + j_l$.

Output: Reduced order model $(\tilde{M}, \tilde{D}, \tilde{K}, \tilde{\mathcal{B}}_\star, \tilde{\mathcal{C}}_\star)$.

$r_0 = \left(s_1^2 M + s_1 D + K\right)^{-1} \mathcal{B}_\star$ % Initialize first Krylov subspace
for $i = 1, \ldots, l$ **do**
  for $j = 1, \ldots, j_i$ **do**
    $k = \sum_{c=1}^{i-1} j_c + j$
    $v_k = r_{k-1} / \| r_{k-1} \|_2$ % New orthonormal vector
    if $j = j_i$ and $i \leq l$ **then**
      $r_k = \left(s_{i+1}^2 M + s_{i+1} D + K\right)^{-1} \mathcal{B}_\star$ % Initialize subsequent Krylov subspace
    else
      $r_k = -\left(s_i^2 M + s_i D + K\right)^{-1} M v_k$ % New vector of Krylov subspace
    end if
    for $t = 1, \ldots, k$ **do**
      $r_k = r_k - (v_t^{\mathrm{T}} r_k) v_t$ % Modified Gram-Schmidt procedure
    end for
  end for
end for
Application of the QR decomposition (4.3.7) to the orthonormal matrix $V = [v_1, \ldots, v_{n_r}] \in \mathbb{C}^{n \times n_r}$ leading to $\bar{V} \in \mathbb{R}^{n \times 2n_r}$.
Compute the reduced order model using the Galerkin projection $\Pi = \bar{V}\bar{V}^{\mathrm{T}}$.

Moreover, the adaptation of the presented greedy-type expansion point selection strategies in Subsection 4.2.4 is as follows: While the AORA-H2 method requires the computation of the Ritz values corresponding to the second-order eigenvalue problem

$$(\lambda_i^2 \tilde{M} + \lambda_i \tilde{D} + \tilde{K}) x = 0, \quad x \neq 0,$$

the application of the WCAWE method in the AORA-MAX method must incorporate the state moments $X^{(j)}(s_i)$ $(j = 0, \ldots, j_i - 1)$ of the second-order linear dynamical system. The upper bound of the output moment error of the AORA-RK method stated in Lemma 4.2.5 allows for an immediate extension to second-order linear dynamical systems by means of the corresponding output moment error, cf. Lemma 4.3.1.

4.4 Divergence-preserving moment matching methods

For first- and second-order linear dynamical systems of Maxwell's equations (3.0.1) and (3.0.3), we have only considered the application of moment matching methods in model order reduction to Faraday's and Ampère's law, cf. (3.1.2) and (3.1.4), respectively. Since Gauss's law for electric and magnetic fields (3.1.6) and (3.1.8) features elementary properties of electric and magnetic fields in classical electromagnetism, this paragraph affects the impact of the discrete divergence conditions $(D_E M_\epsilon)\boldsymbol{E} = 0$ and $(D_H M_\mu)\boldsymbol{H} = 0$ in moment matching based model order reduction, see [19].

At first glance, an explicit projection of the discrete operators D_E and D_H employing the Galerkin projection $\Pi = VV^{\mathrm{T}}$ allows for the application of the discrete divergence operators to the reduced order matrix quadruplet. Since we aim for a more convenient treatment of the discrete divergence conditions in moment matching based model order reduction, we will show that the discrete divergence conditions may be already included in the Krylov subspaces $\mathcal{K}_{j_i}(s_i)$ or $\mathcal{G}_{j_i}(s_i)$ $(i = 1, \ldots, l)$, respectively. By comparison, the numerical simulation of Maxwell's equations requires divergence-free initial conditions $\boldsymbol{E}(0) = \boldsymbol{E}_0$ and $\boldsymbol{H}(0) = \boldsymbol{H}_0$ and a divergence-preserving time-integration scheme for the corresponding state variable $x(t) = [\boldsymbol{E}^{\mathrm{T}}(t), \boldsymbol{H}^{\mathrm{T}}(t)]^{\mathrm{T}} \in \mathbb{R}^n$, e.g. a Leapfrog scheme, see [108].

For an appropriate discussion of divergence-preserving moment matching methods, a distinction between different relations of the mass matrix M_σ on the one hand and the mass matrix M_ϵ and the discrete curl operator C_H on the other hand becomes necessary. Since a general framework on proportional damped and undamped second-order linear dynamical systems has been given in the previous subsection, we adapt the previous definition to first-order linear dynamical systems of Maxwell's equations. More precisely, the following three different cases are present.

- The electric conductivity equals zero in the computational domain.
- The mass matrix M_σ offers a proportional damping of the form

$$M_\sigma = \alpha M_\epsilon + \beta C_H \quad \text{with} \quad \alpha > 0 \quad \text{and} \quad \beta \geq 0. \tag{4.4.1}$$

- The electric conductivity is strictly positive in the computational domain.

As seen for second-order linear dynamical systems, proportional damping arises in different applications of mechanical systems, see [113]. For Maxwell's equations, proportional damping only occurs for very simple model problems with $\epsilon \equiv \epsilon(x)$ and $\sigma \equiv \sigma(x)$, where the material parameters $\epsilon > 0$ and $\sigma > 0$ differ by a positive constant.

A first approach to the analysis on the impact of the divergence conditions to Maxwell's equations follows from the application of the discrete divergence operators D_E and D_H to the first-order linear dynamical system (3.0.1). In due consideration of the discrete divergence conditions $(D_E M_\epsilon)\boldsymbol{E} = 0$ and $(D_H M_\mu)\boldsymbol{H} = 0$, it follows that

$$\begin{aligned} \imath\omega \underbrace{(D_E M_\epsilon \boldsymbol{E})}_{\equiv 0} &= -D_E M_\sigma \boldsymbol{E} + \underbrace{D_E C_H}_{\equiv 0} \boldsymbol{H} + (D_E \mathcal{B}_E)\, u, \\ \imath\omega \underbrace{(D_H M_\mu \boldsymbol{H})}_{\equiv 0} &= -\underbrace{D_H C_E}_{\equiv 0} \boldsymbol{E} + (D_H \mathcal{B}_H)\, u, \end{aligned}$$

cf. (3.0.2), where the control input matrix $\mathcal{B} = [\mathcal{B}_E^{\mathrm{T}}, \mathcal{B}_H^{\mathrm{T}}]^{\mathrm{T}} \in \mathbb{R}^{n\times m}$ has been decomposed in accordance with the dimensions of the electric and magnetic field components, respectively.

Moreover, the discrete nullspace properties of the curl-operator, i.e. $D_E C_H = 0$ and $D_H C_E = 0$, ensure a divergence-free control input matrix for model problems of Maxwell's equations with either $\sigma \equiv 0$ or $\sigma > 0$ on the basis of proportional damping (4.4.1). Since we commonly consider model problems of Maxwell's equations with $\mathcal{B}_H \equiv 0$, which immediately leads to $D_H \mathcal{B}_H \equiv 0$, we have shown the following lemma for first-order descriptor systems.

Lemma 4.4.1. *Let the matrix quadruplet $(\mathcal{E}, \mathcal{A}, \mathcal{B}, \mathcal{C})$ denote the linear dynamical system of Maxwell's equations (3.0.1), where M_ϵ, M_μ and M_σ are symmetric positive definite matrices. If we assume $D_H \mathcal{B}_H = 0$, it follows that*

$$\begin{pmatrix} 0 & 0 \\ 0 & D_H M_\mu \end{pmatrix} X^{(j)}(s_i) = 0. \tag{4.4.2}$$

Moreover, it holds $\mathcal{A}x \neq 0$ for any $x \in \mathcal{K}_{j_i}\left(-(s_i\mathcal{E} - \mathcal{A})^{-1}\mathcal{E}, (s_i\mathcal{E} - \mathcal{A})^{-1}\mathcal{B}\right)$.

Proof. Note that the assumption $D_H \mathcal{B}_H = 0$ may be also written in the form

$$\begin{pmatrix} 0 & 0 \\ 0 & D_H M_\mu \end{pmatrix} \begin{pmatrix} M_\epsilon^{-1}\mathcal{B}_E \\ M_\mu^{-1}\mathcal{B}_H \end{pmatrix} = 0.$$

For the proof of relation (4.4.2), we proceed as follows: First of all we have

$$\begin{aligned} \begin{pmatrix} 0 & 0 \\ 0 & D_H M_\mu \end{pmatrix} \mathcal{E}^{-1}(s\mathcal{E} - \mathcal{A}) &= \begin{pmatrix} 0 & 0 \\ 0 & D_H M_\mu \end{pmatrix} \begin{pmatrix} sI + M_\varepsilon^{-1} M_\sigma & -M_\varepsilon^{-1} C \\ M_\mu^{-1} C^{\mathrm{T}} & sI \end{pmatrix} \\ &= \begin{pmatrix} 0 & 0 \\ D_H C^{\mathrm{T}} & s D_H M_\mu \end{pmatrix} = s \begin{pmatrix} 0 & 0 \\ 0 & D_H M_\mu \end{pmatrix}. \end{aligned}$$

Hence, we obtain the relation

$$\begin{pmatrix} 0 & 0 \\ 0 & D_H M_\mu \end{pmatrix} (s\mathcal{E} - \mathcal{A})^{-1}\mathcal{E} = \frac{1}{s} \begin{pmatrix} 0 & 0 \\ 0 & D_H M_\mu \end{pmatrix}.$$

Finally, we conclude that

$$\begin{aligned}\begin{pmatrix} 0 & 0 \\ 0 & D_H M_\mu \end{pmatrix} X^{(j)}(s) &= \begin{pmatrix} 0 & 0 \\ 0 & D_H M_\mu \end{pmatrix} (-1)^j \left[(s\mathcal{E}-\mathcal{A})^{-1}\mathcal{E}\right]^{j+1} (\mathcal{E}^{-1}\mathcal{B}) \\ &= (-1)^j \left(\frac{1}{s}\right)^{j+1} \begin{pmatrix} 0 & 0 \\ 0 & D_H M_\mu \end{pmatrix} (\mathcal{E}^{-1}\mathcal{B}) = 0. \end{aligned} \tag{4.4.3}$$

Let $x = \left(x_E^{\mathrm{T}}, x_H^{\mathrm{T}}\right)^{\mathrm{T}} \in \mathcal{K}_j(-(s_i\mathcal{E}-\mathcal{A})^{-1}\mathcal{E}, (s_i\mathcal{E}-\mathcal{A})^{-1}\mathcal{B})$ such that

$$\mathcal{A}x = \begin{pmatrix} -M_\sigma x_E + C x_H \\ -C^{\mathrm{T}} x_H \end{pmatrix} = 0,$$

where we already know that $D_H(M_\mu x_H) = 0$, see (4.4.3). Here, $C^{\mathrm{T}} x_H = 0$ indicates that a non-trivial component x_H results from the nullspace of the discrete curl operator. Due to the fact that M_σ is nonsingular and D_E and D_H^{T} span the left and right nullspace of the curl-operator C, we conclude from $-M_\sigma x_E + C x_H = 0$ that

$$x = \begin{pmatrix} 0 \\ D_H^{\mathrm{T}} y_H \end{pmatrix}$$

for a suitably chosen vector y_H. Hence, we have to show that $y_H = 0$ in order to complete the proof of the lemma.

Remember that the mass matrix M_μ is symmetric and positive definite and therefore it defines an inner product. From the decomposition $x_H = D_H^{\mathrm{T}} y_H + (D_H^{\perp})^{\mathrm{T}} z_H$, where the columns of $(D_H^{\perp})^{\mathrm{T}}$ span the M_μ-orthogonal complement of D_H^{T}, we conclude $y_H = 0$, which is equivalent to $D_H(M_\mu x_H) = 0$ from the first part of the proof. □

A divergence-free control input matrix already leads to the preservation of the discrete divergence conditions for each system moment $X^{(j)}(s_i)$ $(j = 0, 1, \ldots, j_i - 1)$. As a consequence, an explicit projection onto the subspace of discrete divergence-free functions of the electric field strength becomes necessary for moment matching methods whenever the part of the control input matrix corresponding to the electric field strength is not divergence-free. Moreover, the result of the previous lemma spreads to the framework of structure-preserving moment matching methods. Another consequence of Lemma 4.4.1 is that the nullspace of the matrix $\mathcal{A} \in \mathbb{R}^{n\times n}$ is independent of the discrete divergence conditions of the electric field strength. Hence, we refer to the matrix pencil $\lambda\mathcal{E} - \mathcal{A}$, $\lambda \in \mathbb{C}$, as stable at least for $\sigma > 0$.

If the state moments $X^{(j)}(s_i)$ are computed by means of iterative Krylov subspace solvers [13], the previous results are no longer valid due to the inexactness of the nullspace properties of the discrete curl operator. In this case, the explicit projection onto the subspace of discrete

divergence-free becomes indispensable. Generally speaking, the application of direct solvers should also comprise the projection onto the orthogonal complement of the discrete divergence operators D_E and D_H due to the appearance of numerical round-off errors.

Throughout the chapter, we have seen that moment matching methods in model order reduction are essentially based on the expansion of the transfer function at different expansion points. Since the Galerkin projection at hand is constructed by computing a sequence of orthonormal vectors corresponding to the Krylov subspaces $\mathcal{K}_{j_i}(s_i)$ and $\mathcal{G}_{j_i}(s_i)$ $(i = 1, \ldots, l)$, an incorporation of the projection onto the subspace of discrete divergence-free functions to the Krylov subspaces at hand is given. More precisely, we will show how to obtain a divergence-free state variable $x(t) = [\boldsymbol{E}(t)^{\mathrm{T}}, \boldsymbol{H}(t)^{\mathrm{T}}]^{\mathrm{T}}$ in the transfer function (2.1.5).

If we denote the projection onto the space of discrete divergence-free functions field separately for the electric and magnetic field strength by

$$P_E = I - D_E \left(D_E M_\epsilon D_E^{\mathrm{T}}\right)^{-1} D_E^{\mathrm{T}} M_\epsilon \quad \text{and} \quad P_H = I - D_H \left(D_H M_\mu D_H^{\mathrm{T}}\right)^{-1} D_H^{\mathrm{T}} M_\mu,$$

the left projection matrix onto the subspace of discrete divergence-free functions follows from

$$P_l = \begin{bmatrix} P_E & 0 \\ 0 & P_H \end{bmatrix}. \tag{4.4.4}$$

The discrete divergence conditions $D_E(M_\epsilon \boldsymbol{E}) = 0$ and $D_H(M_\mu \boldsymbol{H}) = 0$ may be already included in the computation of a reduced order model in terms of moment matching methods.

Remark 4.4.2. *Let $\hat{x}(s)$, $\hat{u}(s)$ and $\hat{y}(s)$ denote the Laplace transformation of the state variable $x(t) \in \mathbb{R}^n$, the input variable $u(t) \in \mathbb{R}^m$ and the output variable $y(t) \in \mathbb{R}^p$. The application of the Laplace transformation to the linear dynamical system (2.1.1) leads to*

$$\hat{y}(s) = \mathcal{C}\hat{x}(s), \quad \textit{where} \quad \hat{x}(s) = (s\mathcal{E} - \mathcal{A})^{-1}\mathcal{B}\hat{u}(s).$$

The incorporation of the discrete divergence conditions to the state variable in the frequency domain is given by the projected state variable $\hat{x}_P(s) \equiv P_l\hat{x}(s)$. In this way, we may already include the projection (4.4.4) into the transfer function such that

$$\mathcal{H}_P(s) = \mathcal{C}P_l^{\mathrm{T}}(s\mathcal{E} - \mathcal{A})^{-1}\mathcal{B}.$$

With regard to the initial vector of the output Krylov subspace (4.1.3), the projected transfer function $\mathcal{H}_P(s)$ allows for the suitable incorporation of the projection (4.4.4) using

$$\mathcal{K}_{j_i}\left(-(s_i\mathcal{E} - \mathcal{A})^{-\mathrm{T}}\mathcal{E}^{\mathrm{T}}, (s_i\mathcal{E} - \mathcal{A})^{-\mathrm{T}}P_l\mathcal{C}^{\mathrm{T}}\right)$$

for all expansion points $s_i \in \mathcal{S}_l = \{s_1, \ldots, s_l\}$, see [19].

Due to the fact that a second-order linear dynamical system may be formulated by means of a linearization as a first-order descriptor system, an extension of the previous remark to the corresponding second-order Krylov subspace is straightforward. If we consider the electric field strength in the second-order formulation of Maxwell's equations, it follows that

$$\mathcal{G}_{j_i}\left(-\bar{K}_i^{-\mathrm{T}}\bar{D}_i^{\mathrm{T}}, -\bar{K}_i^{-\mathrm{T}}M^{\mathrm{T}}, -\bar{K}_i^{-\mathrm{T}}P_E\mathcal{C}_*^{\mathrm{T}}\right)$$

in order to explicitly include the projection onto the subspace of discrete divergence-free functions in the computation of the system moments. Although the incorporation of the discrete divergence conditions in the second-order Krylov subspace does not depend on the choice of the material parameters, e.g. $M_\sigma = \alpha M_\epsilon + \beta K_\mu$ with $\alpha, \beta \geq 0$, we still have to be aware of the efficient orthogonalization of the orthonormal vector sequence.

CHAPTER 5

Efficient Krylov subspace methods for model order reduction

We have seen in the previous chapter that the moment matching based model order reduction leads to the computation of a sequence of orthonormal vectors of different first- and second-order Krylov subspaces $\mathcal{K}_{j_i}(s_i)$ and $\mathcal{G}_{j_i}(s_i)$ $(i = 1, \ldots, m)$, respectively. Since moment matching methods require multiply solving a high-dimensional shifted linear system of the form

$$(s_i\mathcal{E} - \mathcal{A})x_j = f_j \quad \text{or} \quad (s_i^2 M + s_i D + K)x_j = f_j \tag{5.0.1}$$

with $s_i \in \mathbb{C}$ and several right hand sides $f_j \in \mathbb{C}^n$, the subsequent application of the AORA method will become a critical factor when the offline-phase in model order reduction plays an important role for the application under consideration. In view of the dimension of the sequence of shifted linear systems (5.0.1), the memory requirement of a direct solver employed for solving the shifted linear systems represents a significant limitation for moment matching based model order reduction.

Therefore, we will initially introduce a modification of the adaptive-order rational Arnoldi method which avoids the (complete) recalculation of the orthonormal vector sequence $V^{(k)} \in \mathbb{C}^{n\times n_r}$ during the k-th subsequent call. The modification of the AORA method represents a special case of a modified generic rational Arnoldi method given in [18]. More precisely, the solution to a shifted linear system is either computed for the latest expansion point $s_{i+1} \in \mathcal{S}_{i+1} = \mathcal{S}_i \cup \{s_{i+1}\}$, $s_{i+1} \in \mathbb{C}$, $(i = 0, \ldots, m-1)$ or a previous expansion point $s_* \in \mathcal{S}_i$ with an increasing number of orthonormal vectors according to the orthonormal vector sequence $V^{(i-1)}$. Numerical experiments have shown that the *modified adaptive-order rational Arnoldi* (mAORA) method allows for a comparable accuracy of the reduced order model by comparison with the AORA method.

The application of a direct solver, e.g. the LU decomposition, to a sequence of shifted linear systems is rather limited due to the increasing size of the linear dynamical system in the first- and second-order formulation (2.1.1) and (2.1.9), respectively. In particular, the application of the LU decomposition to first-order linear dynamical systems of Maxwell's equations would not even exploit the special block-structure of the model problem. Hence, we will introduce an algebraic two-level method (ATLM) employing the block-structure of first-order Maxwell's equations based on the electric and magnetic field strength, see [19]. The ATLM primarily requires solving a linear system corresponding to the Schur complement of the first-order linear dynamical system. For first-order Maxwell's equations, the Schur complement refers to the (complex) symmetric, but highly indefinite discrete version of the second-order formulation. The ATLM primarily makes use of an LDL^{T} decomposition for solving the linear system with the Schur complement.

Efficiently solving the linear system corresponding to the Schur complement of the ATLM has been also discussed by means of the (recycling) Krylov subspace methods, see [18]. Due to the fact that the Schur complement of first-order Maxwell's equations is (complex) symmetric, but highly indefinite, we will provide an extension of the recycling biconjugate gradient (rBiCG) method [1, 2] to a recycling simplified quasi-minimal residual (rSQMR) method. Similar to the SQMR method [50], the rSQMR also employs a (complex) symmetric, but indefinite preconditioner. By comparison with restarted Krylov subspace methods [104], recycling Krylov subspace methods typically lead to a more reliable convergence behaviour, e.g. the appearance of stagnation has never been observed during the numerical experiments in Chapter 6.

The chapter is outlined as follows: To begin with, we will describe the modification of the adaptive-order rational Arnoldi (AORA) method in order to obtain an efficient way for the computation of the Petrov-Galerkin projection $\Pi = VV^{\mathrm{T}}$ with nested sets of expansion points $\mathcal{S}_{i+1} = \mathcal{S}_i \cup \{s_{i+1}\}$, $s_{i+1} \in \mathbb{C}$. Thereafter, we will review the algebraic two-level method (ATLM) for solving a shifted linear system corresponding to first-order Maxwell's equations (3.0.1). In this context, the application of (recycling) Krylov subspace methods to the second-order formulation of Maxwell's equations (3.0.3), which refers to a (complex) symmetric, but highly indefinite linear system, is given.

5.1 A modified adaptive-order rational Arnoldi method

The major drawback of the subsequent application of a rational Arnoldi-type method for the different expansion points $\mathcal{S}_{i+1} = \mathcal{S}_i \cup \{s_{i+1}\}$, $s_{i+1} \in \mathbb{C}$, $(i = 0, \ldots, m-1)$ arises from the following observation: The orthonormal matrix $V \in \mathbb{C}^{n \times n_r}$ corresponding to the Galerkin projection $\Pi = VV^{\mathrm{T}}$ will be completely recomputed during each call of the rational Arnoldi-

type method. Since a single expansion point $s_{i+1} \in \mathbb{C}$ is added for each call of the rational Arnoldi-type method, the already known vector sequence corresponding to the expansion points $\mathcal{S}_i = \{s_1, \ldots, s_i\} \subset \mathbb{C}$ may be reused during the subsequent call of the rational Arnoldi-type method with the expansion points $\mathcal{S}_{i+1} = \{s_1, \ldots, s_i, s_{i+1}\} \subset \mathbb{C}$. Generally speaking, the solution to a shifted linear system is computed for the latest expansion point $s_{i+1} \in \mathbb{C}$ and all previous expansion points $s_l \in \mathcal{S}_i$ with a larger dimension of the Krylov subspace $\mathcal{K}_{j_l}(s_l)$ or $\mathcal{G}_{j_l}(s_l)$ compared with the previous call of the rational Arnoldi-type method. In the following, we will restrict the discussion to the modification of the adaptive-order rational Arnoldi method for first-order linear dynamical systems, cf. Algorithm 9. A generalisation of the mAORA method in terms of a modified generic rational Arnoldi method is given in [18].

Let $V^{(i)} = \left[v_1^{(i)}, \ldots, v_{n_r}^{(i)}\right]$ denote the orthonormal vector sequence corresponding to the expansion points $\mathcal{S}_i = \{s_1, \ldots, s_{i-1}, s_i\} \subset \mathbb{C}$. Remember that the adaptive-order rational Arnoldi selects an arbitrary residual $r^{(j)}(s_l)$ $(l = 1, \ldots, i)$ with the help of the output moment error (4.2.8) in each iteration step. To put it simply, the modification of the adaptive-order rational Arnoldi method either allows for the consecutive selection of a previous residual $r^{(j)}(s_1), \ldots r^{(j)}(s_{i-1})$ depending on the ordering in the orthonormal vector sequence $V^{(i-1)}$ or the residual vector $r^{(j)}(s_i)$ corresponding to the latest expansion point, cf. line 6 in Algorithm 9. Note that $\alpha > 0$ keeps track on the current column of $V^{(i)}$. For the sake of completeness, we additionally consider the residual vectors coming from a Krylov subspace with an increasing dimension between two subsequent calls of the mAORA method, i.e. $j_{k,i+1} > j_{k,i}$ $(k = 1, \ldots, i)$. Nevertheless, the latter case has rarely occurred for numerical experiments of semiconductor structures, see Chapter 6.

Remark 5.1.1. *Let $v_k^{(i-1)} \in V^{(i-1)}$ and $v_{k+1}^{(i-1)} \in V^{(i-1)}$ be two orthonormal vectors corresponding to the expansion points $s_{k_1} \in \mathcal{S}_{i-1}$ and $s_{k_2} \in \mathcal{S}_{i-1}$, respectively. Then, the application of the modified Gram-Schmidt procedure leads to*

$$\tilde{v}_{k+1}^{(i-1)} = -(s_{k_2}\mathcal{E} - \mathcal{A})^{-1}\mathcal{E}v_k^{(i-1)} - \sum_{j=1}^{k} \gamma_j v_j^{(i-1)},$$

where $\gamma_j \in \mathbb{C}$ denote suitable coefficients obtained via the orthonormalization of the vector sequence. If the mAORA method would allow for an arbitrary selection of orthonormal vectors $v_j \in V^{(i-1)}$ independent of the order of appearance, the subsequent orthonormal matrix $V^{(i)}$ may contain undesirable components of individual orthonormal vectors.

For example, the selection of $v_{k+1}^{(i-1)} \in V^{(i-1)}$ for the orthonormal matrix $V^{(i)}$ but simultaneously leaving out $v_k^{(i-1)} \in V^{(i-1)}$ in $V^{(i)}$ suggests the moment matching of a higher-order derivative at the expansion point $s_{k_1} \in \mathbb{C}$. If the following iteration steps do not employ the expansion point $s_{k_1} \in \mathbb{C}$ anymore, we would obtain a larger subspace of the sequence of Krylov subspaces as expected. Hence, the

Algorithm 9 Modified adaptive-order rational Arnoldi (mAORA) method

Input: Descriptor system $(\mathcal{E}, \mathcal{A}, \mathcal{B}, \mathcal{C})$; set of expansion points $\mathcal{S}_{i+1} = \{s_1, \ldots, s_i, s_{i+1}\} \subset \mathbb{C}$; orthonormal matrix $V^{(i)} = \left[v_1^{(i)}, \ldots, v_{n_r}^{(i)}\right]$ with $n_r = j_{1,i} + \ldots + j_{i,i}$ obtained via previous call of mAORA method; sequence of norms of residual vectors $h_1(s_1), \ldots, h_{j_{1,i}}(s_1), \ldots, h_{j_{i,i}}(s_i)$; number of iteration steps $n_r > 0$.

Output: Orthonormal matrix $V^{(i+1)} = \left[v_1^{(i+1)}, \ldots, v_{n_r}^{(i+1)}\right] \in \mathbb{C}^{n \times n_r}$.

Initialize residuals $r^{(1)}(s_1) = v_{l_1}^{(i)}, \ldots, r^{(1)}(s_i) = v_{l_i}^{(i)}$ with suitable $l_1, \ldots, l_i \in \{1, \ldots, n\}$.
Compute $r^{(1)}(s_{i+1}) = (s_{i+1}\mathcal{E} - \mathcal{A})^{-1}\mathcal{B}$ and $h_1(s_{i+1}) = \| r^{(1)}(s_{i+1}) \|_2$.
Let $h_\pi(s_l) = 1$ and $j_{l,i+1} = 1$ for all $l = 1, \ldots, i+1$.
Initialize current index $\alpha = 1$ of orthonormal vector sequence $v_\alpha^{(i)} \in V^{(i)}$, where $\alpha > 0$ refers to as the current column of $V^{(i)}$.
for $j = 1, \ldots, n_r$ **do**
  Determine $s_{i^\star} = \arg\max_{s \in \mathcal{S}_*} | h_\pi(s)\mathcal{C}r^{(j)}(s) |$, where it holds that
  - $s_{i+1} \in \mathcal{S}_*$ corresponding to the residual vector $r^{(j)}(s_{i+1})$,
  - $s_\alpha \in \mathcal{S}_*$ with $s_\alpha \in \mathcal{S}_i$ corresponding to the current column $v_\alpha^{(i)} \in V^{(i)}$,
  - $s_k \in \mathcal{S}_*$ with $s_k \in \mathcal{S}_i$ such that $j_{k,i+1} > j_{k,i}$ $(k = 1, \ldots, i)$.
  Define $v_j^{(i+1)} = r^{(j)}(s_{i^\star}) / \| r^{(j)}(s_{i^\star}) \|_2$ and compute $h_\pi(s_{i^\star}) = h_\pi(s_{i^\star}) h_{j_{i^\star,i+1}}(s_{i^\star})$.
  Update $j_{i^\star,i+1} = j_{i^\star,i+1} + 1$.
  if $s_{i^\star} = s_{i+1}$ **then**
    Compute $r^{(j+1)}(s_{i+1}) = -(s_{i+1}\mathcal{E} - \mathcal{A})^{-1}\mathcal{E}v_j^{(i+1)}$.
  else
    if $j_{i^\star,i+1} \leq j_{i^\star,i}$ **then**
      Select $r^{(j+1)}(s_{i^\star}) = v_l^{(i)}$ with a suitable $l \in \{1, \ldots, n_r\}$.
    else
      Compute $r^{(j+1)}(s_{i^\star}) = -(s_{i^\star}\mathcal{E} - \mathcal{A})^{-1}\mathcal{E}v_j^{(i+1)}$.
      Update norm of residual $h_{j_{i^\star,i+1}}(s_{i^\star}) = \| r^{(j+1)}(s_{i^\star}) \|_2$.
    end if
    Update $\alpha \equiv \alpha + 1$.
  end if
  Update $r^{(j+1)}(s_l) = r^{(j)}(s_l)$ for all $l = 1, \ldots, i+1$ with $i \neq i^\star$.
  for $k = 1, \ldots, i+1$ **do**
    for $l = 1, \ldots, j$ **do**
      $r^{(j+1)}(s_k) = r^{(j+1)}(s_k) - \left(\left(v_l^{(i+1)} \right)^{\mathrm{T}} r^{(j+1)}(s_k) \right) v_l^{(i+1)}$
    end for
  end for
end for

appropriate formulation of the theoretical framework of moment matching methods requires the consideration of the order of the orthonormal vector sequence $V^{(i-1)}$.

The previous remark leads to the confirmation that the selection of the subsequent residual vector is given by

- $r^{(j)}(s_i)$ with the latest expansion point $s_i \in \mathcal{S}_i$ or
- $r^{(j)}(s_k) \equiv v_\alpha \in V^{(i-1)}$ $(k = 1, \ldots, i-1)$ with the index $\alpha = 1, \ldots, n_r$ corresponding to the current column or
- $r^{(j)}(s_k) = -(s_k\mathcal{E} - \mathcal{A})^{-1}\mathcal{E}v_{j_*}$ for an increasing dimension $j_{k,i} > j_{k,i-1}$ of the Krylov subspace $\mathcal{K}_{j_{k,i}}(s_k)$.

In doing so, the selection of the residual vectors corresponds to the adaptation of the output moment error, cf. line 6 in Algorithm 9. For the appropriate evaluation of the output moment error (4.2.8), the product of the norm of the residuals $\prod_j \| r^{(j)}(s) \|_2$, $s \in \mathcal{S}_i$, is preserved from the initial computation of each residual vector. In this way, a comparable result for the different dimensions $j_{1,i}, \ldots, j_{i,i} > 0$ in the subsequent calls of the AORA and mAORA method may be expected. Numerical experiments for a selection of model problems of Maxwell's equations in semiconductor structures have confirmed this assumption, see Chapter 6.

In [18], we have given a theoretical comparison between the Galerkin projection $\Pi = VV^{\mathrm{T}}$ obtained via the subsequent calls of a generic rational Arnoldi method and a modified generic rational Arnoldi method. Here, we adapt the existing results to the special case of the modified adaptive-order rational Arnoldi method. For the expansion points $s_1 \in \mathbb{C}$ and $s_2 \in \mathbb{C}$, two subsequent calls of the AORA and mAORA method lead to the same Galerkin projection in model order reduction with moment matching methods.

Lemma 5.1.2. *Let $s_1 \in \mathbb{C}$ and $s_2 \in \mathbb{C}$ denote two arbitrary expansion points. Moreover, the columns of the orthonormal matrix $V^{(2)} = [v_1^{(2)}, \ldots, v_{n_r}^{(2)}] \in \mathbb{C}^{n \times n_r}$ have been obtained from two subsequent calls of the modified AORA method. Then, the span of the orthonormal matrix $V^{(2)}$ fulfils*

$$\operatorname{colspan}(V^{(2)}) = \mathcal{K}_{j_1}(-(s_1\mathcal{E} - \mathcal{A})^{-1}\mathcal{E}, \mathcal{B}_1) + \mathcal{K}_{j_2}(-(s_2\mathcal{E} - \mathcal{A})^{-1}\mathcal{E}, \mathcal{B}_2), \tag{5.1.1}$$

where $\mathcal{B}_1 = (s_1\mathcal{E} - \mathcal{A})^{-1}\mathcal{B}$ and $\mathcal{B}_2 = (s_2\mathcal{E} - \mathcal{A})^{-1}\mathcal{B}$ with $n_r = j_1 + j_2$ and $j_1, j_2 \geq 0$.

Proof. Let $V^{(1)} = \left[v_1^{(1)}, \ldots, v_{n_r}^{(1)}\right] \in \mathbb{C}^{n \times n_r}$ denote the orthonormal matrix of the initial call of the modified generic rational Arnoldi method with $s_1 \in \mathbb{C}$. The statement of the lemma is proven via induction on the dimension of the reduced order model $n_r > 0$.

For $n_r = 1$, we will either employ the initial vector $v_1^{(1)} \in \operatorname{span}\{(s_1\mathcal{E} - \mathcal{A})^{-1}\mathcal{B}\}$ or compute the solution to the linear system $\tilde{v}_1^{(2)} = (s_2\mathcal{E} - \mathcal{A})^{-1}\mathcal{B}$. Hence, the initial expansion point selection during the second call of the mAORA method leads to

$$v_1^{(2)} \in \mathcal{K}_1(-(s_1\mathcal{E} - \mathcal{A})^{-1}\mathcal{E}, \mathcal{B}_1) \quad \text{or} \quad v_1^{(2)} \in \mathcal{K}_1(-(s_2\mathcal{E} - \mathcal{A})^{-1}\mathcal{E}, \mathcal{B}_2).$$

Otherwise, we have to distinguish between the choice $v_i \in V^{(1)}$ $(i = 1, \ldots, n_r)$ on the one hand and the computation of the subsequent orthonormal vector via $\tilde{v}_1 = (s_2\mathcal{E} - \mathcal{A})^{-1}\mathcal{B}$ or $\tilde{v}_i = -(s_2\mathcal{E} - \mathcal{A})^{-1}\mathcal{E}v_{i-1}$ $(i = 2, \ldots, n_r)$ on the other hand. Initially, we will assume that

$$\operatorname{span}\left\{v_1^{(2)}, \ldots, v_{n_r-1}^{(2)}\right\} \in \mathcal{K}_{j_1}(-(s_1\mathcal{E} - \mathcal{A})^{-1}\mathcal{E}, \mathcal{B}_1) + \mathcal{K}_{j_2-1}(-(s_2\mathcal{E} - \mathcal{A})^{-1}\mathcal{E}, \mathcal{B}_2), \tag{5.1.2}$$

which suggests that we have to select the expansion point $s_2 \in \mathbb{C}$ during the last iteration step. From $n_r - 1$ iteration steps of the modified adaptive-order rational Arnoldi method, we obtain

$$\gamma_{n_r,n_r-1}\tilde{v}_{n_r}^{(2)} = -(s_2\mathcal{E} - \mathcal{A})^{-1}\mathcal{E}v_{n_r-1}^{(2)} + \sum_{i=1}^{n_r-1} \gamma_{i,n_r-1}v_i^{(2)},$$

where $\gamma_{i,n_r-1} \in \mathbb{C}$ $(i = 1, \ldots, n_r - 1)$ refer to the coefficients of the modified Gram-Schmidt procedure and $\gamma_{n_r,n_r-1} \in \mathbb{R}$ resembles a normalization coefficient. Following the induction hypothesis (5.1.2), we are able to introduce the decomposition $v_{n_r-1}^{(2)} \equiv w_{j_1}^{(1)} + w_{j_2-1}^{(2)}$, where

$$w_{j_1}^{(1)} \in \mathcal{K}_{j_1}(-(s_1\mathcal{E} - \mathcal{A})^{-1}\mathcal{E}, \mathcal{B}_1) \quad \text{and} \quad w_{j_2-1}^{(2)} \in \mathcal{K}_{j_2-1}(-(s_2\mathcal{E} - \mathcal{A})^{-1}\mathcal{E}, \mathcal{B}_2).$$

The application of Lemma 4.2.1 ensures that $-(s_2\mathcal{E}-\mathcal{A})^{-1}\mathcal{E}w_{j_1}^{(1)}$ is already contained in the subspace (5.1.1). Since $-(s_2\mathcal{E} - \mathcal{A})^{-1}\mathcal{E}w_{j_2-1}^{(2)}$ simply extends the Krylov subspace of the expansion point $s_2 \in \mathbb{C}$, we obtain the proposition of the lemma. On the other hand, if we assume that

$$\operatorname{span}\left\{v_1^{(2)}, \ldots, v_{n_r-1}^{(2)}\right\} \in \mathcal{K}_{j_1-1}(-(s_1\mathcal{E} - \mathcal{A})^{-1}\mathcal{E}, \mathcal{B}_1) + \mathcal{K}_{j_2}(-(s_2\mathcal{E} - \mathcal{A})^{-1}\mathcal{E}, \mathcal{B}_2), \tag{5.1.3}$$

we will select the expansion point $s_1 \in \mathbb{C}$ during the last iteration step of the modified generic rational Arnoldi method. Therefore, we consider

$$\gamma_{n_r,n_r-1}\tilde{v}_{n_r}^{(2)} = v_{j_1}^{(1)} + \sum_{i=1}^{n_r-1} \gamma_{i,n_r-1}v_i^{(2)},$$

during the last iteration step, where the coefficients $\gamma_{i,n_r-1} \in \mathbb{C}$ $(i = 1, \ldots, n_r)$ refer to the modified Gram-Schmidt procedure. We know from the initial call of the modified adaptive-order rational Arnoldi method that

$$v_{j_1}^{(1)} \in \mathcal{K}_{j_1}(-(s_1\mathcal{E} - \mathcal{A})^{-1}\mathcal{E}, \mathcal{B}_1) \subset \mathcal{K}_{n_r}(-(s_1\mathcal{E} - \mathcal{A})^{-1}\mathcal{E}, \mathcal{B}_1).$$

The mAORA method suggests the choice of the vector $v_{j_1}^{(1)}$ from the already known vector sequence $v_1^{(1)}, \ldots, v_{n_r-1}^{(1)}$ including an orthonormalization against the previous computed subspace (5.1.3). Hence, the proposition of the lemma follows. □

Similar to the AORA method with the expansion points $s_1 \in \mathbb{C}$ and $s_2 \in \mathbb{C}$, the second call of the mAORA method allows for the selection of either the residual $r^{(j)}(s_1)$ or $r^{(j)}(s_2)$. Hence, the output moment error leads to the same dimensions of each Krylov subspace $\mathcal{K}_{j_1}(s_1)$ and $\mathcal{K}_{j_2}(s_2)$, where the order of appearance of the residual vectors $r^{(j)}(s_1)$ and $r^{(j)}(s_2)$ is identically equal to the selection in the AORA method. As a consequence, the moment matching property (4.2.5) remains valid for the two subsequent calls of the mAORA method.

The major difference for the adaptive selection of each expansion point in the modified adaptive-order rational Arnoldi method occurs for more than two expansion points. On the one hand, the AORA method allows for the computation of the output moment error for all residuals $r^{(j)}(s_k)$ $(k = 1, \ldots, i)$ in each iteration step. On the other hand, assuming that $j_{l,i+1} \leq j_{l,i}$ $(l = 1, \ldots, i)$ between subsequent calls the mAORA method computes the output moment error only for the residuals $r^{(j)}(s_k) \equiv v_\alpha \in V^{(i-1)}$ with an arbitrary $k = 1, \ldots, i-1$ and $r^{(j)}(s_i)$.

Hence, an extension of Lemma 5.1.2 follows from the subsequent application of the modified AORA method to a sequence of expansion points $s_1, \ldots, s_i \in \mathbb{C}$. Under the simplified assumption that the dimensions $j_{1,l}, \ldots, j_{l,l} > 0$ of the subsequent calls of the AORA and the mAORA method coincide for all $l = 1, \ldots, i$, we are again able to formulate a special case of the corresponding result of a modified generic rational Arnoldi method.

Lemma 5.1.3. *Let $s_1, \ldots, s_i \in \mathbb{C}$ denote a given set of expansion points. If the columns of the orthonormal matrix $V^{(i)} = [v_1^{(i)}, \ldots, v_{n_r}^{(i)}] \in \mathbb{C}^{n \times n_r}$ have been obtained from the modified adaptive-order rational Arnoldi (mAORA) method after $i > 0$ subsequent calls, then the relation*

$$\operatorname{colspan}(V^{(i)}) = \sum_{l=1}^{i} \mathcal{K}_{j_{l,i}}(-(s_l\mathcal{E} - \mathcal{A})^{-1}\mathcal{E}, \left(s_l\mathcal{E} - \mathcal{A}\right)^{-1}\mathcal{B})$$

holds, where $n_r = j_{1,i} + \ldots + j_{i,i}$, $j_{l,i} > 0$ $(l = 1, \ldots, i)$, denote the dimensions of each Krylov subspace resulting from the i-th call of the mAORA method.

Proof. We only provide a sketch of the proof due to the fact that the proof of Lemma 5.1.2 may immediately extended to the more general case with $l > 2$ expansion points.

Employing a single expansion point $s_1 \in \mathbb{C}$ refers to the application of the SPRIM algorithm for Maxwell's equations, cf. Algorithm 2, i.e. we simply focus on the case $l > 1$ in the following. Remember that the mAORA method, cf. Algorithm 9, considers the order of the orthonormal matrix $V^{(i-1)}$, while selecting a residual vector corresponding to the expansion points $s_1, \ldots, s_{i-1} \in \mathbb{C}$, cf. Remark 5.1.1. Assume that the subspace of the orthonormal vector sequence $V^{(i-1)}$ corresponds to the subspace (4.2.4) for a suitable selection of the dimensions $j_{1,i-1}, \ldots, j_{i-1,i-1}$.

As seen in Corollary 4.2.3, each variant of a rational Arnoldi method is equal to the rational Arnoldi method as long as the dimensions of the different Krylov subspaces coincide. Note

that the mAORA method refers to a special case of a (modified) rational Arnoldi method with a specific way of selecting the dimensions $j_{1,i}, \ldots, j_{i,i}$. For this reason, the statement of the Lemma follows by means of an inductive argument employing Lemma 4.2.1. □

As a general rule, the mAORA method will lead to different dimensions for each Krylov subspace $\mathcal{K}_{j_k}(-(s_k\mathcal{E}-\mathcal{A})^{-1}\mathcal{E}, (s_k\mathcal{E}-\mathcal{A})^{-1}\mathcal{B})$ $(k = 1, \ldots, l)$ due to the restriction of the selectable residuals in the adaptation of the output moment error, cf. line 6 in Algorithm 9. Consequently, the computed reduced order models by means of the mAORA method offer a different accuracy as for the AORA method. For example, the incorporation of the mAORA method in the AORA-RK method, cf. Algorithm 6, naturally results in a different selection of expansion points.

Nevertheless, numerical experiments for the first- and second-order Maxwell's equations given by (3.0.1) and (3.0.3) have confirmed that the differences between the AORA and the mAORA method either for a fixed set of expansion points or by means of the AORA-RK method do not have a significant impact on the accuracy of the reduced order model, see Chapter 6. In addition, the mAORA method leads to a remarkable speed-up with respect to the computational time and the memory requirement in the offline-stage of moment matching based model order reduction.

5.2 An algebraic two-level method

The *algebraic two-level method* (ATLM) represents a direct solver for solving a linear system of the first-order Maxwell's equations (3.0.1) in due consideration of the block-structure of the electric and magnetic field strength, see [19]. For a given expansion point $s_i \in \mathbb{C}$ and an arbitrary right-hand side $f \in \mathbb{C}^n$, we consider a shifted linear system of the first-order Maxwell's equations of the form

$$(s_i\mathcal{E} - \mathcal{A})x = f, \quad \text{where} \quad s_i\mathcal{E} - \mathcal{A} = \begin{pmatrix} s_iM_\epsilon + M_\sigma & -C \\ C^{\mathrm{T}} & s_iM_\mu \end{pmatrix}.$$

By decomposing the solution vector $x \equiv x(t) = [\boldsymbol{E}(t)^{\mathrm{T}}, \boldsymbol{H}(t)^{\mathrm{T}}]^{\mathrm{T}}$ and the right hand side $f = [f_1^{\mathrm{T}}, f_2^{\mathrm{T}}]^{\mathrm{T}}$ according to the dimensions of the electric and magnetic field strength, one step of block Gaussian elimination leads to

$$\begin{pmatrix} s_iM_\epsilon + M_\sigma & -C \\ C^{\mathrm{T}} & s_iM_\mu \end{pmatrix} = \begin{pmatrix} I & -CU_1^{-1} \\ 0 & L_1 \end{pmatrix} \begin{pmatrix} S & 0 \\ 0 & I \end{pmatrix} \begin{pmatrix} I & 0 \\ L_1^{-1}C^{\mathrm{T}} & U_1 \end{pmatrix}, \tag{5.2.1}$$

where $s_iM_\mu = L_1U_1$ and $S = (s_iM_\epsilon + M_\sigma) + C(s_iM_\mu)^{-1}C^{\mathrm{T}}$ refers to as the Schur complement of first-order Maxwell's equations. The decomposition (5.2.1) allows for solving a shifted linear

system by a backward substitution step, solving a linear system obtained via the corresponding Schur complement and a forward substitution step, cf. Algorithm 10.

Algorithm 10 Algebraic two-level method (ATLM) [19]

Input: Matrix pair $\mathcal{E}$ and $\mathcal{A}$; expansion point $s_i \in \mathbb{C}$; right-hand side $f \in \mathbb{C}^n$.

Output: Solution of linear system $(s_i\mathcal{E} - \mathcal{A})x = f$ with $x = [x_1^{\mathrm{T}}, x_2^{\mathrm{T}}]^{\mathrm{T}} \in \mathbb{C}^n$.

1: Determine the LU decomposition $s_i M_\mu = L_1 U_1$.
2: Backward-substitution: $z_2 = L_1^{-1} f_2$ and $z_1 = f_1 + C U_1^{-1} z_2$.
3: Compute Schur complement $S = (s_i M_\epsilon + M_\sigma) + C U_1^{-1} L_1^{-1} C^{\mathrm{T}}$.
4: Determine the LU decomposition $S = L_S U_S$.
5: Solve Schur complement system: $x_1 = U_S^{-1} L_S^{-1} z_1$.
6: Forward-substitution: $x_2 = U_1^{-1}(z_2 - L_1^{-1} C^{\mathrm{T}} x_1)$.

We see that solving a shifted linear system of the first-order Maxwell's equations by means of the ATLM basically consists of solving a linear system with the Schur complement. Numerical experiments have indicated a remarkable speed-up in the computational time required for solving a shifted linear system as compared to the application of the LU decomposition applied to the whole system, see Chapter 6.

Additionally, we will provide an extension of the algebraic two-level method by applying an iterative (recycling) Krylov subspace method for solving the shifted linear system corresponding to the Schur complement, cf. line 5 in Algorithm 10. In Section 5.3, we will review recycling Krylov subspace methods with an application to (complex) symmetric, but highly indefinite sparse linear systems corresponding to second-order Maxwell's equations.

The explicit construction of the Schur complement is impracticable for a non-diagonal mass matrix M_μ, e.g. the finite element method typically leads to a block-tridiagonal mass matrix. In this case, a mass lumping technique [27,35] or an explicit discretization of the second-order formulation of the Maxwell's equations becomes indispensable, cf. Section 3.3. Be aware that mass lumping techniques require an appropriate construction of the finite element employing higher-order edge elements, see [27].

5.3 Recycling Krylov subspace methods

This paragraph reviews *recycling Krylov subspace methods* for solving a sequence of high-dimensional linear systems of the form

$$A^{(j)} x^{(j)} = f^{(j)}, \quad j = 1, 2, \ldots,$$

where $A^{(j)} \in \mathbb{C}^{n \times n}$, $x^{(j)} \in \mathbb{C}^n$ and $f^{(j)} \in \mathbb{C}^n$. Recycling Krylov subspace methods benefit from the computation of a recycling subspace after solving the current linear system in order to

improve the convergence behaviour for the subsequent linear systems, see [91]. The principal idea behind the application of a recycling subspace in a Krylov subspace method has been originally introduced in the GCROT method, see [30].

Generally speaking, the *recycling subspace* $U_{i+1} \in \mathbb{C}^{n\times p}$ after solving the $(i+1)$-th linear system is computed by

$$C_{i+1} = A^{(i+1)}U_{i+1} \quad \text{with} \quad C_{i+1}^* C_{i+1} = I. \tag{5.3.1}$$

The application of the Arnoldi- or Lanczos-type method for solving the subsequent linear system is carried out with respect to the orthogonal complement of the subspace $C_{i+1} \in \mathbb{C}^{n\times p}$. Moreover, the selection of an appropriate sequence of orthonormal vectors for the recycling subspace is based on a generalized eigenvalue problem by means of the harmonic Ritz values, see [91].

At first, we will recapitulate the basic idea of Krylov subspace methods for iteratively solving a sparse linear system and give a short overview on the most important methods, e.g. the generalized minimal residual (GMRES) method, the biconjugate gradient (BiCG) method and the quasi-minimal residual (QMR) method, see [104]. Thereafter, an extension to the iterative recycling Krylov subspace methods based on the recycling subspace (5.3.1) is given. Finally, we will discuss the key ingredients of the recycling quasi-minimal residual (rQMR) method and the recycling simplified quasi-minimal residual (rSQMR) method.

5.3.1 Survey on Krylov subspace methods

We consider solving a high-dimensional linear system $Ax = f$, where $A \in \mathbb{C}^{n\times n}$, $x \in \mathbb{C}^n$ and $f \in \mathbb{C}^n$, with *Krylov subspace methods*, see [104]. A Krylov subspace employed for solving a linear system is constituted by

$$\mathcal{K}_k(A, r_0) = \operatorname{span}\{r_0, Ar_0, \ldots, A^{k-1}r_0\} \quad \text{with} \quad r_0 = f - Ax_0, \tag{5.3.2}$$

where $x_0 \in \mathbb{C}^n$ refers to as the initial guess of the approximate solution to the linear system $Ax = f$. If the columns of the orthonormal matrix $V_k \in \mathbb{C}^{n\times k}$ span the Krylov subspace (5.3.2), the k-th iterate $x_k \in \mathbb{C}^n$ of a Krylov subspace method is given by the (Petrov-) Galerkin projection, i.e.

$$x_k = x_0 + V_k y_k \quad \text{subject to} \quad r_k = f - Ax_k \perp \mathcal{L}_k. \tag{5.3.3}$$

Typically, the Krylov subspace $\mathcal{L}_k$ simply denotes the Krylov subspace $\mathcal{K}_k(A, r_0)$ or the Krylov subspace $\mathcal{K}_k(A^*, \tilde{r}_0)$, where $\tilde{r}_0 = \tilde{f} - A^*\tilde{x}_0$ refers to as the initial residual of the dual linear system $A^*\tilde{x} = \tilde{f}$ with the initial guess $\tilde{x}_0 \in \mathbb{C}^n$.

The first variant, i.e. $\mathcal{L}_k \equiv \mathcal{K}_k(A, r_0)$, leads to the computation of an orthonormal basis of the Krylov subspace $\mathcal{K}_k(A, r_0)$ with the *Arnoldi method*, which has been previously introduced in Algorithm 1 for moment matching based model order reduction. Recall that the Arnoldi method provides the relation

$$AV_k = V_{k+1}\underline{H}_k, \tag{5.3.4}$$

where the columns of the orthonormal matrix $V_k \in \mathbb{C}^{n\times k}$ span the Krylov subspace $\mathcal{K}_k(A, r_0)$ and $\underline{H}_k \in \mathbb{C}^{(k+1)\times k}$ denotes an upper Hessenberg matrix, see [6]. Here, the initialization of the orthonormal vector sequence follows from $v_1 = r_0/\| r_0 \|_2$.

The second variant, i.e. $\mathcal{L}_k \equiv \mathcal{K}_k(A^*, \tilde{r}_0)$, is based on the *unsymmetric Lanczos method* with biorthonormal matrices $V_k \in \mathbb{C}^{n\times k}$ and $W_k \in \mathbb{C}^{n\times k}$, $W_k^* V_k = I$, such that

$$AV_k = V_{k+1}\underline{T}_k \quad \text{and} \quad A^*W_k = W_{k+1}\underline{\tilde{T}}_k \tag{5.3.5}$$

where $\underline{T}_k \in \mathbb{C}^{(k+1)\times k}$ and $\underline{\tilde{T}}_k \in \mathbb{C}^{(k+1)\times k}$ are tridiagonal matrices and $v_1 = r_0/\| r_0 \|_2$ and $w_1 = \tilde{r}_0/\left(r_0^*\tilde{r}_0\right)$. As compared to the Arnoldi method, the Lanczos method uses a three-term recurrence in the computation of the biorthonormal vector sequence. Since the Lanczos method allows for a freedom of scaling each vector sequence $V_k \in \mathbb{C}^{n\times k}$ and $W_k \in \mathbb{C}^{n\times k}$, we will assume in the following that the relation $W_k^* V_k = D_k$ holds, where $D_k \in \mathbb{C}^{k\times k}$ represents a diagonal matrix, see [57].

The general framework of a Krylov subspace method (5.3.3) based on the Arnoldi method (5.3.4) leads to the norm of the residual

$$\| r_k \|_2 = \| f - Ax_k \|_2 = \| r_0 - AV_k y_k \|_2 = \| V_{k+1}(\rho_0 e_1 - \underline{H}_k y_k) \|_2 = \| \rho_0 e_1 - \underline{H}_k y_k \|_2,$$

where $\rho_0 = \| r_0 \|_2$. More precisely, the *generalized minimal residual (GMRES) method* [105] computes the solution update $x_k^G = x_0^G + V_k y_k^G$ during the k-th iteration step by means of the least squares problem

$$\| \rho_0 e_1 - \underline{H}_k y_k^G \|_2 = \min_{y\in\mathbb{C}^k} \| \rho_0 e_1 - \underline{H}_k y \|_2. \tag{5.3.6}$$

Since $\underline{H}_k \in \mathbb{C}^{(k+1)\times k}$ represents an upper Hessenberg matrix, the subsequent solution to the least squares problem (5.3.6) is computed by a sequence of Householder orthogonalizations or Givens rotations, see [104].

Whenever the application at hand depends on the simultaneous solution to the primary and dual linear system $Ax = f$ and $A^*\tilde{x} = \tilde{f}$, the *biconjugate gradient (BiCG) method* represents the method of choice, see [42, 73]. More precisely, the BiCG method computes the solution update of the primary system

$$x_k^B = x_0^B + V_k y_k^B \quad \text{subject to} \quad r_k^B = f - Ax_k^B \perp W_k \tag{5.3.7}$$

and the corresponding solution update of the dual system

$$\tilde{x}_k^B = \tilde{x}_0^B + W_k \tilde{y}_k^B \quad \text{subject to} \quad \tilde{r}_k^B = \tilde{f} - A^* \tilde{x}_k^B \perp V_k.$$

Similar to the conjugate gradients (CG) method by Hestenes and Stiefel [59], the solution updates of the primary and dual system are obtained via

$$T_k y_k^B = \rho_0 e_1 \quad \text{and} \quad \tilde{T}_k \tilde{y}_k^B = \tilde{\rho}_0 e_1,$$

where $T_k \in \mathbb{C}^{k\times k}$ and $\tilde{T}_k \in \mathbb{C}^{k\times k}$ refer to as the tridiagonal matrices from the unsymmetric Lanczos method (5.3.5) and $\rho_0 = \| r_0^B \|_2$ and $\tilde{\rho}_0 = \| \tilde{r}_0^B \|_2$. A practical implementation of the BiCG method is typically based on a subsequently updated LDU decomposition of the tridiagonal matrix.

The BiCG method breaks down when the relation $(\tilde{r}_i^B)^* r_i^B = 0$ occurs or the LDU factorization without permutations of the tridiagonal matrix T_k fails due to a zero pivot element. An appropriate treatment of a breakdown situation in the BiCG method is given by the *look-ahead Lanczos method* [47]. For the Maxwell's equations, the situation of a breakdown has never been observed during our numerical experiments in Chapter 6.

The *quasi-minimal residual (QMR) method* makes use of the biorthogonal vector sequence $V_k \in \mathbb{C}^{n\times k}$ obtained via the unsymmetric Lanczos method and leads to to the minimization of an upper bound of the norm of the residual, see [48]. Since a straightforward computation shows that

$$\begin{aligned} \| r_k^Q \|_2 &= \| f - A x_k^Q \|_2 \\ &= \| V_{k+1} \Omega_{k+1}^{-1} (\rho_0 e_1 - \Omega_{k+1} \underline{T}_k y_k^Q) \|_2 \\ &\leq \| V_{k+1} \Omega_{k+1}^{-1} \|_2 \| \rho_0 e_1 - \Omega_{k+1} \underline{T}_k y_k^Q \|_2, \end{aligned}$$

where $\Omega_{k+1} = \mathrm{diag}(\omega_1, \ldots, \omega_{k+1})$, $\omega_i \in \mathbb{R}$, refers to as an arbitrary scaling matrix and $\rho_0 = \omega_1 \| r_0^Q \|_2$, the solution update $x_k^Q = x_0^Q + V_k y_k^Q$ of the primary system is achieved by the least squares problem

$$\| \rho_0 e_1 - \Omega_{k+1} \underline{T}_k y_k^Q \|_2 = \min_{y\in\mathbb{C}^k} \| \rho_0 e_1 - \Omega_{k+1} \underline{T}_k y \|_2. \tag{5.3.8}$$

A single Givens rotation in each iteration step typically allows for solving the least squares problem (5.3.8) due to the fact that $\underline{T}_k \in \mathbb{C}^{(k+1)\times k}$ is a tridiagonal matrix. Moreover, a common choice for each entry of the general scaling matrix Ω_{k+1} is given by $\omega_i = \| v_i \|_2$ $(i = 1, \ldots, k+1)$, see [47].

For the special case of a J-symmetric or J-hermitian coefficient matrix $A \in \mathbb{C}^{n\times n}$, i.e. $A^{\mathrm{T}} J = JA$ or $A^* J = JA$ with a non-singular matrix $J \in \mathbb{C}^{n\times n}$, the QMR method allows for a significant simplification. Defining $w_i \equiv J v_i$ leads to the following biorthonormal condition in

unsymmetric Lanczos method, i.e.

$$(Jv_i)^{\mathrm{T}} v_j = \delta_{ij} \quad \text{or} \quad (Jv_i)^* v_j = \delta_{ij}$$

depending on the (complex) symmetric or hermitian case, see [50]. The advantage of the *simplified quasi-minimal residual (SQMR) method* is that the unsymmetric Lanczos method (5.3.5) only requires the vector sequence $V_k \in \mathbb{C}^{n\times k}$ due to the fact that $w_j = \xi_j J v_j$ holds for all $j = 1, \ldots, k$. Here, $\xi_j \in \mathbb{C}$ $(j = 1, \ldots, k)$ refers to as an appropriate scaling factor of the dual vector sequence.

An important example of J-symmetry has been introduced by Freund and Nachtigal for a preconditioned linear system, see [50]. The application of the complex symmetric preconditioner $M = M_1 M_2 = M_2^{\mathrm{T}} M_1^{\mathrm{T}} = M^T$ to the linear system $Ax = f$ with a complex symmetric coefficient matrix $A \in \mathbb{C}^{n\times n}$ results in the preconditioned linear system[1]

$$A'x' = f', \quad \text{where} \quad A' = M_1^{-1} A M_2^{-1}, \quad x' = M_2 x \quad \text{and} \quad f' = M_1^{-1} f.$$

Hence, the J-symmetric of the matrix A', i.e. $(A')^{\mathrm{T}} J = JA'$, follows immediately by setting $J \equiv M_1^{\mathrm{T}} M_2^{-1}$. Typically, we leave out the preconditioner $M = M_1 M_2$ within the discussion of the J-symmetry of a coefficient matrix. This simplification is in due consideration of the fact that preconditioned Krylov subspace methods may be rewritten in such a way that the explicit computation of the matrix-vector product $A'y = M_1^{-1} A M_2^{-1} y$, $y \in \mathbb{C}^n$, will never be performed.

5.3.2 The recycling biconjugate gradient method

The *recycling biconjugate gradient (rBiCG) method* consists of simultaneously solving a sequence of primary and dual linear systems of the form

$$A^{(j)} x^{(j)} = f^{(j)} \quad \text{and} \quad (A^{(j)})^* \tilde{x}^{(j)} = \tilde{f}^{(j)}, \quad j = 1, 2, \ldots,$$

see [2]. Thereby, the solution update of the rBiCG method is obtained via a suitable adaptation of the solution update of the BiCG method in order to benefit from the introduction of a pair of recycling subspaces. In this context, we also review a common framework for the computation of recycling subspaces by means of the harmonic Ritz values, see [91].

First of all, an extension of the recycling subspace $U_{i+1} \in \mathbb{C}^{n\times p}$ (5.3.1) is given in order to properly incorporate the biorthonormal vector sequence $V_k \in \mathbb{C}^{n\times k}$ and $W_k \in \mathbb{C}^{n\times k}$ obtained via the unsymmetric Lanczos method. For convenience, we will leave out the index notation for the $(i+1)$-th linear system, i.e. we refer to as $A \equiv A^{(i+1)}$ and $A^* \equiv (A^{(i+1)})^*$ on the hand, while we denote $U \equiv U_{i+1}$ $(\tilde{U} \equiv \tilde{U}_{i+1})$ and $C \equiv C_{i+1}$ $(\tilde{C} \equiv \tilde{C}_{i+1})$ on the other hand.

[1] Note that $M_1 = M_2^{\mathrm{T}}$ is not necessarily required [50].

The recycling biconjugate gradient method requires a pair of recycling subspaces $U \in \mathbb{C}^{n\times p}$ and $\tilde{U} \in \mathbb{C}^{n\times p}$ with $C = AU$ and $\tilde{C} = A^*\tilde{U}$ subject to

$$\begin{bmatrix}\tilde{C}, & W_k\end{bmatrix} \perp_b \begin{bmatrix}C, & V_k\end{bmatrix}, \tag{5.3.9}$$

see [2]. As a consequence of the three term recurrence of the unsymmetric Lanczos method and the biorthogonal condition (5.3.9), the biorthogonal vector sequence $v_{j+1} \in V_k$ and $w_{j+1} \in W_k$ achieved by the corresponding j-th and $(j-1)$-th Lanczos vectors and the recycling subspaces C and $\tilde{C}$, respectively. This observation results in an extension of the unsymmetric Lanczos method (5.3.5) with respect to the pair of recycling subspaces, i.e.

$$(I - C\hat{C}^*)AV_k = V_{k+1}\underline{T}_k \quad \text{and} \quad (I - \tilde{C}\check{C}^*)A^*W_k = W_{k+1}\underline{\tilde{T}}_k \tag{5.3.10}$$

where $\hat{C} = \tilde{C}D_c^{-*}$ and $\check{C} = CD_c^{-1}$ with $D_c = \operatorname{diag}\left((\tilde{c}_1)^{\mathrm{T}}c_1, \ldots, (\tilde{c}_p)^{\mathrm{T}}c_p\right)$.

We will only discuss the solution update of the primary system in the recycling BiCG method since a similar argument holds for the corresponding dual linear system $A^*\tilde{x} = \tilde{f}$. In [2], the authors extend the solution update (5.3.7) of the BiCG method to the solution update of the rBiCG method by

$$x_k^{rB} = x_0^{rB} + Uz_k^{rB} + V_k y_k^{rB}. \tag{5.3.11}$$

Hence, the biorthogonal condition (5.3.9) is used to require

$$r_k^{rB} = f - Ax_k^{rB} = r_0^{rB} - AUz_k^{rB} - AV_k y_k^{rB} \perp \begin{bmatrix}\tilde{C}, & W_k\end{bmatrix}.$$

Remember that the solution update of the BiCG method follows from the subsequent computation of an LDU decomposition of the tridiagonal matrix $T_k \in \mathbb{C}^{k\times k}$. Since the solution update of the recycling BiCG method (5.3.11) simply appends the recycling subspace $U \in \mathbb{C}^{n\times p}$ to the solution update of the BiCG method (5.3.7), each iterate of the rBiCG method can be computed solving a tridiagonal system with T_k, see [2]. From the unsymmetric Lanczos relation (5.3.10), the solution update of the rBiCG method (5.3.11) and the recycling subspace property $C = AU$, it follows that

$$A\begin{bmatrix}U, & V_k\end{bmatrix}\begin{bmatrix}z_k^{rB}\\ y_k^{rB}\end{bmatrix} = \begin{bmatrix}C, & V_{k+1}\end{bmatrix}\begin{bmatrix}I & \hat{C}^*AV_k\\ 0 & \underline{T}_k\end{bmatrix}\begin{bmatrix}z_k^{rB}\\ y_k^{rB}\end{bmatrix}. \tag{5.3.12}$$

Ahuja et al. have shown that the application of the orthogonal condition (5.3.9) to the augmented Lanczos relation (5.3.12) leads to the solution update of the primary linear system

$$x_k^{rB} = x_0^{rB} + U\hat{C}^*r_0^{rB} + (I - U\hat{C}^*A)V_k y_k^{rB}, \tag{5.3.13}$$

where $T_k y_k^{rB} = \| (I - C\hat{C}^*) r_0^{rB} \|_2 e_1$, see [2]. An efficient implementation of the matrix-matrix multiplication $U\hat{C}^* A$ at the end of solving the j-th linear system $(j = 1, 2, \ldots)$ has been given by Ahuja in [1].

Note that solving a sequence of linear systems allows for different approaches within the computation of a pair of recycling subspaces $C_{i+1} \in \mathbb{C}^{n\times p}$ and $\tilde{C}_{i+1} \in \mathbb{C}^{n\times p}$, see [1]. For example, Ahuja et al. have introduced a subspace recycling technique based on the subspaces $C_0 \in \mathbb{C}^{n\times p}$ and $C_{j+1} \in \mathbb{C}^{n\times p}$. The subspace C_0 represents the latest recycling subspace arising from solving the j-th linear system, while C_{j+1} refers to as the subsequently updated recycling subspace corresponding to solving the $(j+1)$-th linear system, see [2]. For simplicity, we will only consider the subspace $C \equiv C_{j+1}$ within the computation of the subsequent recycling subspace [18].

For the appropriate computation of a recycling subspace, remember that *harmonic Ritz values* $\theta = 1/\mu$ of a matrix $A \in \mathbb{C}^{n\times n}$ are defined by means of the generalized eigenvalue problem

$$A^{-1} y - \mu y \perp w \quad \forall\, w \in AP \;\text{ and }\; y \in AP, \tag{5.3.14}$$

where $P = \mathcal{K}_k(A, r_0)$, see [91]. In view of the augmented Lanczos relation (5.3.12), Ahuja et al. [2] have introduced $\Phi_k = \begin{bmatrix} U, & V_k \end{bmatrix}$ and $\Psi_k = \begin{bmatrix} C, & V_{k+1} \end{bmatrix}$ such that

$$A\Phi_k = \Psi_k H_k, \quad \text{where} \quad H_k = \begin{bmatrix} I & \hat{C}^* A V_k \\ 0 & \underline{T}_k \end{bmatrix}. \tag{5.3.15}$$

The corresponding relation of the dual linear system follows from $\tilde{\Phi}_k = \begin{bmatrix} \tilde{U}, & W_k \end{bmatrix}$ and $\tilde{\Psi}_k = \begin{bmatrix} \tilde{C}, & W_{k+1} \end{bmatrix}$ such that

$$A^* \tilde{\Phi}_k = \tilde{\Psi}_k \tilde{H}_k, \quad \text{where} \quad \tilde{H}_k = \begin{bmatrix} I & \check{C}^* A^* W_k \\ 0 & \underline{\tilde{T}}_k \end{bmatrix}. \tag{5.3.16}$$

Thus, a combination of the augmented Lanczos relations (5.3.15) and (5.3.16) leads to the formulation of the generalized eigenvalue problem

$$(\tilde{H}_k^* \tilde{\Psi}_k^* \Psi_k H_k) W = (\tilde{H}_k^* \tilde{\Psi}_k^* \Phi_k) W \Lambda. \tag{5.3.17}$$

If we refer to the columns of W_p as the $p > 0$ right eigenvectors corresponding to the harmonic Ritz values of smallest magnitude, the recycling subspace is given by $U = \Phi_k W_p$. An efficient computation of the matrix pair $(\tilde{H}_k^* \tilde{\Psi}_k^* \Psi_k H_k, \tilde{H}_k^* \tilde{\Psi}_k^* \Phi_k)$ required for the generalized eigenvalue problem (5.3.17) was previously discussed by Ahuja et al. in [2].

If the solution to the first linear system is computed without a pair of recycling subspaces, the initial pair of recycling subspaces [2] follows from the eigenvalue problems

$$T_k W = W \Lambda \quad \text{and} \quad \tilde{T}_k \tilde{W} = \tilde{W} \Theta, \tag{5.3.18}$$

where T_k and $\tilde{T}_k$ denote the tridiagonal matrices of the unsymmetric Lanczos method (5.3.5). As before, the recycling subspaces $U = W_p$ and $\tilde{U} = \tilde{W}_p$ correspond to the Ritz values of smallest magnitude.

5.3.3 A recycling simplified quasi-minimal residual method

In the following, we will provide an extension of the rBiCG method to a *recycling quasi-minimal residual (rQMR) method* and a *recycling simplified quasi-minimal residual (rSQMR) method*. The formulation of the (recycling) SQMR method is based on the coupled two-term recurrences variant of the unsymmetric Lanczos method given by Freund and Nachtigal [49].

It is important to note that the QMR and SQMR method on the one hand and the recycling QMR and recycling SQMR method on the other hand are based on the unsymmetric Lanczos method but employing a completely different solution update due to the introduction of a recycling subspace. Nevertheless, we will see that the derivation of the recycling (simplified) quasi-minimal residual method also requires the minimization of an upper bound of the norm of the residual, cf. (5.3.8).

To begin with, note that solution update of the QMR method may be obtained via the solution update of the BiCG method, see [44].

Lemma 5.3.1 ([44, Lemma 4.1])**.** *Let $\omega_1 > 0$, $m \geq 1$ and*

$$\underline{H}_m = \begin{bmatrix} H_m \\ h_{m+1,m}\tilde{e}_m^{\mathrm{T}} \end{bmatrix} = \begin{bmatrix} \underline{H}_{m-1} & * \\ 0 & h_{m+1,m} \end{bmatrix},$$

where $\tilde{e}_m^{\mathrm{T}} = \begin{bmatrix} 0 & \dots & 0 & 1 \end{bmatrix} \in \mathbb{R}^m$, be an $(m+1)\times m$ upper Hessenberg matrix of full column rank. For $k = m-1$, let $z_k \in \mathbb{C}^k$ denote the solution to the least-squares problem $\tau_k \equiv \min_{z\in\mathbb{C}^k} \| f_{k+1} - \underline{H}_m z \|_2$, where $f_{k+1} = \omega_1 e_1 \in \mathbb{R}^{k+1}$. Moreover, assume that the $m \times m$ matrix T_m is non-singular and set $\tilde{z}_m \equiv H_m^{-1} f_m$. Then,

$$z_m = (1 - c_m^2) \begin{bmatrix} z_{m-1} \\ 0 \end{bmatrix} + c_m^2 \tilde{z}_m, \quad \tau_m = \tau_{m-1}\vartheta_m c_m, \tag{5.3.19}$$

where

$$\vartheta_m = \frac{1}{\tau_{m-1}} \| f_{m+1} - \underline{T}_m \tilde{z}_m \|_2 \quad \textit{and} \quad c_m = \frac{1}{\sqrt{1+\vartheta_m^2}}.$$

The result of Lemma 5.3.1 has been formulated for the more general case of an upper Hessenberg matrix. Nevertheless, the relationship (5.3.19) makes an extension to the solution update of the BiCG and the QMR method possible.

By comparison with the initial approach for the solution update of the rBiCG method, we extend the solution update of the QMR method by means of the recycling subspace $U \in \mathbb{C}^{n\times p}$ such that

$$x_k^{rQ} = x_0^{rQ} + Uz_k^{rQ} + V_k y_k^{rQ}. \tag{5.3.20}$$

As seen before for the rBiCG method, cf. (5.3.10), the unsymmetric Lanczos method will be applied to the matrices $(I - C\hat{C}^*)A$ and $(I - C\check{C}^*)A^*$. Together with the initial approach for the solution update of the rQMR method and the recycling subspace property $C = AU$, we obtain

$$A\begin{bmatrix} U, & V_k \end{bmatrix}\begin{bmatrix} z_k^{rQ} \\ y_k^{rQ} \end{bmatrix} = \begin{bmatrix} C, & V_{k+1} \end{bmatrix}\begin{bmatrix} I & \hat{C}^*AV_k \\ 0 & \underline{T}_k \end{bmatrix}\begin{bmatrix} z_k^{rQ} \\ y_k^{rQ} \end{bmatrix}. \tag{5.3.21}$$

Hence, the computation of the norm of the residual of the rQMR method leads to

$$\begin{aligned} \| r_k^{rQ} \|_2 &= \| r_0^{rQ} - AUz_k^{rQ} - AV_k y_k^{rQ} \|_2 \\ &= \| r_0^{rQ} - \begin{bmatrix} C, & V_{k+1} \end{bmatrix}\begin{bmatrix} I & \hat{C}^*AV_k \\ 0 & \underline{T}_k \end{bmatrix}\begin{bmatrix} z_k^{rQ} \\ y_k^{rQ} \end{bmatrix} \|_2 \\ &= \| \begin{bmatrix} C, & V_{k+1}\Omega_{k+1}^{-1} \end{bmatrix}\left(\begin{bmatrix} \hat{C}^* r_0^{rQ} \\ \rho_0 e_1 \end{bmatrix} - \begin{bmatrix} I & \hat{C}^*AV_k \\ 0 & \Omega_{k+1}\underline{T}_k \end{bmatrix}\begin{bmatrix} z_k^{rQ} \\ y_k^{rQ} \end{bmatrix} \right) \|_2 \\ &\leq \| \begin{bmatrix} C, & V_{k+1}\Omega_{k+1}^{-1} \end{bmatrix} \|_2 \| \begin{bmatrix} \hat{C}^* r_0^{rQ} \\ \rho_0 e_1 \end{bmatrix} - \begin{bmatrix} I & \hat{C}^*AV_k \\ 0 & \Omega_{k+1}\underline{T}_k \end{bmatrix}\begin{bmatrix} z_k^{rQ} \\ y_k^{rQ} \end{bmatrix} \|_2, \end{aligned}$$

where $\rho_0 = \omega_1 \| (I - C\hat{C}^*) r_0 \|_2$. Due to the fact that $\| \begin{bmatrix} C, & V_{k+1}\Omega_{k+1}^{-1} \end{bmatrix} \|_2 \leq \text{const.}$ holds, the minimization of the upper bound of the norm of the residual is given by the least squares problem

$$\| \rho_0 e_1 - \Omega_{k+1}\underline{T}_k y_k^{rQ} \|_2 = \min_{y\in\mathbb{C}^k} \| \rho_0 e_1 - \Omega_{k+1}\underline{T}_k y \|_2, \tag{5.3.22}$$

where $\underline{T}_k \in \mathbb{C}^{(k+1)\times k}$ represents the tridiagonal matrix of the unsymmetric Lanczos method (5.3.10) with respect to the orthogonal complement of the pair of recycling subspaces, and

$$z_k^{rQ} = \hat{C}^* r_0^{rQ} - \hat{C}^* AV_k y_k^{rQ}. \tag{5.3.23}$$

In summary, (5.3.22) and (5.3.23) allow for rewriting the initial approach of the solution update (5.3.20) of the rQMR method, i.e.

$$x_k^{rQ} = x_0^{rQ} + U\hat{C}^* r_0^{rQ} + (I - U\hat{C}^*A)V_k y_k^{rQ}. \tag{5.3.24}$$

For efficiently computing the solution update of the rQMR method (5.3.24), we make use of the previous results of the rBiCG method. More precisely, the relation between the iterative process of the QMR and the BiCG method, cf. Lemma 5.3.1, allows for an extension to the rQMR

and the rBiCG method. It is important to note that the derivation of (5.3.19) only depends on an upper Hessenberg matrix $\underline{H}_k \in \mathbb{C}^{(k+1)\times k}$ or a tridiagonal matrix $\underline{T}_k \in \mathbb{C}^{(k+1)\times k}$, respectively, see [44]. Hence, employing (5.3.19) with respect to the solution update of the rBiCG and the rQMR method $y_k^{rB} \in \mathbb{C}^k$ and $y_k^{rQ} \in \mathbb{C}^k$ to the iterative rule of the rQMR method (5.3.24), we obtain

$$\begin{aligned} x_k^{rQ} &= x_0^{rQ} + (I - U\hat{C}^*A)V_k y_k^{rQ} \\ &= x_0^{rQ} + (1-c_k^2)(I - U\hat{C}^*A)V_{k-1}y_{k-1}^{rQ} + c_k^2(I - U\hat{C}^*A)y_k^{rB} \\ &= x_{k-1}^{rQ} - c_k^2 x_{k-1}^{rQ} + c_k^2 x_k^{rB}. \end{aligned}$$

The replacement of the k-th iterate of the rBiCG method via $x_k^{rB} = x_{k-1}^{rB} + \alpha_{k-1}(I - U\hat{C}^*A)p_{k-1}$, see [2], extends the latter equation such that

$$\begin{aligned} x_k^{rQ} &= x_{k-1}^{rQ} - c_k^2 x_{k-1}^{rQ} + c_k^2(x_{k-1}^{rB} + \alpha_{k-1}(I - U\hat{C}^*A)p_{k-1}) \\ &= x_{k-1}^{rQ} + c_k^2(x_{k-1}^{rB} - x_{k-1}^{rQ}) + c_k^2\alpha_{k-1}(I - U\hat{C}^*A)p_{k-1}. \end{aligned}$$

Similar to the derivation of Proposition 5.2 in [48], we extend $y_k^B = y_k^Q + \vartheta_k^2 d_k$, where $d_k = x_k^{rQ} - x_{k-1}^{rQ}$, with respect to the recycling subspace. In other words, it follows that

$$x_k^{rB} - x_k^{rQ} = \vartheta_k^2(I - U\hat{C}^*A)d_k.$$

Therefore, the solution update of the recycling quasi-minimal residual (rQMR) method is obtained via

$$x_k^{rQ} = x_{k-1}^{rQ} + c_k^2\vartheta_{k-1}^2(I - U\hat{C}^*A)d_{k-1} + c_k^2\alpha_{k-1}(I - U\hat{C}^*A)p_{k-1}. \tag{5.3.25}$$

Since the solution update of the rQMR and rSQMR method coincides[2], an appropriate definition of the recycling subspaces C and $\tilde{C}$ with respect to the J-symmetry or the J-hermitian of the coefficient matrix becomes necessary. In view of shifted linear systems corresponding to the Maxwell's equations, we restrict the following discussion to a J-(complex-)symmetric coefficient matrix.

Let $A^{\mathrm{T}}J = JA$ be a J-(complex-)symmetric coefficient matrix with $J = J^{\mathrm{T}}$. At first glance, the J-symmetric property of the matrix $A \in \mathbb{C}^{n\times n}$ leads to the formulation of the recycling subspace of the dual linear system as follows:

$$C = AU \Rightarrow JC = (JA)U = A^{\mathrm{T}}(JU),$$

[2]For a J-symmetric or J-complex-symmetric coefficient matrix, we require the scalar product $u^{\mathrm{T}}v$ for arbitrary vectors $u, v \in \mathbb{C}^n$.

such that $\tilde{C} \equiv JC$ and $\tilde{U} \equiv JU$, see [18]. Moreover, the coefficient matrix of the extension of the unsymmetric Lanczos method (5.3.10) also permits the formulation of the J-(complex-)symmetric property, in detail

$$J(I - C\hat{C}^{\mathrm{T}})A = (I - \tilde{C}\check{C}^{\mathrm{T}})A^{\mathrm{T}}J.$$

Hence, we have shown that the J-(complex-)symmetry property of the matrix $A \in \mathbb{C}^{n\times n}$ spreads to the framework of iterative recycling Krylov subspace methods. A similar argument to the SQMR method shows that the previous results remain also valid for the corresponding preconditioned linear system $A'x' = f'$.

Throughout the thesis, we denote by $k > 0$ the number of eigenvectors preserved from solving the generalized eigenvalue problem (5.3.17) or (5.3.18), while $m - k > 0$ refers to as the number of iteration steps before an update of the recycling subspace.

The appropriate treatment of the solution update of the rQMR and the rSQMR method (5.3.24) in terms of the expression $U\hat{C}^{*}r_0^{rQ}$ requires an adaptation of the initial guess $x_{0,*} \in \mathbb{C}^n$ and the corresponding residual $r_{0,*} = f - Ax_{0,*}$. Therefore, the initialization of the rSQMR method reads as

$$x_0 \equiv x_{0,*} + U\hat{C}^{*}r_{0,*} \quad \text{and} \quad r_0 \equiv (I - C\hat{C}^{*})r_{0,*}, \tag{5.3.26}$$

cf. line 1 in Algorithm 11. In doing so, the unsymmetric Lanczos method avoids computing the subsequent biorthogonal matrices V_k and W_k from a subspace used for the solution of the previous linear system.

Finally, we summarize the application of the recycling simplified quasi-minimal residual method to a sequence of linear systems $A^{(j)}x^{(j)} = f^{(j)}$, where $(A^{(j)})^{\mathrm{T}}J = JA^{(j)}$ and $J = J^{\mathrm{T}}$. For example, let $s_i \in \mathbb{C}$ refer to as an arbitrary expansion point. Then, the first-order Maxwell's equations (3.0.1) satisfy

$$(s_i\mathcal{E} - \mathcal{A})^{\mathrm{T}}\begin{pmatrix} I & 0 \\ 0 & -I \end{pmatrix} = \begin{pmatrix} I & 0 \\ 0 & -I \end{pmatrix}(s_i\mathcal{E} - \mathcal{A}), \quad \text{where} \quad s_i\mathcal{E} - \mathcal{A} = \begin{pmatrix} s_iM_\epsilon + M_\sigma & -C \\ C^{\mathrm{T}} & s_iM_\mu \end{pmatrix},$$

while the second-order Maxwell equation (3.0.3) leads to

$$(s_i^2M_\epsilon + s_iM_\sigma + CM_\mu^{-1}C^{\mathrm{T}})^{\mathrm{T}}I = I(s_i^2M_\epsilon + s_iM_\sigma + CM_\mu^{-1}C^{\mathrm{T}}).$$

In view of line 6, line 9 and line 14 in Algorithm 11, an explicit computation of the vector sequences $w_i = \gamma_i Jv_i$ and $q_i = \gamma_i Jp_i$ $(i = 1, \ldots, l)$ may be omitted in this way. Moreover, the computation of the arbitrary scaling factor $\gamma_i > 0$ $(i = 1, \ldots, l)$ adopted from Freund and Nachtigal [50] becomes redundant.

Remember that a complex symmetric coefficient matrix is in need of the scalar product $u^{\mathrm{T}}v$ for arbitrary vectors $u, v \in \mathbb{C}^n$. In particular, this scalar product must be applied to the solution update of the rSQMR method (5.3.25) and the generalized eigenvalue problem (5.3.17). Assuming that $J = I$ holds in the following, the solutions to the sequence of linear systems by means of the rSQMR method are obtained via the following steps:

1. Employ $m > 0$ iteration steps of the SQMR method to the first linear system.
2. Compute the first recycling subspace $U_1 \in \mathbb{C}^{n\times k}$ by means of the eigenvalue problem (5.3.18).
3. If a given tolerance has been reached, proceed to the subsequent linear system.
4. Otherwise, subsequently apply $l \equiv m - k > 0$ iteration steps of the rSQMR method, until convergence of the approximate solution has occurred, cf. Algorithm 11. After each call of the rSQMR method, we require an update of the recycling subspace with the help of the generalized eigenvalue problem (5.3.17), where

$$\Phi_l = [U_1, V_l] \quad \text{and} \quad \Psi_l = [C_1, V_{l+1}].$$

5. For each linear system $A^{(j)}x^{(j)} = f^{(j)}$ $(j = 2, 3, \ldots)$, perform the following steps:
   (a) If a recycling subspace U_{j-1} is available, run $l \equiv m - k > 0$ iteration steps of the rSQMR method, cf. Algorithm 11.
   (b) By means of the biorthonormal matrices $V_l \in \mathbb{C}^{n\times l}$ and $W_l = JV_l \in \mathbb{C}^{n\times l}$ compute an update of the recycling subspace, cf. (5.3.17), where

$$\Phi_l = [U_{j-1}, V_l] \quad \text{and} \quad \Psi_l = [C_{j-1}, V_{l+1}].$$

   (c) If a given tolerance has been reached, proceed to the subsequent linear system, i.e. $j \equiv j + 1$.
   (d) Otherwise, proceed to step 5a with the updated recycling subspace $U_{j-1} \in \mathbb{C}^{n\times k}$.

Algorithm 11 Recycling simplified quasi-minimal residual (rSQMR) method

Input: Let $A \in \mathbb{C}^{n\times n}$, $x \in \mathbb{C}^n$ and $f \in \mathbb{C}^n$ refer to the linear system $Ax = f$ with $A^{\mathrm{T}}J = JA$; $C = AU$ a recycling subspace with $\tilde{C} = JC$ and $\hat{C} = \tilde{C}D_c^{-1}$, where $D_c = \operatorname{diag}\left((\tilde{c}_1)^{\mathrm{T}}c_1, \ldots, (\tilde{c}_p)^{\mathrm{T}}c_p\right)$; $x_{0,*} \in \mathbb{C}^n$ initial guess for iterative solution; maximum number of iteration steps $l > 0$; tolerance tol for convergence criterion.

Output: Approximate solution to linear system $Ax = f$ after $i > 0$ iteration steps.

1: Relating to (5.3.26), compute initial guess $x_0 \in \mathbb{C}^n$ and residual $r_0 \in \mathbb{C}^n$ by means of

$$x_0 \equiv x_{0,*} + U\hat{C}^{\mathrm{T}}r_{0,*} \quad \text{and} \quad r_0 \equiv (I - C\hat{C}^{\mathrm{T}})r_{0,*}.$$

2: Initialize $v_1 = r_0/\rho_1$ with $\rho_1 = \| r_0 \|_2$.

3: Set $p_0 = q_0 = d_0 = 0, c_0 = \epsilon_0 = \xi_1 = 1, \gamma_1 = 1, \vartheta_0 = 0, \eta_0 = -1$.

4: **for** $i = 1, \ldots, l$ **do**

5: Lanczos coefficient: $\delta_i = (\gamma_i J v_i)^{\mathrm{T}} v_i$.

6: Update search direction: $p_i = v_i - p_{i-1}(\xi_i\delta_i/\epsilon_{i-1})$ and $q_i = \gamma_i J p_i$.

7: Compute matrix-vector multiplication: $z = Ap_i$, $y = \hat{C}^{\mathrm{T}}z$ and $w = z - Cy$.

8: Lanczos coefficients: $\epsilon_i = (q_i)^{\mathrm{T}}w$ and $\beta_i = \epsilon_i/\delta_i$.

9: Update biorthogonal vector sequence:

$$\tilde{v}_{i+1} = w - \beta_i v_i, \quad \rho_{i+1} = \| \tilde{v}_{i+1} \|_2 \quad \text{and} \quad \tilde{w}_{i+1} = \gamma_i J v_{i+1}, \quad \xi_{i+1} = \| \tilde{w}_{i+1} \|_2.$$

10: Scaling factor of biorthonormal vector sequence: $\gamma_{i+1} = \gamma_i(\rho_{i+1}/\xi_{i+1})$.

11: Compute solution update:

$$\vartheta_i = \frac{\omega_{i+1}\rho_{i+1}}{\omega_i c_{i-1} |\, \beta_i \,|}, \quad c_i = \frac{1}{\sqrt{1+\vartheta_i^2}}, \quad \eta_i = -\eta_{i-1}\frac{\rho_i c_i^2}{\beta_i c_{i-1}^2},$$
$$d_i = \eta_i(I - U\hat{C}^{\mathrm{T}}A)p_i + (\vartheta_{i-1}c_i)^2(I - U\hat{C}^{\mathrm{T}}A)d_{i-1}, \quad x_i = x_{i-1} + d_i.$$

12: If $\rho_{i+1} = 0$ and $\xi_{i+1} = 0$, then stop.

13: Check i-th residual vector r_i for convergence, e.g. $\| r_i \|_2 < \mathrm{tol} \cdot \| f \|_2$.

14: Define $v_{i+1} = \tilde{v}_{i+1}/\rho_{i+1}$ and $w_{i+1} = \tilde{w}_{i+1}/\xi_{i+1}$.

15: **end for**

CHAPTER 6

Numerical experiments for semiconductor structures

The previous chapters have given a comprehensive overview on the class of moment matching methods in model order reduction of Maxwell's equations given by the linear dynamical systems (3.0.1) and (3.0.3). Apart from the comparison of different greedy-type expansion point selection strategies in moment matching based model order reduction, cf. Subsection 4.2.4, the numerical experiments also affect the improvements from the application of a rational Arnoldi-type method, e.g. the AORA method, with a direct solver to the modified adaptive-order rational Arnoldi (mAORA) method with a recycling Krylov subspace method.

At first, three different model problems of the first- and second-order Maxwell's equations representing individual components of electric circuits are introduced. For the first-order formulation, the discretization primarily follows from the FIT, while the FEM has been applied to second-order Maxwell's equations. Thereafter, the AORA-RK method, cf. Algorithm 6, the AORA-H2 method, cf. Algorithm 4, and the AORA-MAX method, cf. Algorithm 5, are employed to a Coplanar Waveguide, a Branchline Coupler and a Printed Circuit Board[1]. More precisely, the numerical experiments consider the influence of the number of iteration steps of the rational Arnoldi-type method in the AORA-RK method and demonstrate the increasing accuracy within the sequence of reduced order models.

For efficiently solving a sequence of shifted linear systems, we will provide a comparison between the application of the LU decomposition and the algebraic two-level method, cf. Algorithm 10, to high-dimensional model problems of first-order Maxwell's equations. Moreover, we will show that the application of the modified AORA method leads to a significant improve-

[1]The model problems have been developed within the MoreSim4Nano research project, see http://moresim4nano.org – The copyright of the model problems rests with the Computer Simulation Technique (CST) AG and the TEMF Institute (TU Darmstadt).

ment of the computational costs for the subsequent computation of reduced order models. In this context, the recycling SQMR method is applied to a sequence of shifted linear systems of the second-order Maxwell's equations. The main focus of the numerical experiments refers to the improvement of the offline-stage of model order reduction by means of the modified adaptive-order rational Arnoldi method on the one hand and the recycling simplified quasi-minimal residual method on the other hand.

All numerical algorithms have been implemented in MATLAB® R2012a using a desktop computer with 4 CPUs, each Intel® Core™ i7-3770 with 3.40 GHz, and 16 GB RAM. Typically, we aim for an efficient offline-stage in moment matching based model order reduction even on a moderate desktop computer. In this context, the memory requirement for solving a high-dimensional linear system based on a direct solver, e.g. the ATLM, cf. Algorithm 10, represents a crucial limitation. Since the efficiency of the (recycling) iterative Krylov subspace methods depends on a matrix-vector multiplication among others, a moderate desktop computer still leads to the efficient application of moment matching based model order reduction from this point of view.

The notation of the different variables will be clear from the context, e.g. for the application of moment matching methods in model order reduction and the (recycling) Krylov subspace methods, respectively.

6.1 Model problems in semiconductor structures

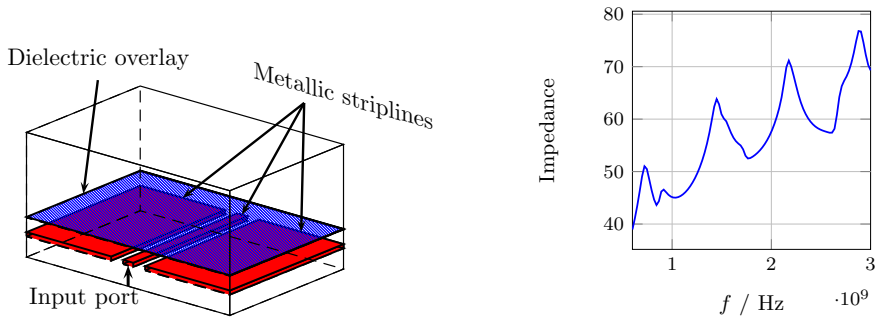

(a) Model problem. (b) Transfer function.

Figure 6.1: Coplanar Waveguide.

The first example of the numerical experiments represents a *Coplanar Waveguide*, which consists of three parallel conducting lines with a dielectric overlay in a metallic box, see Figure 6.1. The Coplanar Waveguide at hand refers to as a special case, since a common model problem would be composed of parallel conducting lines onto the dielectric overlay. Moreover, the PEC boundary condition (3.1.12) is employed on the boundary of the metallic box $\Omega \subset \mathbb{R}^3$ and for

each single transmission line, respectively. The model problem denotes a single-input, single-output (SISO) linear dynamical system, i.e. $p = 1$ and $m = 1$, where the output port has been placed on the opposite side of the input port. Finally, the frequency range of the model problem is given by $[f_{\min}, f_{\max}] = [0.6, 3.0]$ GHz.

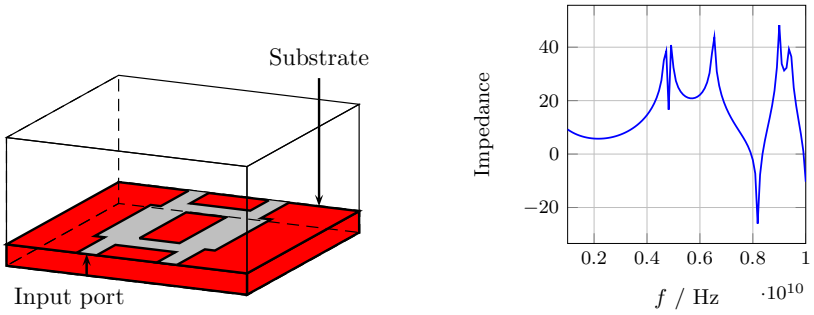

(a) Model problem. (b) Transfer function.

Figure 6.2: Branchline Coupler.

A *Branchline Coupler* with the frequency range $[f_{\min}, f_{\max}] = [1.0, 10.0]$ GHz has been selected as the second example, see Figure 6.2. Here, two parallel strip lines have been connected through a transversal bridge. The PEC boundary condition (3.1.12) has been employed for the metallic ground plane and the metallic box, while the PMC boundary condition (3.1.13) was placed on the other part of the substrate. The output port has been put on the adjacent transmission line opposite to the input port. Similar to the first example, the model problem refers to as a single-input, single-output (SISO) linear dynamical system.

	Coplanar Waveguide	Branchline Coupler	PCB[2]
Electric conductivity	$\sigma_A \equiv 0.01$ and $\sigma_B \equiv 0.02$	$\sigma \equiv 0$	$\sigma \equiv 0$
Frequency range	$[0.6, 3.0]$ GHz	$[1.0, 10.0]$ GHz	$[7.5, 10.0]$ GHz
(3.0.1) with FIT	$n = 32924$	$n = 73385$	$n = 226458$
(3.0.3) with FEM	–	$n = 27679$	–

Table 6.1: Summary on model problems of Maxwell's equations.[3]

The third and last example for the numerical experiments represents an extraction of a *Printed Circuit Board* as a single-input, single-output linear dynamical system of Maxwell's equations, see Figure 6.3. In comparison to the Coplanar Waveguide and the Branchline Cou-

[2]Printed Circuit Board

[3]For the Coplanar Waveguide, a different electric conductivity has been employed above σ_A and below σ_B of the dielectric overlay.

pler, the Printed Circuit Board allows for the application of moment matching based model order reduction to a more complex individual component of an electric circuit. Due to the dimension of the full-order model problem, we will primarily discuss the efficiency of the mAORA method and the rSQMR method in due consideration of the PCB. Moreover, the frequency range of the Printed Circuit Board is given by $[f_{\min}, f_{\max}] = [7.5, 10.0]$ GHz. As seen in the previous examples, the PEC boundary condition has been used for the conducting transmission lines, while the PMC boundary condition is applied to the rest of the substrate.

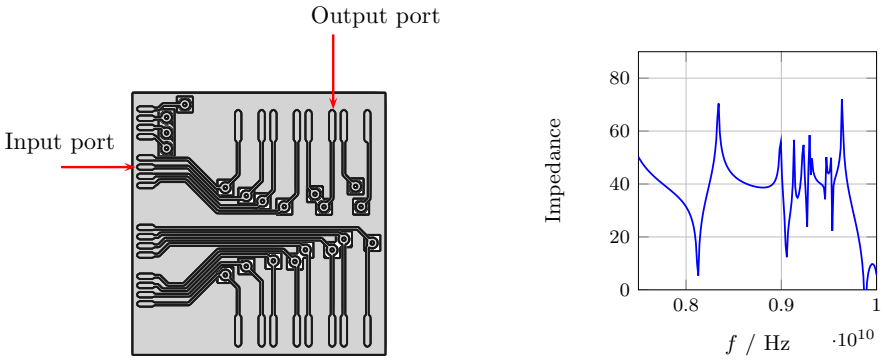

(a) Model problem. (b) Transfer function.

Figure 6.3: Printed Circuit Board.

The most relevant information of a discretization of the Coplanar Waveguide, the Branchline Coupler and the Printed Circuit Board with the corresponding degrees of freedom of the full-order model problem are summarised in Table 6.1.

6.2 Moment matching methods with a greedy-type expansion point selection

Firstly, we will discuss the application of the AORA-RK, AORA-MAX and AORA-H2 method in model order reduction with moment matching methods. Throughout the numerical experiments, we employ the different model problems as follows:

- Coplanar Waveguide: First-order formulation (FIT).
- Branchline Coupler: First-order (FIT) and second-order formulation (FEM).
- Printed Circuit Board: First-order formulation (FIT).

The termination of the adaptive greedy-type expansion point selection based on the AORA-RK method primarily makes use of the heuristic error estimation $\hat{\epsilon}_k > 0$ obtained via the sequence of reduced order models (4.2.10). Moreover, the given number of iteration steps of the

rational Arnoldi-type methods leads to an upper bound for the number of expansion points in order to reasonably benefit from the multiple expansion of the transfer function at each expansion point $\mathcal{S}_{i+1} = \{s_1, \ldots, s_{i+1}\} \subset \mathbb{C}$. Hence, we will not only apply a termination criterion by means of the heuristic error estimation, but also an upper bound for the number of computed reduced order models. Additionally, we will compute the relative error

$$\epsilon_{\text{rel}}(f) = \frac{|\,\mathcal{H}(\imath\omega) - \tilde{\mathcal{H}}(\imath\omega)\,|}{|\,\mathcal{H}(\imath\omega)\,|}, \quad \text{where} \quad \omega = 2\pi f, \quad f \in [f_{\min}, f_{\max}], \tag{6.2.1}$$

for a set of sampling points $\mathcal{S} \subset [f_{\min}, f_{\max}]$ in order to allow for an appropriate comparison of the accuracy of the reduced order models. In practical applications, we do not make use of the relative error (6.2.1) due to the considerable computational costs required for the computation of the transfer function $\mathcal{H}(s)$ corresponding to the high-dimensional full-order model problem, cf. Subsection 4.2.2.

6.2.1 Coplanar Waveguide

Initially, we give an overview on moment matching based model order reduction by means of the AORA-RK, AORA-MAX and AORA-H2 method to the Coplanar Waveguide in Figure 6.4. Due to the application of $n_r = 25$ iteration steps of the AORA method, the real-valued and structure-preserving reduced order models $\tilde{\mathcal{H}}_i(s)$ $(i = 1, \ldots, k)$ are of dimension $n_d = 100$. By comparison with the dimension $n = 32924$ of the full-order model problem, approximately 0.3037% degrees of freedom of the full-order model problem are used within the reduced order model.

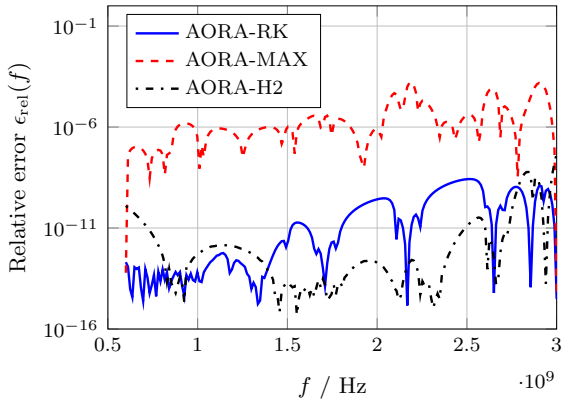

Figure 6.4: Coplanar Waveguide: Adaptive greedy-type expansion point selection. $(n_r = 25)$

At first sight, the AORA-RK method leads to a comparable relative error for the reduced order model in view of the AORA-MAX and AORA-H2 method. Moreover, the number of

iteration steps of the AORA method are already large enough in order to obtain an appropriate reduced order model. Throughout the thesis, we typically aim to achieve the tolerance 10^{-5} - 10^{-8} for the relative error (6.2.1) within the given frequency range $f \in [f_{\min}, f_{\max}]$. For other practices, the prescribed accuracy may significantly differ due to the requirements of the field of application at hand.

According to Table 6.2, the AORA-MAX method fails to achieve the aimed accuracy of the reduced order model. As already mentioned in Subsection 4.2.4, the AORA-MAX method is restricted by the lack of an adequate interpretation of the relative error between two subsequent reduced order models. Although we have chosen the tolerance $\epsilon_0 > 0$ in Algorithm 5 carefully, a suitable selection of expansion points leading to an appropriate relative error $\epsilon_{\text{rel}}(f) > 0$ may not be guaranteed in each and every case.

	AORA-RK	AORA-MAX	AORA-H2
Initial expansion points	$\imath\{\sqrt{f_{\min} f_{\max}}, f_{\max}\}$	$\imath\{f_{\min}, f_{\max}\}$	$\imath\{f_{\min}, \sqrt{f_{\min} f_{\max}}, f_{\max}\}$
$\max\ \epsilon_{\text{rel}}(f)$	$2.66 \cdot 10^{-9}$	$1.66 \cdot 10^{-4}$	$4.63 \cdot 10^{-8}$

Table 6.2: Coplanar Waveguide: Greedy-type moment matching methods. $(n_r = 25)$

Contrary to the AORA-MAX method, the AORA-H2 method leads to a comparable accuracy of the reduced order model in relation to the AORA-RK method. The selection of a sufficiently large tolerance $\eta > 0$ in Algorithm 4 typically results in an adaptation of the tolerance, e.g. $\eta \equiv \eta/2$, in order to compute a prescribed number of expansion points. In this way, the AORA-H2 method leads to an appropriate distribution of the expansion points in the frequency range at hand, see [113].

Nevertheless, the disadvantage of the AORA-H2 method emerges from the following fact: If too few expansion points are left over from the restriction of the Ritz values to the given frequency range, cf. line 4 in Algorithm 4, the restriction of the Ritz values must be omitted. In this case, the expansion of the transfer function is carried out beyond the frequency range of the model problem, which becomes rather impractical for the reliable application of moment matching based model order reduction.

The reliability of the upper bound of the output moment error (4.2.14) employed for the subsequent expansion point selection in the AORA-RK method by means of the relative error $\epsilon_{\text{rel}}(f) > 0$ is given in Figure 6.5. More precisely, we provide a comparison between the adaptive expansion point selection from the AORA-RK method and the maximum relative error $\epsilon_{\text{rel}}(f) > 0$. The latter refers to as a natural way of selecting the subsequent expansion point $s_{i+1} \in \mathbb{C}$ subject to $\mathcal{S}_{i+1} = \mathcal{S}_i \cup \{s_{i+1}\}$. Since the computation of the transfer function $\mathcal{H}(s) \in \mathbb{C}^{p \times m}$ of the full-order model problem is infeasible in view of an efficient offline-stage

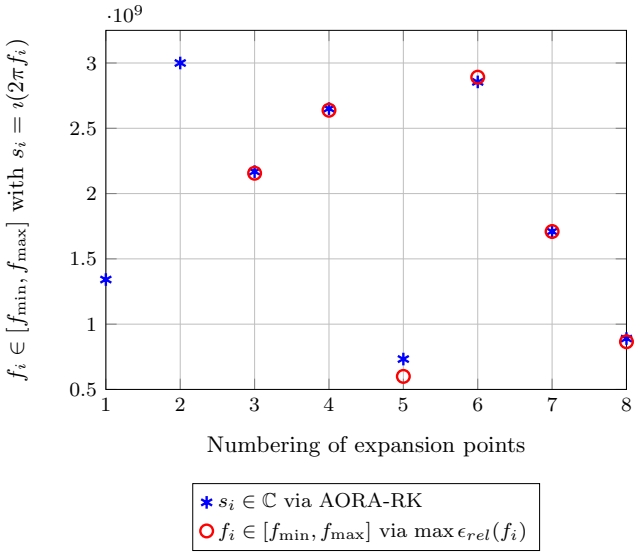

Figure 6.5: Coplanar Waveguide: AORA-RK: Selection of expansion points. $(n_r = 25)$

in model order reduction, we typically aim for a sufficient approximation of the maximum relative error (6.2.1) in moment matching based model order reduction. Numerical experiments of the Coplanar Waveguide suggest that the AORA-RK method offers at least a reliable identification of the regions of the frequency range corresponding to the maximum relative error.

More details on the behaviour of the AORA-RK method are given in Figure 6.6, where we provide the relative error $\epsilon_{\text{rel}}(f) > 0$ for a selection of reduced order models $\tilde{\mathcal{H}}_1(s), \ldots, \tilde{\mathcal{H}}_k(s)$. The initial expansion points of the AORA-RK method are $\mathcal{S}_1 \equiv \imath\{\sqrt{f_{\min} f_{\max}}, f_{\max}\}$, see Table 6.2. Since the reduced order models shall not be optimally with respect to the $\mathbb{H}_2$ norm, the employment of expansion points in the environment of the boundary or the geometric mean of the frequency range represents a common framework for the initial set of expansion points in a greedy-type adaptive expansion point selection strategy, see [19, 26, 113].

Moreover, let us compare the accuracy between the reduced order models corresponding to the expansion points $\mathcal{S}_5 \subset \mathbb{C}$ and $\mathcal{S}_7 \subset \mathbb{C}$ on the one hand and the reduced order models corresponding to $\mathcal{S}_3 \subset \mathbb{C}$ and $\mathcal{S}_5 \subset \mathbb{C}$ on the other hand. This leads to the confirmation that the AORA-RK method primarily selects the expansion points from the region of the frequency range with the largest relative error components. Hence, an appropriate interpretation of the output moment error allows for a suitable greedy-type expansion point selection.

In Figure 6.7, we give an overview on the application of the AORA-RK method for a varying number of iteration steps $n_r > 0$ of the AORA method. Naturally, we obtain a different number

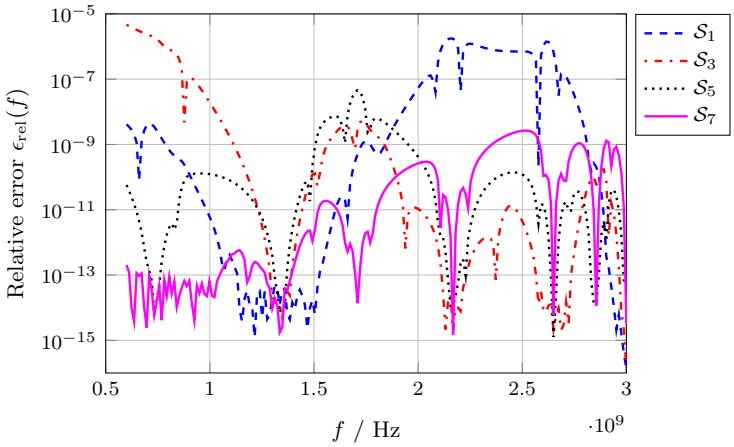

Figure 6.6: Coplanar Waveguide: AORA-RK: Sequence of reduced order models. ($n_r = 25$)

of expansion points $|\,\mathcal{S}_i\,|$ for the different iteration steps due to the termination criterion[4] of the AORA-RK method. The key observation is that we usually do not require a larger number of iteration steps for the AORA method with respect to a given set of expansion points. Rather, an increasing dimension of the reduced order model must be applied to an adequate extension of the already known expansion points in order to benefit from the multiple expansion of the transfer function within the whole frequency range.

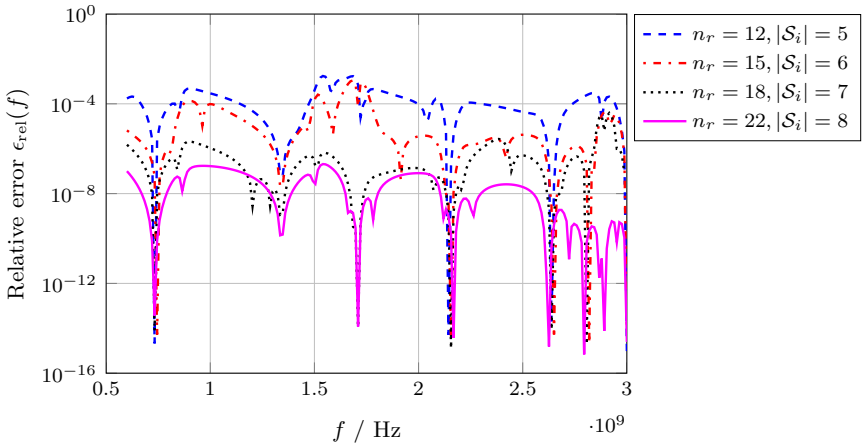

Figure 6.7: Coplanar Waveguide: AORA-RK: Different number of AORA iteration steps.

[4] As mentioned above, we only allow for a specific length of the sequence of reduced order models in order to properly benefit from the multiple expansion of the transfer function with respect to the number of rational Arnoldi-type steps $n_r > 0$.

6.2.2 Branchline Coupler

For the application of moment matching methods to the Branchline Coupler, we initially consider the first-order linear dynamical system of Maxwell's equations (3.0.1) on the basis of the FIT. The accuracy of the reduced order model $\epsilon_{\text{rel}}(f) > 0$ obtained via the AORA-RK, AORA-MAX and AORA-H2 method is given in Figure 6.8. The number of degrees of freedom of the full-order model problem $n = 73385$ has been reduced to the dimension $n_d = 100$ ($n_r = 25$). This represents approximately 0.1362% degrees of freedom of the full-order model problem.

Since the frequency range $[f_{\min}, f_{\max}] = [1.0, 10.0]$ GHz of the Branchline Coupler is even larger as compared to the Coplanar Waveguide, moment matching methods must be carefully applied since they are mainly based on the expansion of the transfer function within the given frequency range. At least for the AORA-RK and AORA-H2 method, the accuracy of the reduced order model decreases rather moderately with respect to the upper part of the frequency range. Nevertheless, the reduced order model still allows for a reliable numerical simulation of the Branchline Coupler. More details on the application of the adaptive greedy-type expansion point selection strategies to the Branchline Coupler are summarised in Table 6.3.

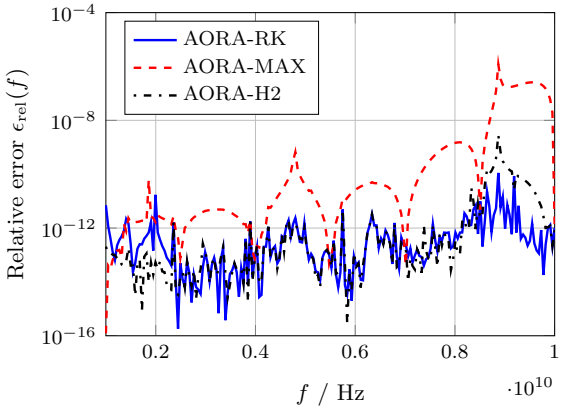

Figure 6.8: Branchline Coupler: Adaptive greedy-type expansion point selection. ($n_r = 25$)

Since the relative error $\epsilon_{\text{rel}}(f)$ corresponding to $n_r = 25$ iteration steps of the adaptive-order rational Arnoldi method is already rather small, we additionally consider the application of moment matching methods in model order reduction with $n_d = 80$ ($n_r = 20$), see Figure 6.9. Thereby, the AORA-RK and AORA-MAX method still ensure the computation of a reduced order model within the accuracy $\max \epsilon_{\text{rel}}(f) \approx 10^{-6}$. Although the AORA-H2 method offers a comparable accuracy of the reduced order model for at least some parts of the frequency range, the principal behaviour of the adaptive expansion point selection significantly differs from the

AORA-RK and AORA-MAX method.

	AORA-RK	AORA-MAX	AORA-H2
Initial expansion points	$\imath\{\sqrt{f_{\min} f_{\max}}, f_{\max}\}$	$\imath\{f_{\min}, f_{\max}\}$	$\imath\{f_{\min}, \sqrt{f_{\min} f_{\max}}, f_{\max}\}$
$\max\ \epsilon_{\mathrm{rel}}(f)$	$1.12 \cdot 10^{-10}$	$1.21 \cdot 10^{-6}$	$2.85 \cdot 10^{-9}$

Table 6.3: Branchline Coupler: Greedy-type moment matching methods. $(n_r = 25)$

Similar to the application of the AORA-H2 method to the Coplanar Waveguide, the tolerance $\epsilon_0 > 0$, cf. line 4 in Algorithm 4, has been chosen small enough in order to aim for a selection of expansion points leading to a small relative error. Nevertheless, the numerical results in Figure 6.9 indicate that the selection of expansion points simply leads to an accurate reduced order model in the vicinity of each expansion point. In comparison to the AORA-RK and AORA-MAX method, the increasing accuracy for the whole frequency range by means of a careful selection of expansion points will not be achieved. We have occasionally observed a similar behaviour of the AORA-H2 method for the other model problems in semiconductor structures and specific settings of the framework of moment matching methods in model order reduction.

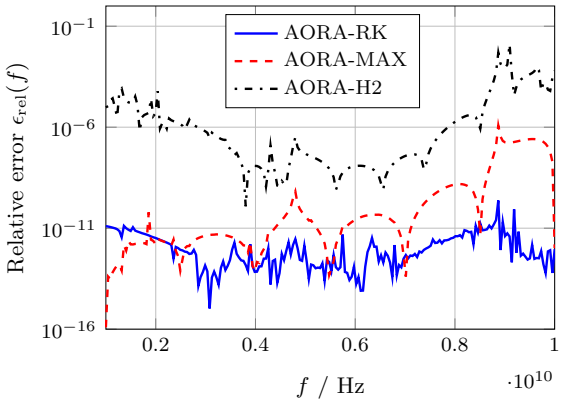

Figure 6.9: Branchline Coupler: Adaptive greedy-type expansion point selection. $(n_r = 20)$

In Figure 6.10, we provide a comparison between the selection of expansion points from the AORA-RK method and the maximum relative error $\epsilon_{\mathrm{rel}}(f) > 0$ corresponding to $n_r = 20$ iteration steps of the AORA method. Remember that the upper bound of the output moment error (4.2.14) does not offer an exact representation of the relative error $\epsilon_{\mathrm{rel}}(f) > 0$, but at least a suitable identification of the regions of the frequency range with the largest error components. For example, the expansion points $s_3 = \imath(2\pi f_{3,*}) \in \mathbb{C}$ and $s_6 = \imath(2\pi f_{6,*}) \in \mathbb{C}$ significantly differ from the expansion points suggested by the maximum relative error. On closer inspection, the

following relative errors have occurred:

- $\epsilon_{\mathrm{rel}}(f_3) \approx 9.91 \cdot 10^{-10}$ and $\epsilon_{\mathrm{rel}}(f_{3,*}) \approx 1.23 \cdot 10^{-12}$,
- $\epsilon_{\mathrm{rel}}(f_6) \approx 2.35 \cdot 10^{-10}$ and $\epsilon_{\mathrm{rel}}(f_{6,*}) \approx 7.61 \cdot 10^{-13}$.

At first, we see that the relative errors $\epsilon_{\mathrm{rel}}(f_3)$ and $\epsilon_{\mathrm{rel}}(f_6)$ are already relatively small. In other words, the number of iteration steps $n_r > 0$ of the AORA method and the initial set of expansion points lead to a sufficient accuracy of the reduced order model. Nevertheless, the example shows that the suitable selection of expansion points by means of the AORA-RK method becomes more challenging for a small relative error.

Regardless of the misleading interpretation of the relative error for the expansion points $s_3 \in \mathbb{C}$ and $s_6 \in \mathbb{C}$, the AORA-RK method still selects the expansion point $s_4 \in \mathbb{C}$ in the vicinity of the largest error components $\max \epsilon_{\mathrm{rel}}(f_3)$ and $\max \epsilon_{\mathrm{rel}}(f_6)$, respectively. In this way, the multiple expansion of the transfer function allows for the conservation of a misleading interpretation of the relative error. We conclude that even for a small tolerance of the heuristic error estimation, e.g. $\hat{\epsilon}_k < 10^{-12}$, the AORA-RK method still leads to a reasonable set of expansion points within the given frequency range.

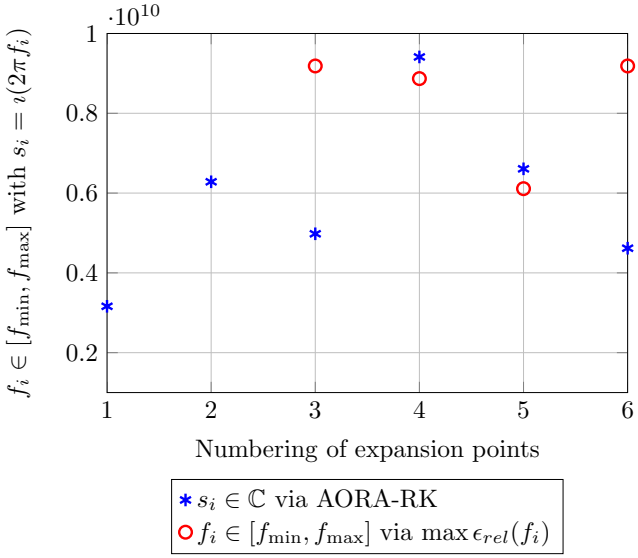

Figure 6.10: Branchline Coupler: AORA-RK: Selection of expansion points. $(n_r = 20)$

Moment matching methods in model order reduction may be also applied to second-order linear dynamical systems of Maxwell's equations (3.0.3). For example, each greedy-type expansion point selection strategy at hand provide an extension to the second-order formulation of a linear dynamical system, cf. Subsection 4.2.4. Therefore, we have given an overview on the ac-

curacy of the reduced order model corresponding to the Branchline Coupler with $n_r = 15$ iteration steps of the second- and adaptive-order rational Arnoldi method in Figure 6.11. Here, the dimension $n = 27679$ of the full-order model problem has been reduced to $n_d = 30$ $(n_r = 15)$, which represents approximately 0.1083% degrees of freedom of the full-order model problem.

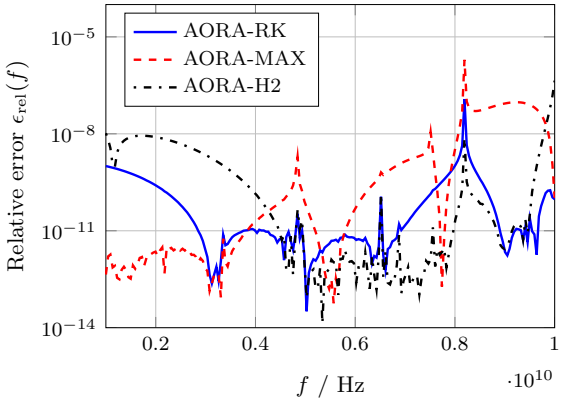

Figure 6.11: Branchline Coupler: Adaptive greedy-type expansion point selection. $(n_r = 15)$

Similar to the previous results of the Branchline Coupler, we observe a comparable accuracy of the reduced order model for each greedy-type expansion point selection. We make use of the second-order formulation of the Branchline Coupler due to the fact that the electric conductivity is equal to zero. In this case, the simplification of the second-order Krylov subspace $\mathcal{G}_{j_i}(s_i)$ to a first-order Krylov subspace leads to an efficient computation of an orthonormal basis of the sequence of Krylov subspaces $\mathcal{G}_{j_1}(s_1), \ldots, \mathcal{G}_{j_l}(s_l)$, where $n_r = j_1 + \ldots + j_l$, $j_i > 0$ $(i = 1, \ldots, l)$, cf. Section 4.3.

Until now, we have given a comprehensive comparison between the application of the AORA-RK, AORA-MAX and AORA-H2 method in moment matching based model order reduction of the first- and second-order Maxwell's equations. In contrast to the AORA-MAX and AORA-H2 method, the AORA-RK method allows for the computation of a suitable reduced order model for a model problem of a Coplanar Waveguide and a Branchline Coupler with a varying number of iteration steps of the rational Arnoldi-type method.

6.2.3 Printed Circuit Board

This paragraph involves the application of the AORA-RK, AORA-MAX and AORA-H2 method to the Printed Circuit Board in the first-order formulation of Maxwell's equations (3.0.1) on the basis of the finite integration technique, cf. Figure 6.3. In comparison to the Coplanar Waveguide and the Branchline Coupler, the dimension of the linear dynamical system of the Printed Circuit Board increases significantly. Moreover, the upper part of the frequency of

the transfer function suggests a more competitive application of moment matching methods in model order reduction due to the computation of the reduced order model with the help of a Taylor expansion of the transfer function at different expansion points.

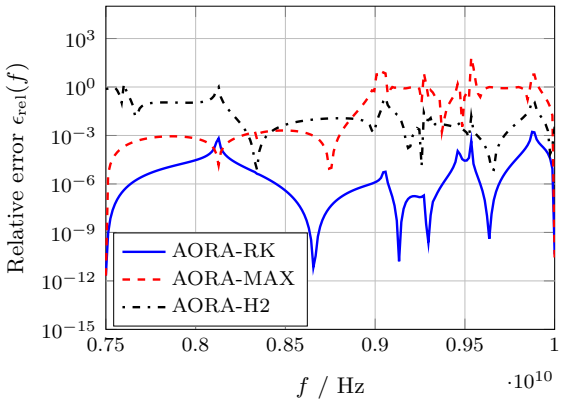

Figure 6.12: PCB: Adaptive greedy-type expansion point selection. ($n_r = 20$)

In Figure 6.12, we give an overview on the accuracy of the reduced order model of dimension $n_d = 80$ ($n_r = 20$) for the AORA-RK, AORA-MAX and AORA-H2 method. In this way, approximately 0.035% of the degrees of freedom of the full-order model problem are required in the reduced order model. By comparison, the AORA-RK method leads to a significantly larger accuracy of the reduced order model. Another major advantage of the AORA-RK method is the reliable treatment of the more challenging regions of the transfer function, i.e. the upper part of the frequency range, corresponding to the Printed Circuit Board. Rather, the adaptive expansion point selection on the basis of the AORA-MAX and AORA-H2 method does not lead to a comparable relative error within the whole frequency range. Typically, an increasing accuracy simply occurs in the near vicinity of each expansion point. More details on the application of moment matching methods to the Printed Circuit Board are given in Table 6.4.

	AORA-RK	AORA-MAX	AORA-H2
Initial expansion points	$\imath\{\sqrt{f_{\min} f_{\max}}, f_{\max}\}$	$\imath\{f_{\min}, f_{\max}\}$	$\imath\{f_{\min}, \sqrt{f_{\min} f_{\max}}, f_{\max}\}$
$\max\ \epsilon_{\text{rel}}(f)$	$1.66 \cdot 10^{-3}$	$6.86 \cdot 10^{1}$	$1.57 \cdot 10^{1}$

Table 6.4: PCB: Greedy-type moment matching methods. ($n_r = 20$)

It is important to note that the application of the Printed Circuit Board within the frequency range $[f_{\min}, f_{\max}] = [7.5, 8.5]$ GHz would lead to a significant simplification of the model problem. Since this case would lead to a comparable behaviour of the different greedy-type expansion point selection strategies, we have introduced an artificial extension of the frequency

range in order to verify the competitive of the AORA-RK method.

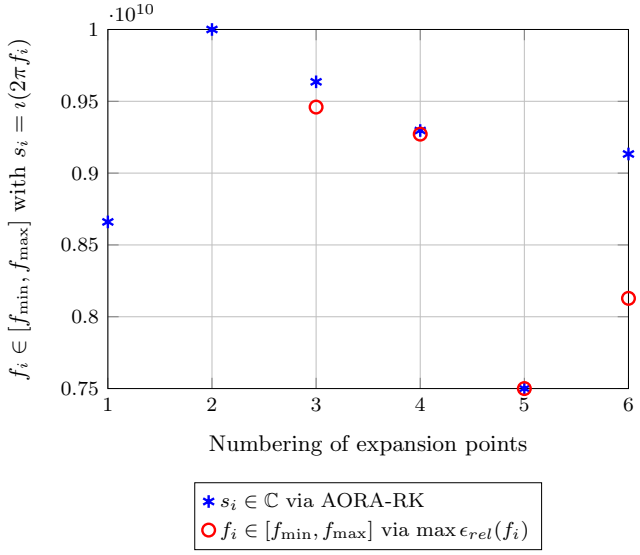

Figure 6.13: PCB: AORA-RK: Selection of expansion points. $(n_r = 20)$

Similar to the numerical results of the Branchline Coupler, the AORA-RK method selects the subsequent expansion points at least from the parts of the frequency range with the largest relative error components, see Figure 6.13. For example, the reduced order model corresponding to the expansion points $\mathcal{S}_5 = \{s_1, \ldots, s_5\} \subset \mathbb{C}$ leads to the following relative errors:

- $\max \epsilon_{\text{rel}}(f) \approx 8.5 \cdot 10^{-2}$ with $f \in [f_{\min}, f_{\max}]$,
- $\epsilon_{\text{rel}}(f_\star) \approx 3.0 \cdot 10^{-3}$ with $s_6 = \imath(2\pi f_\star)$.

An increasing accuracy in the reduced order model would require a larger number of iteration steps $n_r > 0$ of the rational Arnoldi-type method in combination with an appropriate extension of the expansion points. Although the expansion point selection does not coincide with the maximum relative error $\epsilon_{\text{rel}}(f) > 0$ in each and every case, we still obtain an expansion point selection from the challenging region of the upper part of the frequency range.

Nevertheless, the AORA-RK method offers a limitation in the approximation of the relative error in case different regions with a comparable relative error are present. The latter case still allows for the selection of an expansion point from at least one of these regions with a large relative error. As seen in Section 4.2.5, another attempt would be to compute the upper bound of the output moment error (4.2.14) for different regions of the frequency range or an increasing number of iteration steps of the rational Arnoldi-type method.

Nevertheless, we are still able to employ the AORA-RK method, cf. Algorithm 6, to the model problem of the Printed Circuit Board in a more convenient way. In Figure 6.14, we make

use of $n_r = 25$ iteration steps of the adaptive-order rational Arnoldi method leading to a reduced order model of dimension $n_d = 100$. Since a comparable setting for the framework of each adaptive Greedy-type expansion point selection strategy has been employed, we emphasise the reliability of the expansion point selection by the AORA-RK method. More precisely, an increasing number of iteration steps already leads to an improving accuracy of the reduced order models.

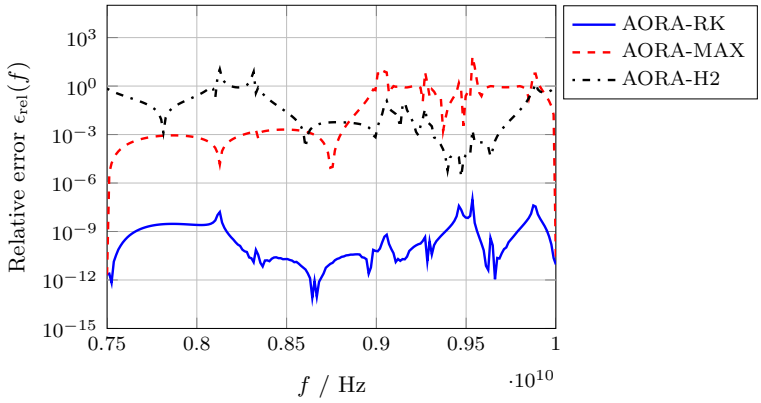

Figure 6.14: PCB: Adaptive greedy-type expansion point selection. $(n_r = 25)$

Since the selection of the subsequent expansion point in the AORA-RK method does not depend on a specific parameter, e.g. $\eta > 0$ (AORA-H2 method) and $\epsilon_0 > 0$ (AORA-MAX method), the application of the adaptive expansion point selection simplifies for a varying number of iteration steps of the rational Arnoldi-type method.

Finally, we give a comparison between the selection of the subsequent expansion point by the AORA-RK method and the maximum relative error $\epsilon_{\text{rel}}(f)$ in Figure 6.15. Summarising, the AORA-RK method allows for a sufficient accurate approximation of the maximum relative error (6.2.1) in each iteration step. Again, we do not claim to establish an exact representation of the relative error by Lemma 4.2.5 but a suitable selection of expansion points.

6.3 Efficient offline-stage for moment matching methods

As major conclusion of the numerical experiments in Section 6.2, the AORA-RK method allows for the suitable application of moment matching methods in model order reduction of Maxwell's equations. Since we require solving a sequence of high-dimensional shifted linear systems, we discuss different approaches leading to an improvement of the offline-stage in model order reduction, see Chapter 5. Thereby, we primarily focus on the computational costs for the subsequent computation of the Galerkin projection obtained via the nested sets of

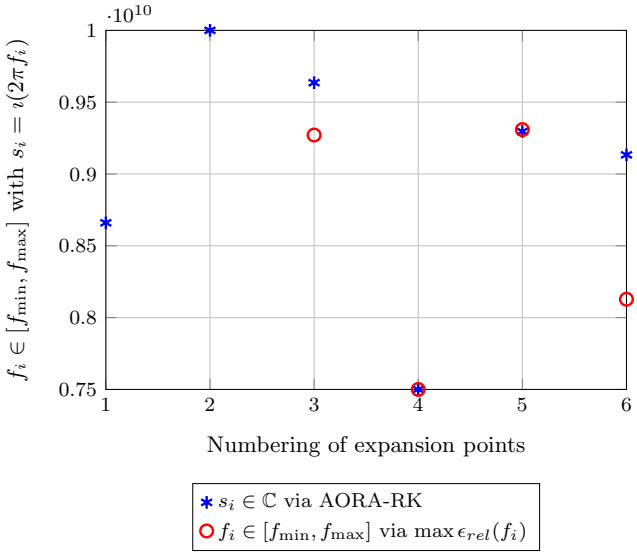

Figure 6.15: PCB: AORA-RK: Selection of expansion points. ($n_r = 25$)

expansion points $\mathcal{S}_{i+1} = \mathcal{S}_i \cup \{s_{i+1}\}$, $s_{i+1} \in \mathbb{C}$.

At first, we will consider the application of the modified adaptive-order rational Arnoldi (mAORA) method in the AORA-RK method. In view of the theoretical framework of the modified generic rational Arnoldi method, cf. Section 5.1, a comparable accuracy for the reduced order model between the application of the AORA and mAORA method in a greedy-type adaptive expansion point selection is achieved. As we will presently see, the major advantage of the mAORA method is the significantly smaller number of systems solves of the shifted linear systems within the subsequent computation of the Galerkin projection.

Thereafter, we will discuss the efficiency of the algebraic two-level method (ATLM) allowing for solving a shifted linear system of first-order Maxwell's equations in due consideration of the special block-structure of the electric and magnetic field strength. We will show that the recycling simplified quasi-minimal residual (rSQMR) method leads to an efficient iterative solution technique for second-order Maxwell's equations. Finally, we will provide a short overview on the application of (recycling) Krylov subspace methods to moment matching based model order reduction, see [13].

6.3.1 Modified adaptive-order rational Arnoldi method

To begin with, we discuss the application of the AORA-RK method to the Coplanar Waveguide, where the subsequent reduced order models are computed by means of the modified adaptive-order rational Arnoldi method. We refer to this extension of the greedy-type expan-

sion point selection as the mAORA-RK method. According to Figure 6.16, the accuracy of the reduced order model of the mAORA-RK method compares with the AORA-RK method. The reason for this is that the adaptive expansion point selection from the application of the AORA and mAORA method in the AORA-RK method does not significantly differ. For example, the numerical experiment at hand shows that only one out of eight expansion points of the mAORA-RK method has been selected in a completely different way. Otherwise the expansion points of the mAORA-RK method arise at least in the near vicinity of the expansion points computed by the AORA-RK method.

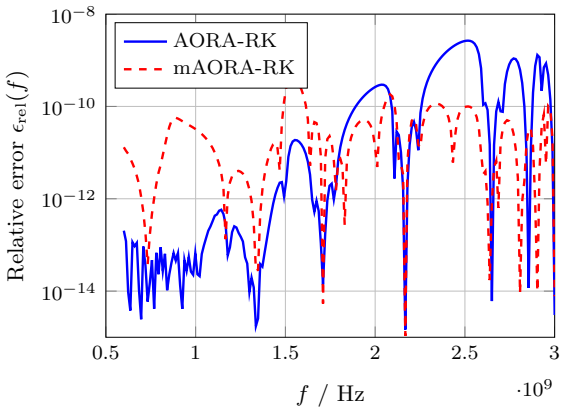

Figure 6.16: Coplanar Waveguide: AORA-RK vs. mAORA-RK. ($n_r = 25$)

Another important aspect of the comparison between the AORA and mAORA method affects the differences in the accuracy of the reduced order model. Therefore, we fix the expansion points of the AORA-RK method and consider the subsequent application of the mAORA method in Figure 6.17. In accordance with the theoretical framework in Section 5.1, the application of the mAORA method leads to a comparable accuracy of the reduced order model in terms of the moment matching property (4.2.5). Additionally, we obtain a significant speed-up in the subsequent computation of the Galerkin projection by the mAORA method even for moderate dimensions of the full-order model problem. More precisely, the computational time refers to the subsequent computation of the Galerkin projection $\Pi = VV^{\mathrm{T}}$, $V \in \mathbb{C}^{n \times n_r}$, on the basis of the expansion points $\mathcal{S}_{i+1} = \mathcal{S}_i \cup \{s_{i+1}\}$, $s_{i+1} \in \mathbb{C}$.

By comparison with the AORA method, the way of selecting an expansion point in each iteration step of the modified AORA method, cf. line 6 in Algorithm 9, leads to a comparable sequence of the dimensions of the different Krylov subspaces, see Table 6.5. Here, the dimensions $j_{1,l}, \ldots, j_{l,l}$ $(l = 1, \ldots, m)$ of the Krylov subspace corresponding to the expansion points $s_1, \ldots, s_l \in \mathbb{C}$ form a decreasing sequence between the subsequent calls. Nevertheless, the differences between the accuracy of the reduced order model can be explained as follows: While

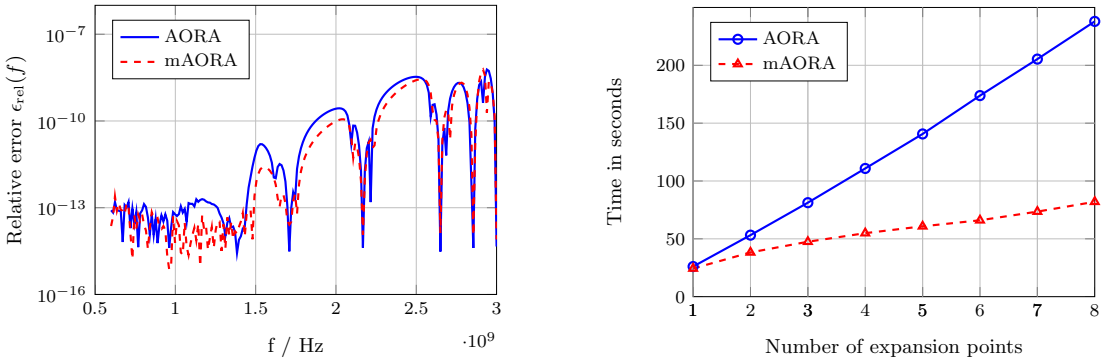

(a) (b)

Figure 6.17: Coplanar Waveguide: mAORA vs. AORA method. ($n_r = 25$)

the AORA method allows for the selection of an arbitrary residual vector in each iteration step, the mAORA method selects in simplified terms either the residual vector corresponding to the latest expansion point or the expansion point corresponding to the current index $\alpha > 0$ of the previous orthonormal vector sequence, cf. Section 5.1. In addition to this, we still have to be aware of numerical round-off errors.

# Call	$s_1 \in \mathbb{C}$		$s_2 \in \mathbb{C}$		$s_3 \in \mathbb{C}$		$s_4 \in \mathbb{C}$		$s_5 \in \mathbb{C}$		$s_6 \in \mathbb{C}$		$s_7 \in \mathbb{C}$		$s_8 \in \mathbb{C}$	
1	25	25														
2	12	13	13	12												
3	8	8	9	8	8	9										
4	6	6	7	6	6	6	6	7								
5	5	4	5	4	5	4	5	6	5	7						
6	4	3	4	3	5	3	4	5	4	5	4	6				
7	3	3	4	3	4	3	4	3	3	4	4	4	3	5		
8	3	3	4	3	3	3	3	3	3	3	3	3	3	3	3	4

Table 6.5: Coplanar Waveguide: Comparison between selection of expansion points. (AORA / mAORA)

As seen before, the application of the modified adaptive-order rational Arnoldi method to the Coplanar Waveguide leads to a significant speed-up in the computational time. We will now consider the model problem of the Printed Circuit Board with a significantly larger dimension of the full-order model problem as compared to the Coplanar Waveguide. Remember that the reliable application of moment matching based model order reduction to the PCB depends on a suitable expansion point selection, cf. Figure 6.12. Due to the comparable selection of expansion points in the mAORA-RK method, we obtain similar results for the accuracy of

the reduced order model, see Figure 6.18. In view of the model problems in semiconductor structures given in Section 6.1, the adaptive expansion point selection based on the AORA-RK and the mAORA-RK method allows for the computation of a comparable reduced order model.

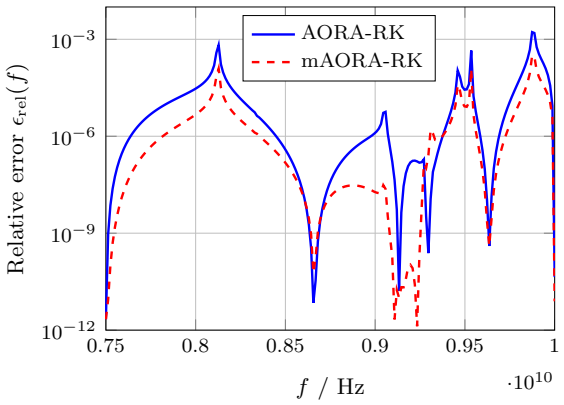

Figure 6.18: PCB: AORA-RK vs. mAORA-RK. ($n_r = 20$)

Moreover, the expansion points obtained via the AORA-RK method have been also used for the subsequent computation of a reduced order model with the modified AORA method, see Figure 6.19. Although the transfer function of the reduced order model maintains a comparable accuracy for the modified AORA method, a slightly less accurate reduced order model occurs for the upper part of the frequency range. Nevertheless, the accuracy of the reduced order model would still allow for a suitable application of model order reduction within the numerical simulation of the Printed Circuit Board. The major advantage of the application of the modified AORA method is that the number of high-dimensional shifted linear systems to be solved will be significantly reduced. More precisely, the subsequent calls of the AORA method require in total 120 times solving a high-dimensional shifted linear system, while the mAORA method only needs 41 computations.

The significantly smaller number of solutions to shifted linear systems is a consequence of the observation that we only require solving a shifted linear system corresponding to the latest expansion point $s_{i+1} \in \mathbb{C}$ in each call of the mAORA method. Due to the fact that $j_{l,i+1} \leq j_{l,i}$ holds for all $l = 1, \ldots, i$, the already known orthonormal vector sequence $V^{(i)} \in \mathbb{C}^{n \times n_r}$ may be reused for all other expansion points $s_1, \ldots, s_i \in \mathbb{C}$, see Table 6.6.

In summary, it can be stated that the application of the modified AORA method to the Coplanar Waveguide and the Printed Circuit Board leads to a gain in the computational time by a factor of approximately 2.5 in the offline-stage of moment matching based model order reduction. Moreover, the reduced order models provide a comparable accuracy from the ap-

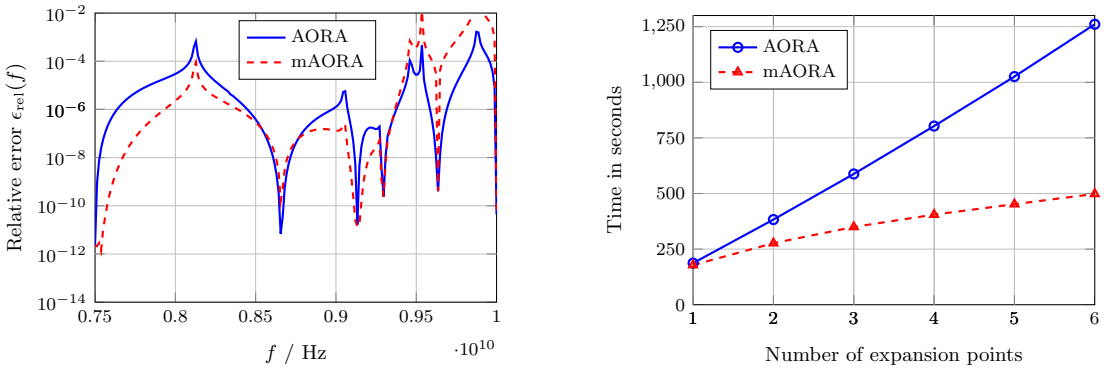

(a) (b)

Figure 6.19: PCB: mAORA vs. AORA method. ($n_r = 20$)

plication of the mAORA method either for a fixed set of expansion points or by means of a comparison between the AORA-RK and mAORA-RK method.

# Call	$s_1 \in \mathbb{C}$		$s_2 \in \mathbb{C}$		$s_3 \in \mathbb{C}$		$s_4 \in \mathbb{C}$		$s_5 \in \mathbb{C}$		$s_6 \in \mathbb{C}$	
1	20	20										
2	10	9	10	11								
3	7	6	6	6	7	8						
4	5	4	5	4	5	5	5	7				
5	4	2	4	3	4	4	4	5	4	6		
6	3	2	3	2	4	2	4	4	3	5	3	5

Table 6.6: PCB: Comparison between selection of expansion points. (AORA / mAORA)

6.3.2 Recycling Krylov subspace methods

The basic idea behind the application of the class of (recycling) Krylov subspace methods to shifted linear systems of the first-order Maxwell's equations is given by the algebraic two-level method (ATLM). Since we make use of the FIT for model problems of first-order Maxwell's equations, we are able to explicitly formulate and compute the Schur complement

$$S = (s_i M_\epsilon + M_\sigma) + C(s_i M_\mu)^{-1} C^{\mathrm{T}} \quad \text{with} \quad s_i \in \mathbb{C}, \tag{6.3.1}$$

cf. Section 5.2. In Table 6.7, we provide a comparison between the computational time of the LU decomposition and the ATLM to a shifted linear system of first-order Maxwell's equations. For a more convenient comparison, we have increased the number of degrees of freedom corresponding to the discretization of the Coplanar Waveguide. Similar to the increasing accuracy

of structure-preserving moment matching methods in model order reduction, we also benefit from the exploitation of the block-structure of first-order Maxwell's equations for solving the shifted linear system $(s\mathcal{E} - \mathcal{A})x = f$, $s \in \mathbb{C}$.

Dimension	LU decomposition	Two-level approach
42764	1.3e+01s	1.2e+00s
78442	6.1e+01s	5.5e+00s
140992	4.5e+02s	1.5e+01s
208996	6.2e+02s	3.0e+01s

Table 6.7: Coplanar Waveguide: Algebraic two-level approach for $(s\mathcal{E} - \mathcal{A})x = f$, $s \in \mathbb{C}$.

Although we still require an explicit formulation of the Schur complement (6.3.1), the preservation of the block-structure in the ATLM leads to an efficient solution method for solving a shifted linear system of first-order Maxwell's equations with respect to the computational time. It is important to note that a discretization of the first-order formulation of the Maxwell's equations by means of the FEM would require an explicit discretization of the Schur complement in order to apply the ATLM, see Chapter 3.

In view of (recycling) Krylov subspace methods, we mainly focus on solving a time-harmonic, second-order Maxwell's equations because the key ingredient of the ATLM comes from solving a linear system with the Schur complement. To be more precise, we restrict the discussion to the application of the (recycling) SQMR method to the Schur complement of first-order Maxwell's equations (6.3.1). For the preconditioner of the (recycling) Krylov subspace method, we apply the decomposition $M_1 M_2 \equiv L D L^{\mathrm{T}}$ of the (complex) symmetric, but indefinite Schur complement $S = (s_\star M_\epsilon + M_\sigma) + C(s_\star M_\mu)^{-1} C^{\mathrm{T}}$ with $s_\star = \imath\sqrt{f_{\min} f_{\max}}$. The focus of the preconditioner is mainly based on efficiently solving a sequence of shifted linear systems for moment matching methods in model order reduction.

In Figure 6.20, we compare the application of the SQMR and rSQMR method to a sequence of shifted linear systems arising from the Schur complement (6.3.1) of the Printed Circuit Board. The expansion points are obtained via an evenly distributed set of sampling points in the frequency range $[7.5, 10.0]$ GHz. The stopping tolerance has been chosen as $\| r_k \|_2 \leq 10^{-6} \| r_0 \|_2$, while $m = 40$ and $k = 20$ have been employed for the rSQMR method. We see that the rSQMR method requires a significantly smaller number of iteration steps for solving the sequence of shifted linear systems corresponding to the Schur complement with a single preconditioner. Due to the application of a recycling subspace, we obtain a significantly smaller number of iteration steps for the upper part of the frequency range as compared to the SQMR method. Although we have to be aware of the computational effort for the computation of a recycling

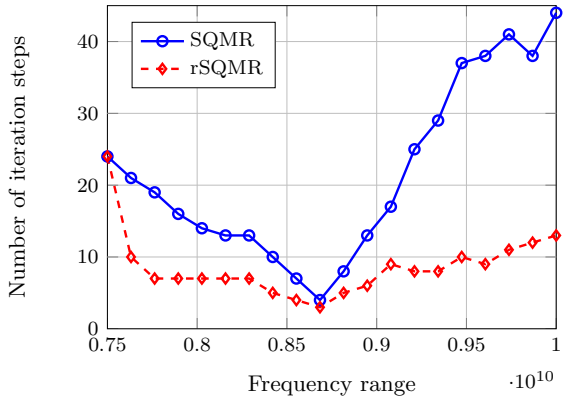

Figure 6.20: PCB: Sequence of shifted linear system with rSQMR method.

subspace, the major advantage of the rSQMR method is that the single preconditioner may be employed within a large frequency range.

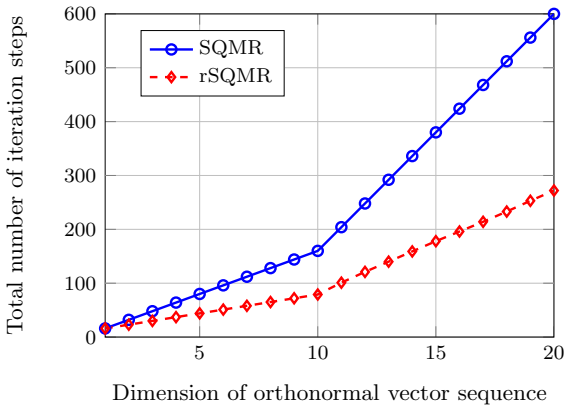

Figure 6.21: PCB: Initialization of mAORA method with rSQMR method.

Furthermore, we extend the application of the recycling SQMR method to the initialization of the modified AORA method with the expansion points $s_1 = \imath(2\pi \cdot 9.0 \cdot 10^9)$ and $s_2 = \imath(2\pi \cdot 10.0 \cdot 10^9)$. For the initial call of the mAORA method, we have employed $j_{1,1} = 10$ iteration steps leading to an (inexact) orthonormal basis of the Krylov subspace $\mathcal{K}_{j_{1,1}}(s_1)$. Assuming that the second call of the mAORA method leads to $j_{1,2} = 10$ and $j_{2,2} = 10$ iteration steps for the expansion points $s_1 \in \mathbb{C}$ and $s_2 \in \mathbb{C}$. Hence, we are able to reuse the orthonormal vector sequence $V^{(1)} \in \mathbb{C}^{n \times j_{1,1}}$ and only require the subsequent solution to a shifted linear system for the expansion point $s_2 \in \mathbb{C}$. As before, we have applied an LDL^{T} decomposition of the Schur complement at the expansion point $s_\star = \imath\sqrt{f_{\min} f_{\max}}$ as preconditioner.

The corresponding numerical results in Figure 6.21 show that here the rSQMR method with

$m = 40$ and $k = 10$ only requires half of iteration steps as compared to the SQMR method in the initialization of the mAORA method. Here, the initial expansion points $\mathcal{S}_1 \subset \mathbb{C}$ for the AORA-RK method have been chosen in a different way, cf. Table 6.4, in order to demonstrate the benefit from the application of a recycling subspace in the iterative Krylov subspace methods.

Further details on the efficiency gain of the rSQMR method have been given with respect to the norm of the residual $\| r_k \|_2$ $(k = 1, 2, \ldots)$ in Figure 6.22. Similar to the previous results, the application of a recycling subspace $U \in \mathbb{C}^{n \times p}$ significantly improves the convergence behaviour of the rSQMR method solving $(s_1\mathcal{E} - \mathcal{A})x = f$, $s_1 \in \mathbb{C}$, a second time and solving $(s_2\mathcal{E} - \mathcal{A})x = f$, $s_2 \in \mathbb{C}$, for the first time, respectively.

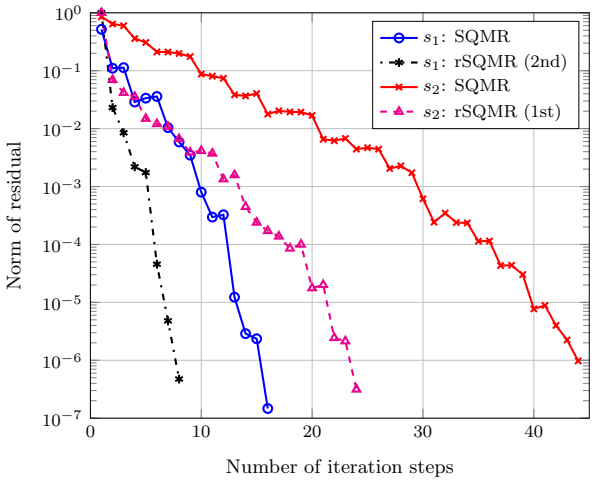

Figure 6.22: PCB: Relative error of init. of mAORA method with rSQMR method.

Finally, we provide a comparison between the accuracy of the reduced order model obtained via the subsequent application of the (modified) AORA method on the basis of the LU decomposition and the rSQMR method for solving the linear system with the Schur complement in the algebraic two-level method, cf. Figure 6.23 and 6.24, respectively. In order to allow for a reliable comparison, we restrict the discussion to the expansion points obtained via the AORA-RK method. Nevertheless, we expect at least comparable results for the employment of the rSQMR method within the mAORA-RK method.

The orthonormal vectors of the Krylov subspaces for the Galerkin projection are only determined up to the tolerance $\| r_k \|_2 \leq 10^{-8} \| r_0 \|_2$ in the recycling SQMR method. Naturally, a less accurate reduced order model will be obtained, while increasing the computational efficiency for solving the sequence of shifted linear systems with respect to the computational time and the memory requirement. Nevertheless, the numerical experiments indicate that a suitable accuracy for the reduced order model from the application of the recycling simplified

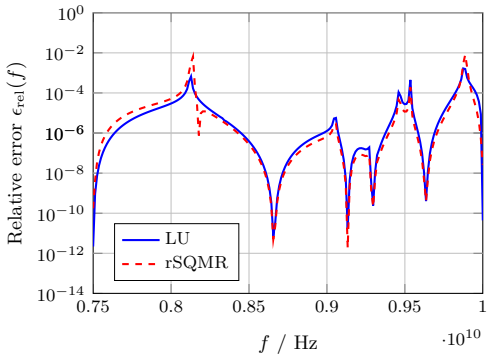

Figure 6.23: PCB: LU decomposition vs. rSQMR method in AORA method.

quasi-minimal residual (rSQMR) method within the frequency range at hand may be expected. Similar to the comparison between the AORA and mAORA method, we have obtained a comparable set of expansion points from the application of the recycling SQMR method in the greedy-type expansion point selection with the AORA-RK method.

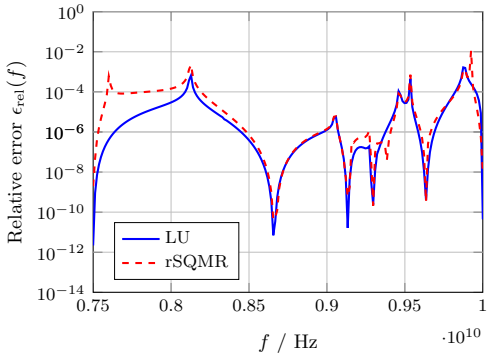

Figure 6.24: PCB: LU decomposition vs. rSQMR method in mAORA method.

The numerical results in Figure 6.24 provide an appropriate summary for the main contribution of the thesis at hand. The application of the modified adaptive-order rational Arnoldi (mAORA) method on the one hand and the recycling SQMR (rSQMR) method on the other hand leads to an efficient framework for the offline-stage of moment matching methods in model order reduction. The major advantage of the adequate application of the proposed framework is the comparable accuracy of the reduced order model with respect to the AORA method on the basis of the LU decomposition. Overall, we are able to efficiently deal with high-dimensional model problems of Maxwell's equations in view of the computational effort and the memory requirement.

In Table 6.8, we provide an overview on the subsequent iteration steps of the rSQMR

method for the different expansion points $\mathcal{S}_{i+1} = \mathcal{S}_i \cup \{s_{i+1}\}$, $s_{i+1} \in \mathbb{C}$. We only require subsequently solving a shifted linear system $(s_{i+1}\mathcal{E} - \mathcal{A})x = f$ with the latest expansion point $s_{i+1} \in \mathbb{C}$ during the $(i+1)$-th call of the mAORA method. Due to the fact that $j_{l,i+1} \leq j_{l,i}$ holds for all $l = 1, \ldots, i$, we may reuse the already known orthonormal vectors from the subspace $V^{(i)} \in \mathbb{C}^{n \times n_r}$. Here, the tolerance $\| r_k \|_2 \leq 10^{-8} \| r_0 \|_2$ still leads to a suitable number of iteration steps of the rSQMR method with $m = 40$ and $k = 10$.

Expansion point	# rSQMR	# SQMR
$s_1 = 5.44\text{e+}10\imath$	–	–
$s_2 = 6.28\text{e+}10\imath$	54, 24, 25, 24, 25, 24, 24, 24, 25, 25, 25	55
$s_3 = 6.05\text{e+}10\imath$	23, 20, 19, 20, 20, 20, 20, 20, 19	50
$s_4 = 5.84\text{e+}10\imath$	16, 13, 13, 13, 13, 13, 13	35
$s_5 = 4.71\text{e+}10\imath$	23, 21, 21, 18, 21	29
$s_6 = 5.73\text{e+}10\imath$	25, 11, 11, 10, 11	26

Table 6.8: PCB: Iteration steps of rSQMR method in mAORA method.

The larger number of iteration steps in the initial call of the rSQMR method for each expansion point results from the varying expansion points in the frequency range at hand. Nevertheless, the total number of iteration steps for solving each shifted linear system with the rSQMR method is still significantly smaller than the subsequent application of the SQMR method. For convenience, the number of iteration steps of the SQMR method for solving the linear system with the Schur complement may be obtained from the last column of Table 6.8.

CHAPTER 7

Conclusion

In the thesis at hand, we have given a comprehensive overview on the application of structure- and passivity-preserving moment matching methods in model order reduction of the first- and second-order Maxwell's equations. Apart from the introduction of an adaptive greedy-type expansion point selection based on the output moment error, we have shown different improvements for the offline-stage in model order reduction, e.g. the modified adaptive-order rational Arnoldi (mAORA) method and the recycling simplified quasi-minimal residual (rSQMR) method. These advancements lead to a significantly decreasing computational effort and memory requirement in the offline-stage of moment matching based model order reduction.

More precisely, the AORA-RK method refers to as a greedy-type expansion point selection strategy on the basis of an upper bound of the output moment error. Numerical experiments have proven its efficiency and reliability in model order reduction of linear dynamical systems arising from the Maxwell's equations in semiconductors structures. As compared to other greedy-type expansion point selection strategies, the AORA-RK method does not make use of an individual tolerance required for the selection of the subsequent expansion point by means of a heuristic error estimation. Moreover, the key ingredient of the AORA-RK method – the adaptive-order rational Arnoldi (AORA) method – already ensures the computation of a structure- and passivity-preserving reduced order model corresponding to linear dynamical systems of the Maxwell's equations.

An extension of the AORA method follows from the modified adaptive-order rational Arnoldi (mAORA) method in order to avoid the (complete) recomputation of an orthonormal basis for different sequences of Krylov subspaces, see Section 5.1. In principle, the employment of the mAORA method allows for an efficient offline-stage in moment matching based

model order reduction. While we typically benefit from the application of a reduced order model within a specific accuracy for numerical simulations, the offline-stage in model order reduction may become a challenging task with respect to the computational effort and the memory requirement. For example, the computation of a sequence of reduced order models with moment matching methods requires multiply solving a sequence of high-dimensional shifted linear systems. Numerical experiments have shown that the mAORA method allows for the efficient computation of the Galerkin projection within an appropriate accuracy of the reduced order model.

In due consideration of the memory requirement, the application of a direct solver, e.g. the LU decomposition, to a sequence of high-dimensional shifted linear systems is only possible for moderate dimensions of the full-order model problem. Rather, an algebraic two-level method (ATLM) makes the efficient computation of the solution to a shifted linear system of the first-order Maxwell's equations possible through exploiting the specific block-structure of the electric and magnetic field strength. The main computational effort of the ATLM is solving a linear system corresponding to the Schur complement of the algebraic two-level decomposition of the first-order Maxwell's equations. Typically, the Schur complement refers to as a (complex) symmetric, but highly indefinite time-harmonic, second-order Maxwell's equations.

The increasing memory requirement for the application of direct solvers leads to the framework of (recycling) Krylov subspace methods solving a sequence of shifted linear systems. In this context, the simplified quasi-minimal residual (SQMR) method represents the natural candidate of Krylov subspace methods for the time-harmonic, second-order Maxwell's equations. A significant improvement of the convergence behaviour of Krylov subspace methods solving a sequence of shifted linear systems is obtained via the class of recycling Krylov subspace methods, see [2,91]. Here, an extension of the SQMR method to the recycling simplified quasi-minimal residual (rSQMR) method on the basis of the recycling biconjugate gradient (rBiCG) method has been given.

Since the rSQMR method allows for the application of a (complex) symmetric, but indefinite preconditioning technique, we employ an LDL^{T} decomposition of a shifted linear system of the second-order Maxwell's equations at the geometric mean of the frequency range as the preconditioner $M \equiv M_1 M_2$. In many cases, the single preconditioner already allows for efficiently solving a sequence of shifted linear systems for a large frequency range. Numerical experiments have shown the competitive of the application of the recycling SQMR method for moment matching methods in model order reduction.

Although the upper bound of the output moment error (4.2.15) leads to a sufficient identification of the parts of the frequency range with the largest relative error components, moment matching methods are still restricted by the lack of an a-priori error estimator. In order to

provide a more convenient connection between the stopping criterion of a (recycling) Krylov subspace method and the accuracy of the reduced order model, we also have to incorporate the application of iterative Krylov subspace methods within the computation of the system moments $X^{(j)}(s_l)$ $(j = 0, \ldots, j_l - 1)$ for all $l = 1, \ldots, m$, see [13].

The demand for an efficient offline-stage in model order reduction also affects the class of parametric model problems with varying geometric or material parameters, see [12,130]. Here, multiple reduced order models corresponding to a given parameter selection, e.g. interpolation points in the parameter domain, are required in order to obtain the reduced order model of a specific parameter setting via interpolation of the reduced order models. In this context, we may even think about an extension of the upper bound of the output moment error in the AORA-RK method for parametrized linear dynamical systems.

Apart from parametrized linear dynamical systems, Krylov based model order reduction has been also applied to time-delay systems, see [84]. Thereby, the time-delay system is rewritten in terms of a finite-dimensional approximation and projected onto a low-dimensional subspace in order to guarantee a specific moment matching property. Similar to the delay eigenvalue problem [64], the corresponding Krylov subspace is constructed in a dynamic fashion. Here, we might discuss the necessity of improving the given moment matching property at zero and at infinity with respect to the structure of the time-delay system.

An extension of the previous framework to multiple-input, multiple-output (MIMO) linear dynamical systems follows from the application of the adaptive-order rational global Arnoldi (AORGA) method, see [65]. For example, the AORA-RK method and the modified adaptive-order rational Arnoldi method allow for a straightforward extension to multiple-input, multiple-output linear dynamical systems. Nevertheless, the computation of the upper bound of the output moment error (4.2.15) with the Frobenius norm requires an appropriate adaptation of the AORA-RK method in order to avoid the multiple selection of the same expansion point, cf. Subsection 4.2.5. An important example is given by a linear dynamical system with a quadratic output, i.e. $y(t) = x(t)^{\mathrm{T}} S x(t)$, where $S \in \mathbb{R}^{n \times n}$ is a symmetric matrix of rank $r \ll n$. In this case, an equivalent formulation of the linear dynamical system results in a linear dynamical system with multiple outputs, see [119].

Moreover, we require a more general preconditioning technique solving a linear system corresponding to the time-harmonic, second-order Maxwell's equations. For example, we may extend previous results on the efficient preconditioning of Helmholtz equations with a complex shifted mass matrix, see [38]. In this context, the application of a multilevel incomplete LU decomposition as preconditioner has proven its efficiency in [21]. A preconditioning technique for the time-harmonic, second-order Maxwell's equations based on a moving PML boundary condition has been also discussed recently, see [36,118].

Since the numerical experiments have been primarily carried out with MATLAB, we expect a further computational gain from the implementation of the modified AORA method and the recycling SQMR method in C or FORTRAN. We may even think about the efficient parallelization of the rational Arnoldi-type methods [111] and the corresponding iterative Krylov subspace methods. The parallelization also affects the efficient computation of the state moments for multiple right hand sides arising from multiple-input, multiple-output linear dynamical systems.

Bibliography

[1] K. AHUJA, *Recycling bi-Lanczos algorithms: BiCG, CGS, and BiCGSTAB*, Master's thesis, Department of Mathematics, Virginia Tech, 2009.

[2] K. AHUJA, E. DE STURLER, S. GUGERCIN, AND E. CHANG, *Recycling BiCG with an Application to Model Reduction*, SIAM Journal on Scientific Computing, 34 (2012), pp. 1925–1949.

[3] B. ANDERSON AND S. VONGPANITLERD, *Network Analysis and Synthesis*, Prentice Hall, Englewood Cliffs, NJ, 1973.

[4] A. C. ANTOULAS, *Approximation of Large-Scale Dynamical Systems*, Society for Industrial Mathematics, 2009.

[5] A. C. ANTOULAS, D. SORENSEN, AND S. GUGERCIN, *A survey of model reduction methods for large-scale systems*, Contemporary Mathematics, 280 (2001), pp. 193–219.

[6] W. E. ARNOLDI, *The principle of minimized iterations in the solution of the matrix eigenvalue problem*, Quarterly of Applied Mathematics, 9 (1951), pp. 17–29.

[7] K. ATKINSON AND W. HAN, *Theoretical Numerical Analysis: A Functional Analysis Framework*, Springer-Verlag, 2009.

[8] Z. BAI, *Krylov subspace techniques for reduced-order modeling of large-scale dynamical systems*, Applied Numerical Mathematics, 43 (2002), pp. 9–44.

[9] Z. BAI AND Y. SU, *Dimension Reduction of Large-Scale Second-Order Dynamical Systems via a Second-Order Arnoldi Method*, SIAM Journal on Scientific Computing, 26 (2005), pp. 1692–1709.

[10] ——, *SOAR: A Second-order Arnoldi Method for the Solution of the Quadratic Eigenvalue Problem*, SIAM Journal on Matrix Analysis and Applications, 26 (2005), pp. 640–659.

[11] G. A. BAKER JR. AND P. GRAVIES-MORRIS, *Padé Approximants, Part I: Basic Theory*, MA: Addison-Wesley, 1981.

[12] U. BAUR, C. BEATTIE, P. BENNER, AND S. GUGERCIN, *Interpolatory Projection Methods for Parameterized Model Reduction*, SIAM Journal on Scientific Computing, 33 (2011), pp. 2489–2518.

[13] C. BEATTIE, S. GUGERCIN, AND S. WYATT, *Inexact solves in interpolatory model reduction*, Linear Algebra and its Applications, 436 (2012), pp. 2916 – 2943.

[14] C. A. BEATTIE AND S. GUGERCIN, *Krylov-based model reduction of second-order systems with proportional damping*, in Proceedings of the 44th IEEE Conference on Decision and Control, and the European Control Conference, 2005.

[15] R. BECK, *Algebraic Multigrid by Component Splitting for Edge Elements on Simplicial Triangulations*, in Preprint SC 99-40, Konrad-Zuse-Zentrum für Informationstechnik, 1999.

[16] G. BENDERSKAYA, *Numerical Methods for Transient Field-Circuit Coupled Simulations Based on the Finite Integration Technique and a Mixed Circuit Formulation*, PhD thesis, Technical University Darmstadt, 2007.

[17] P. BENNER, J.-R. LI, AND T. PENZL, *Numerical Solution of Large Lyapunov equations, Riccati Equations, and Linear-Quadratic Control Problems*, Numer. Lin. Alg. w. Appl., 15 (2008), pp. 755–777.

[18] A. BODENDIEK AND M. BOLLHÖFER, *Efficient Krylov subspace methods in moment-matching model order reduction*, tech. rep., TU Braunschweig, 2013. Submitted.

[19] A. BODENDIEK AND M. BOLLHÖFER, *Adaptive-order rational Arnoldi-type methods in computational electromagnetism*, BIT Numerical Mathematics, (2013), pp. 1–24.

[20] C. BOESS, A. LAWLESS, N. NICHOLS, AND A. BUNSE-GERSTNER, *State estimation using model order reduction for unstable systems*, Computers & Fluids, 46 (2011), pp. 155 – 160.

[21] M. BOLLHÖFER, M. J. GROTE, AND O. SCHENK, *Algebraic Multilevel Preconditioner for the Helmholtz Equation in Heterogeneous Media*, SIAM J. Sci. Comput., 31 (2009), pp. 3781–3805.

[22] D. BRAESS, *Finite Elemente: Theorie, schnelle Löser und Anwendungen in der Elastizitätstheorie*, Springer-Verlag, 3 ed., 2003.

[23] S. C. BRENNER AND L. R. SCOTT, *The Mathematical Theory of Finite Element Methods*, Springer-Verlag, 30 ed., 2008.

[24] A. BUNSE-GERSTNER, D. KUBALIŃSKA, G. VOSSEN, AND D. WILCZEK, *h_2-norm optimal model reduction for large scale discrete dynamical MIMO systems*, Journal of Computational and Applied Mathematics, 233 (2010), pp. 1202 – 1216.

[25] BUREAU INTERNATIONAL DES POIDS ET MESURES, *The International System of Units (SI)*, www.bipm.org, 2006.

[26] R.-U. BÖRNER, O. G. ERNST, AND K. SPITZER, *Fast 3-D simulation of transient electromagnetic fields by model reduction in the frequency domain using Krylov subspace projection*, Geophysical Journal International, 173 (2008), pp. 766–780.

[27] G. COHEN, X. FERRIERES, P. MONK, AND S. PERNET, *Mass-lumped edge elements for the lossy maxwell's equations*, in Mathematical and Numerical Aspects of Wave Propagation WAVES 2003, G. C. Cohen, P. Joly, E. Heikkola, and P. Neittaanmäki, eds., Springer Berlin Heidelberg, 2003, pp. 383–388.

[28] L. DAI, *Singular Control Systems*, Springer-Verlag, 1989.

[29] L. DANIEL, O. C. SIONG, L. CHAY, K. H. LEE, AND J. WHITE, *A multiparameter moment-matching model-reduction approach for generating geometrically parameterized interconnect performance models*, Computer-Aided Design of Integrated Circuits and Systems, IEEE Transactions on, 23 (2004), pp. 678–693.

[30] E. DE STURLER, *Truncation Strategies for Optimal Krylov Subspace Methods*, SIAM Journal on Numerical Analysis, 36 (1999), pp. 864–889.

[31] V. DRUSKIN, C. LIEBERMAN, AND M. ZASLAVSKY, *On Adaptive Choice of Shifts in Rational Krylov Subspace Reduction of Evolutionary Problems*, SIAM J. Scientific Computing, 32 (2010), pp. 2485–2496.

[32] V. DRUSKIN AND V. SIMONCINI, *Adaptive rational Krylov subspaces for large-scale dynamical systems*, Systems & Control Letters, 60 (2011), pp. 546–560.

[33] P. L. DUREN, *Theory of $\mathcal{H}_p$ spaces*, Academic Press, New York, 1970.

[34] R. EID, B. SALIMBAHRAMI, AND B. LOHMANN, *Parametric Order Reduction of Proportionally Damped Second-Order Systems*, Journal of Sensors and Materials, 19 (2007), pp. 149–164.

[35] A. ELMKIES AND P. JOLY, *Éléments finis d'arête et condensation de masse pour les équations de maxwell: le cas 2d*, Comptes Rendus de l'Académie des Sciences - Series I - Mathematics, 324 (1997), pp. 1287 – 1293.

[36] B. ENGQUIST AND L. YING, *Sweeping Preconditioner for the Helmholtz Equation: Moving Perfectly Matched Layers*, Multiscale Modeling & Simulation, 9 (2011), pp. 686–710.

[37] A. K. EPPLER AND M. BOLLHÖFER, *An alternative way of solving large Lyapunov equations*, PAMM, 10 (2010), pp. 547–548.

[38] Y. A. ERLANGGA, C. VUIK, AND C. W. OOSTERLEE, *On a class of preconditioners for solving the Helmholtz equation*, Appl. Numer. Math., 50 (2004), pp. 409–425.

[39] H. FASSBENDER AND A. SOPPA, *Machine tool simulation based on reduced order FE models*, Mathematics and Computers in Simulation, 82 (2011), pp. 404–413.

[40] J. FEHR, C. TOBIAS, AND P. EBERHARD, *Automated and error controlled model reduction for durability based structural optimizationof mechanical systems*, in 5th Asian Conference on Multibody Dynamics, 2010.

[41] P. FELDMANN AND R. FREUND, *Efficient Linear Circuit Analysis by Pade Approximation via the Lanczos Process*, Computer-Aided Design of Integrated Circuits and Systems, IEEE Transactions on, 14 (1995), pp. 639–649.

[42] R. FLETCHER, *Conjugate gradient methods for indefinite systems*, in Numerical Analysis, G. A. Watson, ed., vol. 506 of Lecture Notes in Mathematics, Springer Berlin Heidelberg, 1976, pp. 73–89.

[43] F. FREITAS, J. ROMMES, AND N. MARTINS, *Gramian-Based Reduction Method Applied to Large Sparse Power System Descriptor Models*, Power Systems, IEEE Transactions on, 23 (2008), pp. 1258–1270.

[44] R. FREUND, *A Transpose-Free Quasi-Minimal Residual Algorithm for Non-Hermitian Linear Systems*, SIAM Journal on Scientific Computing, 14 (1993), pp. 470–482.

[45] ——, *Krylov-subspace methods for reduced-order modeling in circuit simulation*, J. Comp. Appl. Math., 123 (2000), pp. 395 – 421.

[46] ——, *SPRIM: Structure-preserving reduced-order interconnect macromodeling*, in Proceedings of the 2004 IEEE/ACM International conference on Computer-aided design, ICCAD '04, IEEE Computer Society, 2004, pp. 80–87.

[47] R. FREUND, M. GUTKNECHT, AND N. NACHTIGAL, *An Implementation of the Look-Ahead Lanczos Algorithm for Non-Hermitian Matrices*, SIAM Journal on Scientific Computing, 14 (1993), pp. 137–158.

[48] R. FREUND AND N. NACHTIGAL, *QMR: a quasi-minimal residual method for non-hermitian linear systems*, Numerische Mathematik, 60 (1991), pp. 315–339.

[49] ——, *An Implementation of the QMR Method Based on Coupled Two-Term Recurrences*, SIAM Journal on Scientific Computing, 15 (1994), pp. 313–337.

[50] ——, *Software for simplified Lanczos and QMR algorithms*, Applied Numerical Mathematics, 19 (1995), pp. 319 – 341.

[51] R. W. FREUND, *Model reduction methods based on krylov subspaces*, Acta Numerica, 12 (2003), pp. 267–319.

[52] K. GALLIVAN, E. GRIMME, AND P. V. DOOREN, *A rational Lanczos method for model reduction*, Numer. Algorithms, 12 (1995), pp. 33–63.

[53] G. H. GOLUB AND C. F. VAN LOAN, *Matrix Computations*, The Johns Hopkins University Press, 3rd ed., 1996.

[54] E. GRIMME AND K. GALLIVAN, *A Rational Lanczos Algorithm for Model Reduction II: Interpolation Point Selection*, Numerical Algorithms, 12 (1998), pp. 33–63.

[55] E. J. GRIMME, *Krylov Projection Methods for Model Reduction*, PhD thesis, University of Illinois at Urbana-Champaign, 1997.

[56] S. GUGERCIN, A. C. ANTOULAS, AND C. BEATTIE, *$\mathcal{H}_2$ Model Reduction for Large-Scale Linear Dynamical Systems*, SIAM Journal on Matrix Analysis and Applications, 30 (2008), pp. 609–638.

[57] M. H. GUTKNECHT, *Lanczos-type solvers for nonsymmetric linear systems of equations*, Acta Numerica, 6 (1997), pp. 271–397.

[58] M. HESS AND P. BENNER, *Fast Evaluation of Time Harmonic Maxwellś Equations Using the Reduced Basis Method*, IEEE Trans. Microwave Theory and Techniques, 61 (2013), pp. 2265–2274.

[59] M. R. HESTENES AND E. STIEFEL, *Methods of Conjugate Gradients for Solving Linear Systems*, Journal of Research of the National Bureau of Standards, 49 (1952), pp. 409–436.

[60] M. HINZE AND S. VOLKWEIN, *Proper Orthogonal Decomposition Surrogate Models for Nonlinear Dynamical Systems: Error Estimates and Suboptimal Control*, in Dimension Reduction of Large-Scale Systems, P. Benner, V. Mehrmann, and D. Sorensen, eds., vol. 45 of Lecture Notes in Computational Science and Engineering, Springer-Verlag, Berlin/Heidelberg, Germany, 2005, pp. 261–306.

[61] R. HIPTMAIR, *Multigrid method for Maxwell's equations*, SIAM J. Numer. Anal., 36 (1999), pp. 204–225.

[62] ——, *Finite elements in computational electromagnetism*, Acta Numerica, Cambridge University Press, (2002), pp. 237–339.

[63] P. HOLMES, J. L. LUMLEY, AND G. BERKOOZ, *Turbulence, Coherent Structures, Dynamical Systems and Symmertry*, Cambridge, New York, 1996.

[64] E. JARLEBRING, K. MEERBERGEN, AND W. MICHIELS, *A Krylov Method for the Delay Eigenvalue Problem*, SIAM Journal on Scientific Computing, 32 (2010), pp. 3278–3300.

[65] K. JBILOU, A. MESSAOUDI, AND H. SADOK, *Global FOM and GMRES algorithms for matrix equations*, Applied Numerical Mathematics, 31 (1999), pp. 49–63.

[66] M. KAMON, N. MARQUES, L. SILVEIRA, AND J. WHITE, *Automatic generation of accurate circuit models of 3-d interconnect*, Components, Packaging, and Manufacturing Technology, Part B: Advanced Packaging, IEEE Transactions on, 21 (1998), pp. 225–240.

[67] G. KERSCHEN, J.-C. GOLINVAL, A. VAKAKIS, AND L. BERGMAN, *The Method of Proper Orthogonal Decomposition for Dynamical Characterization and Order Reduction of Mechanical Systems: An Overview*, Nonlinear Dynamics, 41 (2005), pp. 147–169.

[68] P. KOOSIS, *Introduction to $\mathcal{H}^p$ spaces*, Cambridge University Press, Cambrigde, 1980.

[69] D. KRESSNER, M. PLEŠINGER, AND C. TOBLER, *A preconditioned low-rank CG method for parameter-dependent Lyapunov matrix equations*, tech. rep., ETH Zurich, 2012.

[70] A. KÖHLER, S. REITZ, AND P. SCHNEIDER, *Sensitivity analysis and adaptive multi-point multi-moment model order reduction in MEMS design*, Analog Integrated Circuits and Signal Processing, 71 (2012), pp. 49–58.

[71] A. KÖHLER AND S. REITZINGER, *An adaptive multi-point multi-moment model order reduction algorithm for fast broadband simulation of large-scale 3D electromagnetic models*, in ANALOG 2010. Entwicklung von Analogschaltungen mit CAE-Methoden., VDE-Verlag, Berlin, 2010, pp. 39–52.

[72] M.-H. LAI, C.-C. CHU, AND W.-S. FENG, *The Multiple Point Global Lanczos Method for MIMO Interconnect Model-Order Reductions*, in APCCAS, 2006, pp. 1268–1271.

[73] C. LANCZOS, *Solution of systems of linear equations by minimized iterations*, Journal of Research of the National Bureau of Standards, 49 (1952), pp. 33–53.

[74] H.-J. LEE, C.-C. CHU, AND W.-S. FENG, *An adaptive-order rational Arnoldi method for model-order reductions of linear time-invariant systems*, Linear Algebra and its Applications, 415 (2006), pp. 235–261.

[75] R. B. LEHOUCQ AND D. C. SORENSEN, *Deflation Techniques for an Implicitly Restarted Arnoldi Iteration*, SIAM Journal on Matrix Analysis and Applications, 17 (1996), pp. 789–821.

[76] J.-R. LI AND J. WHITE, *Low Rank Solution of Lyapunov Equations*, SIAM Journal on Matrix Analysis and Applications, 24 (2002), pp. 260–280.

[77] R.-C. LI AND Z. BAI, *Structure-preserving model reduction using a Krylov subspace projection formation*, Communications in Mathematical Sciences, 3 (2005), pp. 179–199.

[78] A. LOGG, K.-A. MARDAL, G. N. WELLS, ET AL., *Automated Solution of Differential Equations by the Finite Element Method*, Springer, 2012.

[79] R. LOZANO, B. BROGLIATO, O. EGELAND, AND B. MASCHKE, *Dissipative Systems Analysis and Control*, Communications and Control Engineering, Springer-Verlag, 2000.

[80] J. C. MAXWELL, *A Dynamical Theory of the Electromagnetic Field*, Philosophical Transactions of the Royal Society of London, 155 (1865), pp. 459–512.

[81] K. MEERBERGEN, *The Quadratic Arnoldi Method for the Solution of the Quadratic Eigenvalue Problem*, SIAM Journal on Matrix Analysis and Applications, 30 (2009), pp. 1463–1482.

[82] V. MEHRMANN AND T. STYKEL, *Balanced Truncation Model Reduction for Large-Scale Systems in Descriptor Form*, in Dimension Reduction of Large-Scale Systems, P. Benner, D. C. Sorensen, V. Mehrmann, T. J. Barth, M. Griebel, D. E. Keyes, R. M. Nieminen, D. Roose, and T. Schlick, eds., vol. 45 of Lecture Notes in Computational Science and Engineering, Springer Berlin Heidelberg, 2005, pp. 83–115.

[83] L. MEIER AND D. LUENBERGER, *Approximation of Linear Constant Systems*, IEEE Transactions on Automatic Control, 12 (1967), pp. 585–588.

[84] W. MICHIELS, E. JARLEBRING, AND K. MEERBERGEN, *Krylov-Based Model Order Reduction of Time-delay Systems*, SIAM Journal on Matrix Analysis and Applications, 32 (2011), pp. 1399–1421.

[85] P. MONK, *Finite Element Methods for Maxwell's Equations*, Numerical mathematics and scientific computation, Oxford University Press, 2003.

[86] G. E. MOORE, *Cramming more components onto integrated circuits, reprinted from electronics, volume 38, number 8, april 19, 1965, pp.114 ff.*, Solid-State Circuits Society Newsletter, IEEE, 11 (2006), pp. 33–35.

[87] R. B. MORGAN, *On restarting the Arnoldi method for large nonsymmetric eigenvalue problems*, Mathematics of Computation, 65 (1996), pp. 1213–1230.

[88] I. MUNTEANU, T. WITTIG, T. WEILAND, AND D. IOAN, *FIT/PVL circuit-parameter extraction for general electromagnetic devices*, Magnetics, IEEE Transactions on, 36 (2000), pp. 1421–1425.

[89] J. C. NÉDÉLEC, *Mixed finite elements in* $\mathbb{R}^3$, Numerische Mathematik, 35 (1980), pp. 315–341.

[90] K. H. A. OLSSON AND A. RUHE, *Rational Krylov for eigenvalue computation and model order reduction*, BIT Numerical Mathematics, 46 (2006), pp. 99–111.

[91] M. PARKS, E. DE STURLER, G. MACKEY, D. JOHNSON, AND S. MAITI, *Recycling Krylov Subspaces for Sequences of Linear Systems*, SIAM Journal on Scientific Computing, 28 (2006), pp. 1651–1674.

[92] K. PEARSON, *On Lines and Planes of Closest Fit to Systems of Points in Space*, Philosophical Magazine, 2, p. 559–572.

[93] G. PELOSI, *The finite-element method, Part I: R. L. Courant [Historical Corner]*, Antennas and Propagation Magazine, IEEE, 49 (2007), pp. 180–182.

[94] T. PENZL, *A Cyclic Low-Rank Smith Method for Large Sparse Lyapunov Equations*, SIAM J. Sci. Comput., 21 (1999), pp. 1401–1418.

[95] L. PILLAGE AND R. ROHRER, *Asymptotic waveform evaluation for timing analysis*, Computer-Aided Design of Integrated Circuits and Systems, IEEE Transactions on, 9 (1990), pp. 352–366.

[96] F. RAPETTI AND A. BOSSAVIT, *Whitney Forms of Higher Degree*, SIAM Journal on Numerical Analysis, 47 (2009), pp. 2369–2386.

[97] T. REIS AND T. STYKEL, *Balanced truncation model reduction of second-order systems*, Mathematical and Computer Modelling of Dynamical Systems, 14 (2008), pp. 391–406.

[98] ——, *PABTEC: Passivity-Preserving Balanced Truncation for Electrical Circuits*, Computer-Aided Design of Integrated Circuits and Systems, IEEE Transactions on, 29 (2010), pp. 1354–1367.

[99] ——, *Positive real and bounded real balancing for model reduction of descriptor systems*, 83 (2010), pp. 74–88.

[100] G. ROZZA, D. HUYNH, AND A. PATERA, *Reduced Basis Approximation and a Posteriori Error Estimation for Affinely Parametrized Elliptic Coercive Partial Differential Equations*, Archives of Computational Methods in Engineering, 15 (2007), pp. 229–275.

[101] A. RUHE, *Rational Krylov sequence methods for eigenvalue computation*, Linear Algebra Appl., 58 (1984), pp. 391–405.

[102] ——, *Rational Krylov algorithm for nonsymmetric eigenvalue problems II: Matrix pairs*, Linear Algebra Appl., 197 (1994), pp. 283–295.

[103] ——, *The rational Krylov algorithm for nonsymmetric eigenvalue problems III: complex shifts for real matrices*, BIT, 34 (1994), pp. 165–176.

[104] Y. SAAD, *Iterative Methods for Sparse Linear Systems*, Society for Industrial and Applied Mathematics, 2 ed., 2003.

[105] Y. SAAD AND M. H. SCHULTZ, *GMRES: A generalized minimal residual algorithm for solving nonsymmetric linear systems*, SIAM J. Sci. Statist. Comput., 7 (1986), pp. 856–869.

[106] J. SAAK, *Efficient Numerical Solution of Large Scale Algebraic Matrix Equations in PDE Control and Model Order Reduction*, PhD thesis, TU Chemnitz, 2009.

[107] S. B. SALIMBAHRAMI, *Structure Preserving Order Reduction of Large Scale Second Order Models*, PhD thesis, Technical University München, 2005.

[108] R. SCHUHMANN AND T. WEILAND, *A Stable Interpolation Technique for FDTD on Nonorthogonal Grids*, International Journal on Numerical Modelling, 11 (1998), pp. 299–306.

[109] L. M. SILVEIRA AND J. R. PHILLIPS, *Resampling Plans for Sample Point Selection in Multipoint Model-Order Reduction*, Computer-Aided Design of Integrated Circuits and Systems, IEEE Transactions on, 25 (2006), pp. 2775 –2783.

[110] V. SIMONCINI, *A New Iterative Method for Solving Large-Scale Lyapunov Matrix Equations*, SIAM Journal on Scientific Computing, 29 (2007), pp. 1268–1288.

[111] D. SKOOGH, *A parallel rational Krylov algorithm for eigenvalue computations*, in Applied Parallel Computing Large Scale Scientific and Industrial Problems, B. Kågström, J. Dongarra, E. Elmroth, and J. Waśniewski, eds., vol. 1541 of Lecture Notes in Computer Science, Springer Berlin Heidelberg, 1998, pp. 521–526.

[112] R. SLONE, R. LEE, AND J.-F. LEE, *Well-conditioned asymptotic waveform evaluation for finite elements*, Antennas and Propagation, IEEE Transactions on, 51 (2003), pp. 2442 –2447.

[113] A. SOPPA, *Krylov-Unterraum basierte Modellreduktion zur Simulation von Werkzeugmaschinen*, PhD thesis, Technical University Braunschweig, 2011.

[114] K. STAVRAKAKIS, *Model Order Reduction Methods for Parametrized Systems in Electromagnetic Field Simulations*, PhD thesis, Technical University Darmstadt, 2012.

[115] G. STEWART AND J.-G. SUN, *Matrix Pertubation Theory*, Academic Press, New York, 1990.

[116] T. STYKEL, *Analysis and numerical solution of generalized Lyapunov Equations*, PhD thesis, Technical University Berlin, 2002.

[117] S. TAN AND L. HE, *Advanced Model Order Reduction Techniques in VLSI Design*, Cambridge University Press, 6 2007.

[118] P. TSUJI, B. ENGQUIST, AND L. YING, *A sweeping preconditioner for time-harmonic Maxwell's equations with finite elements*, Journal of Computational Physics, 231 (2012), pp. 3770–3783.

[119] R. VAN BEEUMEN, K. VAN NIMMEN, G. LOMBAERT, AND K. MEERBERGEN, *Model reduction for dynamical systems with quadratic output*, International Journal for Numerical Methods in Engineering, 91 (2012), pp. 229–248.

[120] S. VOLKWEIN, *Model Order Reduction using Proper Orthogonal Decomposition*, TU Graz, 2006. Lecture notes.

[121] E. L. WACHSPRESS, *ADI iterative solution of Lyapunov equations*, Appl. Math. Letter, 1 (1988), pp. 87–90.

[122] ——, *The ADI Model Problem*, tech. rep., Windsor, CA, 1995.

[123] D. S. WATKINS, *The Matrix Eigenvalue Problem: GR and Krylov Subspace Methods*, Society for Industrial Mathematics, 2007.

[124] T. WEILAND, *A discretization method for the solution of Maxwell's equations for six-component fields*, Electronics and Communications, 31 (1977), pp. 116–120.

[125] ——, *Time domain electromagnetic field computation with finite difference methods*, Int. J. Numer. Model., 9 (1996), pp. 295–319.

[126] D. WEILE, E. MICHIELSSEN, E. GRIMME, AND K. GALLIVAN, *A method for generating rational interpolant reduced order models of two-parameter linear systems*, Applied Mathematics Letters, 12 (1999), pp. 93 – 102.

[127] K. WILLCOX, *Unsteady Flow Sensing and Estimation via the Gappy Proper Orthogonal Decomposition*, Computers & Fluids, 35 (2006), pp. 208–226.

[128] T. WITTIG, I. MUNTEANU, R. SCHUHMANN, AND T. WEILAND, *Two-step Lanczos algorithm for model order reduction*, IEEE Transactions on Magnetics, 38 (2002), pp. 673–676.

[129] W.-Y. YAN AND J. LAM, *An approximate approach to h2 optimal model reduction*, Automatic Control, IEEE Transactions on, 44 (1999), pp. 1341–1358.

[130] Y. YUE AND K. MEERBERGEN, *Accelerating Optimization of Parametric Linear Systems by Model Order Reduction*, SIAM Journal on Optimization, 23 (2013), pp. 1344–1370.

[131] S. ZAGLMAYR, *High Order Finite Element Methods for Electromagnetic Field Computation*, PhD thesis, Johannes Kepler University Linz, 2006.

[132] K. ZHOU, J. C. DOYLE, AND K. GLOVER, *Robust and Optimal Control*, Prentice Hall, 1996.

Index